2014

Effect of protons on the biology of human gliomas

Avinash Vinayak Honasoge
University of Alabama at Birmingham

EFFECT OF PROTONS ON THE BIOLOGY OF HUMAN GLIOMAS

by

AVINASH VINAYAK HONASOGE

HARALD SONTHEIMER, COMMITTEE CHAIR
MARK BEVENSEE
MICHELLE OLSEN
J. DAVID SWEATT
JACQUES WADICHE

A DISSERTATION

Submitted to the graduate faculty of The University of Alabama at Birmingham,
in partial fulfillment of the requirements for the degree of
Doctor of Philosophy

BIRMINGHAM, ALABAMA
2014

EFFECT OF PROTONS ON THE BIOLOGY OF HUMAN GLIOMAS

AVINASH VINAYAK HONASOGE

DEPARTMENT OF NEUROBIOLOGY

ABSTRACT

Gliomas are the most common and most deadly primary brain cancer. Patient outcome for the most malignant variety, the World Health Organization (WHO) Type IV glioblastoma multiforme (GBM), has stagnated over the last several decades – the best combination treatment of surgical resection, radiation, and chemotherapy results in median survival of just over a year. To escape treatment, GBM must multiply and migrate in a confined brain environment. Both of these aspects of tumor cell invasion rely on the cell's ability to volume regulate; cell division involves a stage called "pre-mitotic condensation" in which the cells shrink immediately prior to splitting, and migration in the tight brain space necessitates cell shrinkage and expansion to accommodate. This volume regulation is in turn dependent on the osmotic flux of ions through dedicated channels across the lipid bilayer – most commonly K^+ and Cl^-. These channels themselves are regulated by a host of factors including ion concentration, membrane potential (V_m), phosphorylation, and as shown in this thesis, pH. This last component is especially relevant to glioma cells, as they produce copious amounts of protons due to a largely glycolytic metabolism even in the presence of ample oxygen.

Here, I demonstrate that glioma tumor spheroids create steep external pH (pH_e) gradients. These affect glioma ion channels that are tightly regulated by pH_e. By altering the conductance of these pH_e-sensitive K^+ channels, glioma cells set their

V_m based on their location within the tumor mass, and this in turn affects their proliferation state by gating their G_1-to-S transition through the cell cycle. Thus, the glioma controls its growth through autocrine proton signaling.

Additionally, I found that protons directly permeate the cell membrane through the Cl^-/H^+ antiporter ClC-3, movement which depends on extracellular Cl^- and protons and is uncoupled at acidic pH_e. This is a novel finding that adds to the cohort of pH regulators expressed on glioma cells and provides an additional function to a well-described glioma Cl^- channel.

Keywords: glioma, pH, potassium channel, ClC-3, Cl^-/H^+ antiporter

DEDICATION

To my parents, Lakshmi and Ananth, and to my brother, Akilesh.

ACKNOWLEDGMENTS

This work would not be possible were it not for the guidance and mentorship of Dr. Harald Sontheimer. He helped me develop as both a scientist and a person during my time in the lab, and I am forever thankful. I would also like to thank all members of the Sontheimer lab, past and present, for their contributions to this project. Additionally, the members of my committee, Drs. J. David Sweatt, Jacques Wadiche, Michelle Olsen, and Mark Bevensee, have provided excellent feedback during my time in the lab. In particular, Dr. Bevensee shared his vast knowledge of both pH and pH regulation within astrocytes. Finally, I would like to thank Dr. Robin Lorenz and the members of the UAB MSTP for guiding me through my journey.

TABLE OF CONTENTS

Page

ABSTRACT iii

DEDICATION v

ACKNOWLEDGMENTS vi

LIST OF FIGURES viii

INTRODUCTION 1

INVOLVEMENT OF TUMOR ACIDIFICATION IN BRAIN CANCER PATHOPHYSIOLOGY 8

AUTOCRINE REGULATION OF GLIOMA CELL PROLIFERATION VIA pH_e-SENSITIVE K^+ CHANNELS 37

CLC-3 ACTS AS A PLASMA MEMBRANE Cl^-/H^+ ANTIPORTER IN HUMAN GLIOMAS 78

SUMMARY AND DISCUSSION 112

GENERAL LIST OF REFERENCES 120

APPENDIX: IRB APPROVAL FORM 126

LIST OF FIGURES

Figure *Page*

INVOLVEMENT OF TUMOR ACIDIFICATION IN BRAIN CANCER PATHOPHYSIOLOGY

1 Major components of pH_i regulation in glioma cells 12

2 Examples of pH-dependent physiology in solid tumors 19

AUTOCRINE REGULATION OF GLIOMA CELL PROLIFERATION VIA pH_e-SENSITIVE K^+ CHANNELS

1 Quantification of tumor spheroid acidification. 49

2 Human glioma spheroids evolve pH_e and proliferation gradients. 52

3 Glioma cells display a pH_e-sensitive whole-cell conductance 54

4 The pH_e-sensitive conductance is $[K^+]_o$-dependent. 57

5 Inhibition of the pH_e-sensitive K^+ conductance 59

4 Quinine depolarizes glioma spheroids 61

5 pH_e-sensitive conductance modulates glioma cell cycle. 64

CLC-3 ACTS AS A PLASMA MEMBRANE Cl^-/H^+ ANTIPORTER IN HUMAN GLIOMAS

1 Expression of ClC-3 protein in human glioma cells 91

2 Electrogenic movement of protons in human glioma cells. 93

3 pH_e-dependent E_{rev} and current density in human glioma cells. 94

4 Knockdown of ClC-3 protein in human glioma cells 96

LIST OF FIGURES (cont'd)

Figure *Page*

5 ClC-3 determines pH_e-dependence of glioma cells.....97

6 ClC-3 is electrogenically driven by altered $[K^+]_o$.....99

7 Disruption of leading edge pH_i and pH_i covariation in ClC-3 knockdown glioma cells.....102

SUMMARY AND DISCUSSION

1 pH_e CONTROL OF GLIOMA CELL PROLIFERATION VIA pH_e- AND QUININE-SENSITIVE K^+ CHANNELS.....113

2 ROLE OF pH_e CONTROL OF GLIOMA CELL PROLIFERATION IN THE GO-VS.-GROW HYPOTHESIS OF CANCER CELLS.....116

INTRODUCTION

Protons (H^+) are ionized hydrogen atoms. In biology, they represent point sources of charge that interact with every molecule and protein in the human body. This reactiveness necessitates a tight control of free proton concentration, measured as pH, which has evolved into a large biological network of buffers and transporters. This tight control has subsequently given dramatic consequence to even small changes of pH.

pH follows a logarithmic scale, as its equation demonstrates:

$$pH = -\log_{10}[H^+]$$

where $[H^+]$ represents the concentration of free protons in the medium (note: this equation only works when one assumes the concentration and activity of free protons are equal). The pH of cerebrospinal fluid (CSF) which houses the brain is around 7.30 in mammals (Mitchell and Singer, 1965; Javaheri et al., 1984), slightly acidic relative to blood plasma due to the heightened partial pressure of CO_2 (pCO_2) in the brain (Andrews et al., 1994). This pH of 7.30 represents $10^{-7.3}$ M – or 50 nM – $[H^+]$, making protons far scarcer than Na^+, K^+, and Cl^- and roughly as scarce as Ca^{2+} intracellularly. As a result, introduction of new proton sources above and beyond normal cellular physiology can have drastic effects on brain chemistry.

This is best exemplified with gliomas, which are solid primary brain tumors noted for hyperacidification of the interstitium (García-Martín et al., 2001; Garcia-Martin et al., 2006). All cells in the body create protons as a byproduct of normal cell metabolism in an attempt to create adenine triphosphate (ATP) and other energy-rich molecules; however, this process is accelerated in cancer cells in a manner first observed by Otto Warburg, a German scientist in the 1920s (Warburg et al., 1927; Warburg, 1956). He noted that even those cancer cells given ample oxygen to undergo oxidative phosphorylation preferred glycolysis and lactic acid fermentation. As a result, he hypothesized that the primary cause of cancer is this aerobic glycolysis. While it now appears that this metabolism is usually an indirect result of upstream mutations causing upregulation of pro-glycolytic genes including hypoxia-inducible factor 1 (HIF-1), the initial observation of altered metabolism and abundant proton production in tumor cells has been repeatedly verified (Semenza et al., 2001; Papandreou et al., 2006; Cairns et al., 2011).

Gliomas are highly aggressive and deadly, with median survival of just over a year even with the best combination of therapies for the most malignant subtype, glioblastoma multiforme (GBM) (Stupp et al., 2005). Additionally, a number of comorbidities accompany the brain's destruction by the tumor and can be debilitating themselves, most notably glutamate release by the glioma cells causing neuronal excitotoxicity (Buckingham et al., 2011; Sontheimer, 2011; Campbell et al., 2012; Buckingham and Robel, 2013). We must therefore learn how these tumors affect brain chemistry on top of their abilities to invade and proliferate, and the increased tumoral proton load is an underexplored subject in that regard.

The potential effects of these protons on brain chemistry will be speculated in the *Discussion* section of this thesis; but first, it is important to note the many mechanisms by which gliomas counteract their proton buildup and how protons can affect them in an autocrine manner. Gliomas possess a series of transporters and pumps to protect themselves from an otherwise toxic intracellular pH (pH_i) environment. The exact expression pattern of these proteins is the subject of the review included as the first part of this thesis (Honasoge and Sontheimer, 2013), but the highest-expressed transporter is the Na^+/H^+ exchanger NHE1. NHE1 expression is upregulated in gliomas versus their astrocytic counterparts, and results in gliomas relying more on HCO_3^--independent mechanisms of proton movement (McLean et al., 2000). Glioma cells also express lactate-H^+ cotransporters which simultaneously extrude the metabolic byproducts lactate and protons; and in fact, the cells can organize the expression of lactate and proton transporters across the bulk of the tumor mass to reapportion metabolites (Grillon et al., 2011).

If left unchecked, proton buildup can shut down cellular processes. Both low pH_i and pH_e tend to be deleterious to cell function, and in the worst case can trigger cell apoptosis (Park et al., 1999; Lagadic-Gossmann et al., 2004). However, before death, degrees of proton loading can modulate physiology. Glioma cells are especially adept at maximizing their chances of survival in this hostile environment. For instance, low pH_e triggers downstream intracellular functions such as increased expression of vascular endothelial growth factor (VEGF) and carbonic anhydrase IX (CAIX) to enhance blood flow and thus shuttle away protons, CO_2, and other metabolic byproducts (Wykoff et al., 2000; Xu et al., 2002). Additionally, the

aforementioned NHE1 can localize to the leading edge of tumor cells, leading to two escape mechanisms: 1) using a high pH_i leading edge to polarize the tumor cell by inducing actin polymerization and 2) using a low pH_e leading edge to enhance extracellular matrix destruction (Busco et al., 2010; Magalhaes et al., 2011). These processes combine to help tumor cells escape from their self-created acidified tumor microenvironment.

It is important to highlight the impact of pH on ion channels in glioma cells, as it is central to this thesis. pH is one of many regulatory mechanisms of ion channels, usually taking a backseat to phosphorylation, Ca^{2+} sensitivity, voltage, and time. Generally, protons block the pore of cation channels and decrease channel conductance (Lopes et al., 2001; Cohen et al., 2009; Van Slyke et al., 2012). A relevant example is the two-pore K^+ channel family (K2P), especially the members TASK-1 and TASK-3. These are "leak" conductance K^+ channels that are blocked by both low pH_e and by several inhibitors, most robustly quinine (Lotshaw, 2007). However, there are also channels that are activated by low pH_e, including those in the acid-sensing ion channel (ASIC) family (Waldmann et al., 1997). ASICs are expressed on glioma cells, and affect both their migration and their proliferation (Berdiev et al., 2003; Kapoor et al., 2009; Rooj et al., 2012).

Additionally, ion channels are involved in cancer cell proliferation (Becchetti, 2011). These channels are transmembrane proteins and can act as liaisons for extracellular molecules to influence intracellular proliferation signaling in two major ways: 1) the ions that are fluxed through these channels, most notably Ca^{2+},

can serve downstream in intracellular signaling cascades, including those that govern growth; and 2) changing V_m changes the electric field on the cell surface, which can recruit (or repel) charged proteins to (or from) the plasma membrane. Additionally, the profile of open and closed ion channels sets the cell's resting membrane potential (V_m) which feeds back and determines the open and closed states of voltage-gated channels, thus altering V_m and providing an added means of control. In these ways, ion channels act as a fundamental determinant of a cell's "state" and help regulate whether it is free to pass through the checkpoints in the cell cycle or if it is arrested.

In the second part of this thesis, we wondered if the pH_e heterogeneity encountered by glioma cells could serve as a signal for cell growth using pH_e-sensitive ion channels as the transmembrane mediator (Honasoge et al., 2013). To do this, we first established a three-dimensional tumor spheroid model that recapitulated the environment a cell might see *in vivo*. These spheroids showed properties of human gliomas, including outside-out growth and steep pH_e gradients. Once we established this model, we probed individual cells on coverslips to see if they contained pH_e-sensitive electrophysiological currents, and upon finding these we sought to isolate them pharmacologically. Finally, we looked one step downstream and saw the potential impact of pH_e-sensitive ion channels on glioma cell proliferation via V_m control. In total, we discovered a pH_e- and quinine-sensitive K^+ channel that controlled V_m and whose hyperpolarizing effect on glioma cells was necessary for the G_1-to-S phase cell cycle transition, thus assigning autocrine effect to glioma-produced protons on cell proliferation.

A final possible interaction between ion channels on gliomas and protons involves direct proton permeation through these channels. Glioma cells are unique in that they appear to have high surface expression of ClC-3, a protein that is part of the CLC family composed of Cl^- channels and Cl^-/H^+ antiporters (Accardi and Picollo, 2010). In gliomas, ClC-3 allows the cells to volume regulate by fluxing Cl^- in tandem with K^+ and H_2O (Ransom et al., 2001; Mcferrin and Sontheimer, 2006). This volume regulation serves two purposes in glioma cell pathophysiology: 1) it lets glioma cells squeeze through tight spaces and invade distant brain tissue, and 2) it shrinks the cells prior to M-phase in a necessary step of the cell cycle known as "pre-mitotic condensation" (Habela et al., 2008; Cuddapah et al., 2012). Though controversial, in other model systems it is thought that ClC-3 exists as an antiporter and not a strict chloride channel (Matsuda et al., 2008; Matsuda et al., 2010). These antiporters are usually confined to the cell's interior (Accardi and Picollo, 2010), making ClC-3's surface expression on glioma cells both novel and exciting, as it could be a new source of pH_i regulation for these cells and an unexplored role for ClC-3 in glioma pathophysiology. This is the topic that concerns the last section of this thesis: we set out to determine if human glioma cells possessed an electrogenic, chloride-dependent pH_i regulator, and if so, implicate ClC-3 as that antiporter. Through a series of electrophysiological and pH_i-sensitive fluorescence experiments, we probed human glioma cells and found a much more complicated role for pH_e than previously discussed; now, extracellular protons can both gate and permeate the glioma cell membrane by interacting with the Cl^-/H^+ antiporter ClC-3. This proton-ClC-3 interaction is a complicated one, however, as low extracellular proton

concentrations (high pH_e) actually *increase* antiporter conductance, while high extracellular proton concentrations (low pH_e) uncouple Cl^-/H^+ antiport (Matsuda et al., 2010). The currents of human glioma cells in Na^+- and K^+-free conditions seem to fit this signature of ClC-3, and knockdown of ClC-3 protein reduced glioma cell pH_e-dependence. Functionally, this ClC-3 knockdown resulted in augmentation of the low-high pH_i gradient found from the lagging to leading edge of glioma cells, most likely due to the localized surface expression of ClC-3 to the leading edge. As a result, we observe that glioma cells possess a pH_e-sensitive Cl^-/H^+ antiporter, ClC-3, that until now has been described as a strict chloride channel. In this way, gliomas may intertwine their proton dynamics with volume regulation and subsequently growth and invasion.

In conclusion, there were three overarching hypotheses tested for this thesis:

1) Human glioma cells recapitulate their three-dimensional pH physiology *in vitro* even with a clonal population of cells, making cell line usage an appropriate tool of investigation;

2) Proton extrusion from glioma cells affects proliferation in an autocrine manner;

3) The previously-described ClC-3 chloride channel on human glioma cells also fluxes protons through the plasma membrane in an antiport fashion with chloride and impacts pH_i.

INVOLVEMENT OF TUMOR ACIDIFICATION IN BRAIN CANCER PATHOPHYSIOLOGY

by

Avinash Honasoge and Harald Sontheimer

Frontiers in Physiology – Membrane Physiology and Membrane Biophysics
4:316

Format adapted for dissertation

ABSTRACT

Gliomas, primary brain cancers, are characterized by remarkable invasiveness and fast growth. While they share many qualities with other solid tumors, gliomas have developed special mechanisms to convert the cramped brain space and other limitations afforded by the privileged central nervous system into pathophysiological advantages. In this review we discuss gliomas and other primary brain cancers in the context of acid-base regulation and interstitial acidification; namely, how the altered proton (H^+) content surrounding these brain tumors influences tumor development in both autocrine and paracrine manners. As proton movement is directly coupled to movement of other ions, pH serves as both a regulator of cell activity as well as an indirect readout of other cellular functions. In the case of brain tumors, these processes result in pathophysiology unique to the central nervous system. We will highlight what is known about pH-sensitive processes in brain tumors in addition to gleaning insight from other solid tumors.

Keywords: glioma, pH, NHE, brain cancer, solid tumor, acidification

INTRODUCTION

Primary brain tumors stand out amongst solid tumors in both their location and their pathophysiology. The most common and aggressive type of primary brain tumors, glioma, invades brain space while simultaneously destroying surrounding tissue in an attempt to increase brain real estate (Watkins and Sontheimer, 2012). As with other solid tumors, gliomas display enhanced glycolysis and heightened acidification of the tissue interstitium (Vlashi et al., 2011). Unlike other solid tumors, however, gliomas face both brain-specific cellular interactions (Charles et al., 2011) and chemical composition (Irani, 2008). This results in unique pathophysiological consequences. In this review, we will highlight the mechanisms by which brain tumors regulate both their intracellular pH (pH_i) and also the pH of the surrounding tissue (pH_e), and how this pH regulation affects tumor pathogenicity.

pH_i REGULATION

Tumor cells constantly struggle to resist the electrochemical gradients of protons, weak acids, and weak bases generally acidifying the cell (Webb et al., 2011;Bevensee and Boron, 2013). Thus a major driving force in understanding tumor acid-base physiology is understanding the transport of protons across the plasma membrane. This transport uses either energy substrates or is coupled to the electrochemically-favorable transport of a second molecule. The following section explains the roles of various H^+-coupled transporters and exchangers in brain tumor pH_i regulation (Fig. 1).

Most initial studies on glioma cell pH_i regulation used C6 rat glioma cells, which were generated by exposure to *N,N'*-nitroso-methylurea and used throughout the 1980s and 1990s as a convenient cell line for studying astrocytic physiology including cytotoxic edema, cerebral ischemia, and volume regulation under osmotic challenge. For a thorough review of the C6 line, please refer to (Grobben et al., 2002). These studies often used changes in pH_i as a proxy for transport of other ions such as Na^+, K^+, and Cl^-. Only recently did the focus of inquiry shift to human glioma. With this caveat in mind, we will review some older literature that describes pH regulatory systems in C6 followed by newer literature on the biological targets of pH changes in human gliomas.

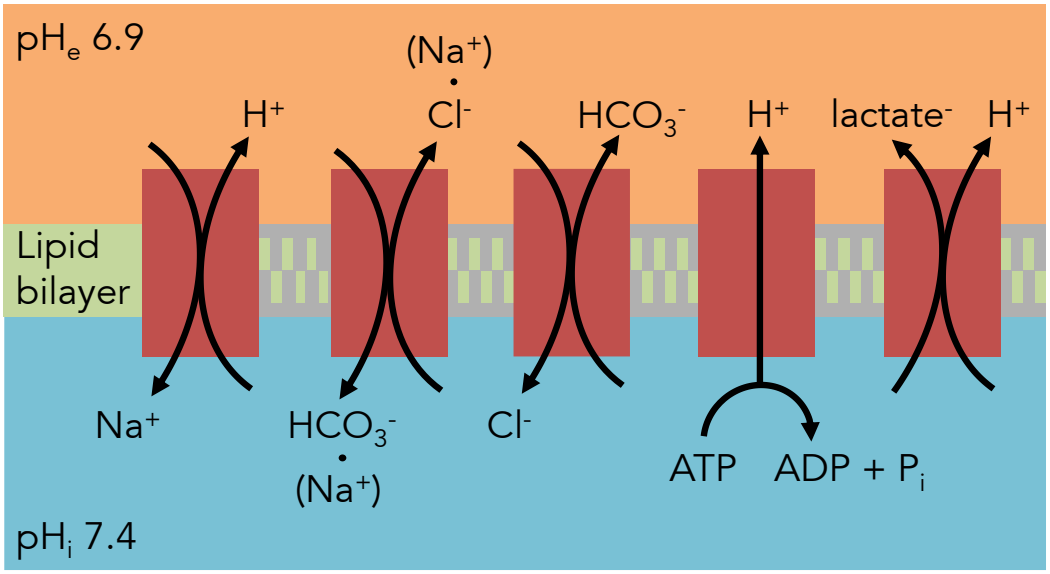

Figure 1. *Major components of pH_i regulation in glioma cells*. Unlike astrocytes, glioma cells rely heavily on HCO_3^--independent mechanisms to regulate their pH_i. The predominant acid extruder is NHE1, a Na^+/H^+ exchanger. All of these components except for the H^+ V-ATPase also contribute to C6 glioma osmotic regulation from the transport of the counter-ion.

Na^+/H^+ exchange

Na^+/H^+ exchange (NHE) was originally identified in mouse muscle fibers (Aickin and Thomas, 1977) where it was shown to be the major regulator of pH_i. Owing to a strong inwardly-directed electrochemical gradient for Na^+, it is ideally suited for proton extrusion, thereby alkalinizing pH_i while simultaneously acidifying the interstitium (Fig. 1). The first implications of NHE in glioma cells came from studies in C6 rat glioma cells and neuroblastoma x glioma hybrid cells (NG108-15), both used as model systems investigating NHE in adrenergic signaling (Hertel and Staehelin, 1983;Isom et al., 1987a;Nunnari et al., 1987). Later studies involved NHE in a wide variety of signaling pathways (Isom et al., 1987b;Neve et al., 1992). C6 glioma cells were also considered a viable model of glial cells during acidosis and postischemic brain edema, where pH_i served as a secondary readout for NHE involvement in osmotic swelling and regulatory volume increase (Jakubovicz et al., 1987;Kempski et al., 1988;Jakubovicz and Klip, 1989;Staub et al., 1994) under mildly acidotic conditions (pH_e 6.0-7.0). Later, it was postulated that NHE served to maintain homeostatic pH_i at the cost of cell swelling (Kempski et al., 1990;Staub et al., 1990). This exchange was temperature-dependent, with increased activity at higher temperatures (Lui et al., 1995;Mountian et al., 1996). While these studies sought to implicate glial cells in cytotoxic edema, they also hinted at a robust NHE mechanism that would soon be implicated as a hallmark of brain tumors.

The initial reports of NHE in brain tumor cell activity came from C6 glioma spheroids, where H^+ production under high glucose conditions was diminished by amiloride (Acker et al., 1992). Subsequently, Shrode et al. characterized differences

in pH_i regulation between C6 glioma cells and astrocytes, with the largest being a lack of Na^+/HCO_3^- transport in glioma cells (Shrode and Putnam, 1994). McLean et al. were the first to look at various human glioma cell lines and noted a significant elevation in Na^+/H^+ exchanger subtype 1 (NHE1) expression, an increase in baseline pH_i, and an increased reliance on HCO_3^--independent pathways versus primary rat astrocytes (McLean et al., 2000). As the NHE1 blocker amiloride is nonspecific and has off-target effects on glioma cells (Hegde et al., 2004), specific blockade of NHE1 with HOE642 (cariporide) confirmed a tonic activity for the NHE1 exchanger in glioma cell pH_i regulation (Glunde et al., 2002). Interestingly, DNA hypermethylation decreases NHE1 expression in oligodendroglioma versus higher-grade gliomas, potentially limiting the growth potential of these lower-grade gliomas (Blough et al., 2012). However, there have not been comprehensive studies of NHE subtypes in gliomas, with one study finding absence of NHE2 and NHE3 expression in C6 glioma cells (Willoughby et al., 2005). More recent studies have hinted at changes in Na^+/H^+ exchanger recruitment to the cell surface (Kislin et al., 2009) and spatial organization within the tumor (Grillon et al., 2011).

Cl^-/HCO_3^- exchange

C6 glioma cells express both Na^+-dependent and Na^+-independent modes of Cl^-/HCO_3^- exchange (Fig. 1). The Na^+-dependent transport is alkalinizing, while the Na^+-independent transport is acidifying in response to an intracellular alkalinization (Shrode and Putnam, 1994); these are blocked by the inhibitors 4,4'-diisothiocyano-2,2'-stilbenedisulfonic acid (DIDS) and 4-acetamido-4-isothiocyanatostilbene-2,2-disulfonic acid (SITS) (Kempski et al., 1988;Shrode and Putnam, 1994;Mountian et

al., 1996;McLean et al., 2000). Cl^-/HCO_3^- antiporter activity helps import Cl^- ions in tandem with Na^+ ions from the NHE to serve as osmotic agents for cell swelling in the face of acidosis (Staub et al., 1990;Mountian et al., 1996). The extrusion of HCO_3^- seems to additionally act as a buffer for lactic acid (Staub et al., 1990), a finding discovered while investigating cerebral ischemia but that extrapolates well to the tumor microenvironment. Unlike nontransformed astrocytes, however, it appears glioma cells strongly lean on CO_2/HCO_3^--independent mechanisms of acid extrusion (McLean et al., 2000).

H^+-lactate cotransport

Proton-coupled lactate transporters help rid the cell of both acid and lactate loads simultaneously and thus play vital roles in tumor cellular metabolism and osmoregulation (Fig. 1). Lactate efflux was first reported in C6 glioma cells to be a pH-dependent phenomenon, with increased efflux at alkaline pH_e (Lust et al., 1975). This transport was reversed in an astrocytoma cell line when the extracellular lactate and proton concentrations were increased (Lomneth et al., 1990;Tomsig et al., 1991), and lactate uptake in glioma cells was saturable at lower concentrations of lactate, indicating a carrier-dependent process (Dringen et al., 1995). This transport can be inhibited by the lactate transport inhibitors quercetin and alpha-cyano-4-hydroxycinnamate (CHC), which when used on C6 glioma cells prevented H^+-lactate efflux and decrease pH_i (Volk et al., 1997). More recently, identification of two specific lactate transporters, MCT1 (Froberg et al., 2001;Mac and Nalecz, 2003;Grillon et al., 2011;Miranda-Goncalves et al., 2013) and MCT4 (Grillon et al.,

2011;Miranda-Goncalves et al., 2013) in various types of brain tumors has provided molecular targets for disrupting brain tumor metabolism and pH_i regulation.

Vacuolar-type H^+-ATPase

Despite predominantly functioning as organellar proton pumps, there is evidence that V-ATPases translocate to the plasma membrane and regulate pH_i in brain tumors (Fig. 1). V-ATPase inhibitors such as bafilomycin A1 depolarized the membranes of NG108-15 neuroblastoma x glioma hybrid cells (Gerard et al., 1994;Gerard et al., 1998) and C6 glioma cells (Philippe et al., 2002). Additionally, this V-ATPase was tonically active and alkalinized C6 glioma cells at physiological pH_i (Volk et al., 1998). It should be noted, however, that plasma membrane expression of this proton pump is not limited to gliomas but also occurs in nontransformed astrocytes (Philippe et al., 2002). A more recent study has isolated the a4 isoform of the V0 subunit in human glioma samples, a subunit usually absent in normal human brain that is expressed in the kidney and epididymis (Gleize et al., 2012).

Aquaporins and carbonic anhydrases

Both of these protein types serve to facilitate a more rapid regulation of pH_i. Carbonic anhydrases do so by catalyzing the reversible interconversion of $CO_2 + H_2O$ and $HCO_3^- + H^+$, while aquaporins may be involved in the direct flux of CO_2 through the plasma membrane (Endeward et al., 2006;Hub and de Groot, 2006). Gliomas predominantly express carbonic anhydrase 9 (CAIX) and aquaporins 1 and 4 (AQP1 and AQP4). Aquaporins have also been shown to play roles in glioma cell adhesion

and maintenance of iso-osmolarity during volume regulation via H_2O flux (McCoy and Sontheimer, 2007). The direct role of these proteins in brain tumor pathophysiology is outside the scope of this review.

CONSEQUENCES OF pH_i REGULATION

The most direct (and obvious) consequence of pH_i regulation is pH_e alteration. The aforementioned mechanisms of pH_i regulation mostly act as intracellular alkalinizing agents, leading to a large proton efflux into the extracellular space (ECS). The magnitude of pH_i and pH_e changes depends on buffering capacity, total compartment volume, and molecular diffusivity (Chesler, 2003). These protons do not dissipate readily in the poorly perfused spaces within solid tumors, resulting in pH_e heterogeneity and pockets of increased acidity. Therefore, protons may serve as messenger molecules that alter both intratumoral and extratumoral physiology (Fig. 2). This section will both review known mechanisms of pH-directed pathophysiology in brain tumors as well as draw lessons from other solid tumor types.

Ion channel signaling

Brain tumors possess several pH-sensitive ion channels, including acid-sensing ion channels (ASICs), transient receptor potential channels (TRPs), two-pore potassium channels (K2Ps), purinergic receptors (P2XRs), and proton-sensing G-protein coupled receptors (GPCRs). Here we will briefly touch upon channel expression, subtype, and pH-sensitivity as discussed in brain tumor literature. For a broader view of pH-sensitive ion channels and cancer, see (Glitsch, 2011); for a more in-depth view of ion channels in brain tumors, see (Ding et al., 2012).

ASICs are cation-nonspecific (Na^+, K^+, and sometimes Ca^{2+}) ion channels that are usually opened by low pH_e and are transiently active. ASICs 1 and 2 have been shown to be expressed in human glioma cells (Berdiev et al., 2003), with sensitivity

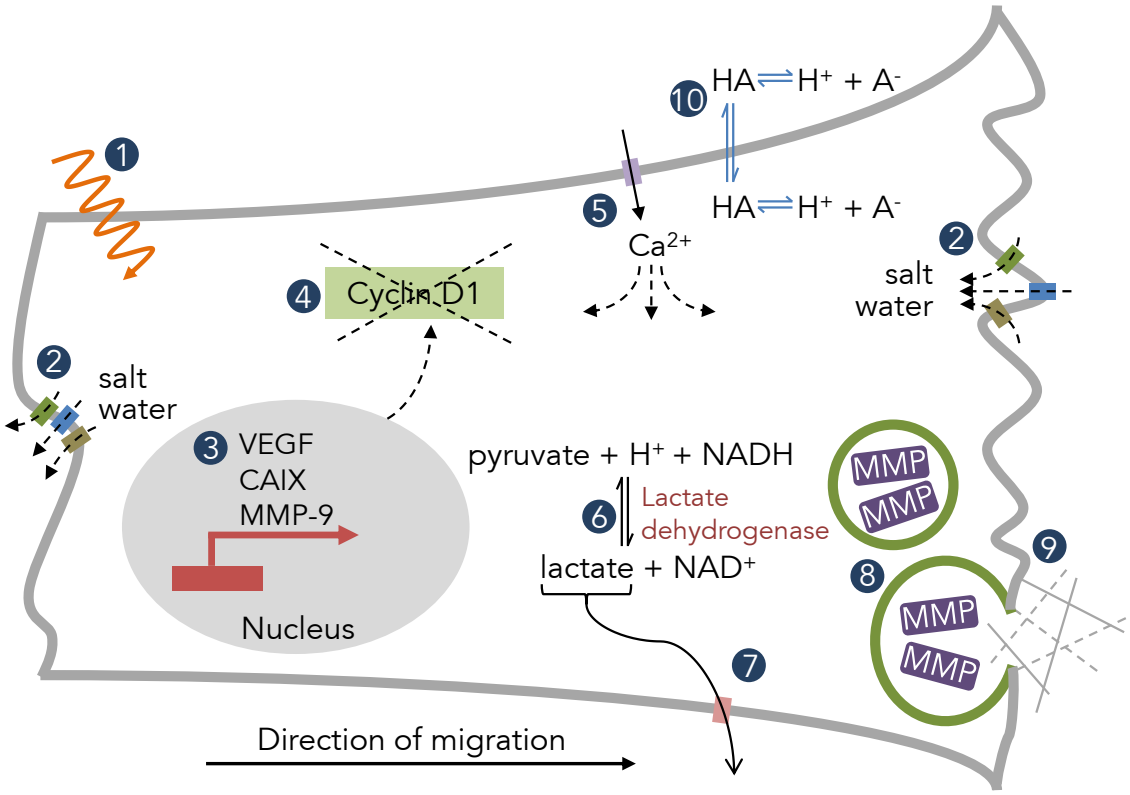

Figure 2. *Examples of pH-dependent physiology in solid tumors*. (1) Radiation efficacy. (2) Salt water flux via K^+, Cl^-, and H_2O channels. (3) Downstream expression patterns of tumorigenic genes. (4) Mislocalization of cyclin D1 and disruption of the cell cycle. (5) Ca^{2+} permeation through ion channels (ASIC, P2X, TRP) and subsequent downstream effects. (6) Metabolic enzyme activity. (7) H^+-coupled lactate efflux. (8) Vesicular fusion and protease enzymatic activity. (9) Interaction with the extracellular matrix. (10) Distribution of weak acids/bases.

to psalmotoxin 1 in addition to amiloride (Bubien et al., 2004). The Na^+ current derived from glioma ASIC expression contributes to their volume regulation (Ross et al., 2007) and migration (Vila-Carriles et al., 2006;Kapoor et al., 2009). Interestingly, a hybrid of ASIC and epithelial sodium channel (ENaC) subunits creates a basally active conductance (Kapoor et al., 2011) that affects glioma cell migration and cell cycle progression (Rooj et al., 2012). This hybrid channel is recruited to the plasma membrane in the face of acidic pH_e as found in the tumor core (Kapoor et al., 2011). Under acidotic conditions, the role of ASIC1a and ASIC2a seems paradoxical: ASIC1a knockdown prevents Ca^{2+}-mediated injury (Weng et al., 2007), while ASIC2a knockdown aggravates it (Liu et al., 2011).

TRPs are also cation-nonspecific channels, whose pH-sensitivities play a role in the proton-heavy environments of taste buds, pain receptors, and cancer cells. In brain tumor cells, the expression of TRPC channels has been especially tied to Ca^{2+} influx mediating changes in cell morphology and movement. This includes cytokinesis (Bomben and Sontheimer, 2008;Bomben and Sontheimer, 2010), Ca^{2+} mobilization (Nakao et al., 2008;Chigurupati et al., 2010), and cell migration (Chigurupati et al., 2010;Bomben et al., 2011). Unlike TRPC channels, TRPV channel expression tends to negatively affect glioma cells, leaving them vulnerable to capsaicin-induced apoptosis (Amantini et al., 2007) and chemotherapeutic cytotoxicity (Nabissi et al., 2013), as well as promoting differentiation (Morelli et al., 2012). Interestingly, neural precursor cells (NPCs) release endogenous TRPV agonists that prevent glioma cells from attacking the juvenile brain (Stock et al., 2012), a phenomenon that is lost with a loss of NPCs during aging.

P2XRs are ATP-gated cation channels, while P2YRs are purinergic-coupled GPCRs. Together, they are most extensively studied for their involvement in Ca^{2+} flux in glioma cell signal transduction, tumor progression, and cell death. In general, these receptors are proton-potentiated (Glitsch, 2011). For a comprehensive review of purinergic signaling in glioma cells, refer to (Barańska, 2013); for the pH-sensitivities of these channels, refer to (Stoop et al., 1997;Gerevich et al., 2007).

K2P channels and pH-sensitive GPCRs have not been studied extensively in brain tumor tissue, though their roles in other cancers have been elucidated (Sin et al., 2004;Innamaa et al., 2013). The K2P members TASK-1 and TASK-3, pH-sensitive background K^+ channels, have functional expression in human medulloblastoma cells (Ernest et al., 2010) and have been functionally implicated in glioma cell survival (Meuth et al., 2008). The pH-sensitive GPCRs OGR1 and G2A are also expressed in human medulloblastoma cells and regulate intracellular Ca^{2+} signaling in response to extracellular pH (Huang et al., 2008).

Volume regulation and cell movement

Gliomas are highly invasive, quickly seeding the brain with satellite tumors. This is especially impressive in the crowded brain space and requires a coordinated effort of cell shrinkage, process extension, and path-clearing. Volume regulation is a vital component of the first two functions and requires salt water flux (cation + anion + H_2O; Fig. 2) (Sontheimer, 2008;Watkins and Sontheimer, 2011). Two of the most well-studied ion channels in glioma cell migration, BK for K^+ ions and ClC-3 for Cl^- ions, are pH-sensitive. More specifically, low pH_e blocks both channels, while low pH_i stimulates BK channels, all within a physiological range of pH 6-8 (Avdonin et

al., 2003;Brelidze and Magleby, 2004;Matsuda et al., 2008;Matsuda et al., 2010). Additionally, as described beforehand, proton flux through glioma cells is directly tied to osmotically-active Na^+ and lactate, which both then contribute to volume regulation (Jakubovicz and Klip, 1989;Staub et al., 1990). Thus, protons can both directly and indirectly contribute to glioma cell volume regulation, which then affects cell movement.

Proton concentrations also both shape and orient tumor cells. This has been most thoroughly studied regarding NHE in melanoma cells, though gliomas similarly possess increased NHE1 activity versus their nontransformed counterparts (McLean 2000) with specific microdomain localization (Willoughby et al., 2005). In melanoma cells, NHE1 creates a local pH gradient that dominates the bulk solution pH and orients the cells via pH-dependence of integrin $\alpha2\beta1$ stickiness (Stock et al., 2005;Stuwe et al., 2007;Martin et al., 2011). Intracellularly, NHE1 also organizes the cytoskeleton of cells. For instance, the Rho GTPase Cdc42 recruits NHE1 to the leading edge of the cell, increasing leading edge pH_i and activating Cdc42 via a guanine nucleotide exchange factor, thus maintaining polarized cytoskeletal growth (Frantz et al., 2007). Similarly, cortactin phosphorylation recruits NHE1 to the invadopodium, where it alkalinizes pH_i and induces actin polymerization via cortactin release of cofilin (Magalhaes et al., 2011), thus playing an integral role in invadopodium protrusion/retraction cycling. NHE1 is further activated at the invadopodium by p90 ribosomal S6 kinase under hypoxic conditions (Lucien et al., 2011).

Tissue destruction

Brain tumors also cause direct destruction of surrounding tissue, including both neuronal death via glutamate excitotoxicity (Ye and Sontheimer, 1999) and degradation of the extracellular matrix via metalloproteinases (MMPs) and other proteases (Nakada et al., 2003). It is well-established that protease activity is pH-dependent (Fasciglione et al., 2000;Gioia et al., 2010). Additionally, however, acidic pH_e both induces MMP-9 expression (Kato et al., 2005) and enhances the rupture of protease-containing vesicles (Taraboletti et al., 2006), hinting at acidosis driving tumor invasion (Fig. 2). RNAi inhibition of MMP-9 and the protease cathepsin B dramatically reduced tumor pathogenicity of gliomas both *in vitro* and *in vivo* (Lakka et al., 2004).

Here again NHE1 plays a role. While in the intracellular compartment NHE1-dependent alkalinization coordinates tumor cell invasion, in the extracellular compartment the consequent acidification is essential for proteolysis of the extracellular matrix (Busco et al., 2010). Interestingly, preventing ion translocation through NHE1 alone was sufficient to alter the gene profile of mammalian fibroblasts, including a decrease in MMP-9 expression (Putney and Barber, 2004).

Finally, the excitotoxic process is itself pH-dependent. Excitatory amino acid transporter 2 (EAAT-2), expressed in low-grade brain tumors (de Groot et al., 2005), cotransports protons along with glutamate and thus is pH-dependent (Vandenberg et al., 1998). The alanine-cysteine-serine transporter 2 (ASCT2) also transports glutamate, and it has shown pH-dependence in C6 glioma cells (Dolińska et al., 2003). Lastly, the NMDA glutamate receptors in part responsible for neuronal excitotoxicity are inhibited by protons (Traynelis and Cull-Candy, 1990).

Metabolic activity

Gliomas, like most other cancers, demonstrate the Warburg effect – a preference for glycolysis over oxidative phosphorylation even in the presence of ample oxygen. This leads to increased intracellular lactate buildup, which is cleared via the cotransport of lactate and protons via MCTs (Fig. 2). Thus, inhibition of these cotransporters via drug or decreased pH_e both decreases pH_i (Volk et al., 1997) and increases intracellular lactate levels (Lomneth et al., 1990). As many glycolytic enzymes prefer the slightly alkaline pH_i of glioma cells – lactate dehydrogenase displays maximal activity at pH_i 7.5 while phosphofructokinase 1 works best between pH_i 7.0 and 7.5 (Webb et al., 2011) – there is an intimate coupling of glioma pH regulation and cell metabolism. This connection likely governs the expression patterns of pH-associated proteins across the glioma mass (Grillon et al., 2011).

Cell signaling

It is often difficult to separate the consequences of the various conditions found within a tumor; levels of CO_2, O_2, lactate, waste products, and pH distribute through the tumor heterogeneously, and all can influence the cellular phenotype. A few studies have specifically implicated acidosis in an alteration of glioma cell state. For instance, a pH_e of 6.6 upregulated VEGF mRNA and protein expression in human GBM cells via the ERK1/2 MAPK signaling cascade (Xu et al., 2002). Acidosis (pH_e 6.5) also maintained the stemness of glioma cells as determined both by stem cell markers and cellular phenotype via hypoxia inducible factor 2α (HIF2α) signaling (Hjelmeland et al., 2011). Acyl-CoA synthetase 5 (ACSL5) promotes glioma cell survival under low pH_e conditions through midkine (MDK) signaling (Mashima et al.,

2009). CA IX, known to be upregulated during times of hypoxia via the HIF1α pathway (Wykoff et al., 2000), is also upregulated by low pH_e independent of hypoxia in GBM cells via the same pathway (Ihnatko et al., 2006). Finally, very low pH_e (6.0) arrested glioma cells in the G_1 phase of the cell cycle as a downstream result of cyclin D_1 mislocalization (Fig. 2) and degradation in T98G human glioma cells (Schnier et al., 2008).

Therapy sensitivity

A heterogeneous pH environment creates a moving target for both radiation and chemotherapeutics. Weak base and weak acid drugs find themselves confined to either the intracellular or extracellular spaces (Fig. 2), depending on pH_e and pH_i, in a phenomenon known as "ion trapping" (Raghunand and Gillies, 2000). This can result in heterogeneous drug potency across the tumor mass, and has led to efforts to either acidify or alkalinize the tumor in an attempt to localize chemotherapeutics to either the intra- or extracellular compartment. In gliomas, mild acidosis inhibits cell growth while protecting cells from chemotherapeutic cytotoxicity (Reichert et al., 2002). Attempts have been made to artificially alkalinize solid tumors with $NaHCO_3$-induced metabolic alkalosis to enhance weak base uptake (Raghunand et al., 2001), though none of these studies have yet been performed in brain tumors. pH also can affect the radiosensitivity of cells (Bosi et al., 1991), though its effect on glioma cells appears inconsistent (Reichert et al., 2002).

With highly buffered ions such as Ca^{2+} and protons, nanomolar changes in the free ion concentration equate to severalfold shifts and drastic changes in central nervous system (CNS) signaling. It is this context that separates brain tumors from

other solid tumors – the pathophysiological implications of large pH heterogeneity in a susceptible environment are greater than in many other, more robust organs. This also leads to great opportunity – brain tumors lean heavily on pH regulation to continue their growth and invasion, and thus disruption of proton transport could devastate tumor function while leaving normal tissue relatively unharmed.

CONFLICT OF INTEREST STATEMENT

The authors declare that the research was conducted in the absence of any commercial or financial relationships that could be construed as a potential conflict of interest.

REFERENCES

Acker, H., Holtermann, G., Bolling, B., and Carlsson, J. (1992). Influence of glucose on metabolism and growth of rat glioma cells (C6) in multicellular spheroid culture. Int. J. Cancer 52, 279–285. doi: 10.1002/ijc.2910520221

Aickin, C. C., and Thomas, R. C. (1977). An investigation of the ionic mechanism of intracellular pH regulation in mouse soleus muscle fibres. J. Physiol. 273, 295–316.

Amantini, C., Mosca, M., Nabissi, M., Lucciarini, R., Caprodossi, S., Arcella, A., et al. (2007). Capsaicin-induced apoptosis of glioma cells is mediated by TRPV1 vanilloid receptor and requires p38 MAPK activation. J. Neurochem. 102, 977–990. doi: 10.1111/j.1471-4159.2007.04582.x

Avdonin, V., Tang, X. D., and Hoshi, T. (2003). Stimulatory action of internal protons on Slo1 BK channels. Biophys. J. 84, 2969–2980. doi: 10.1016/S0006-3495(03)70023-X

Barañska, J. (2013). Glioma Signaling. Dordrecht: Springer. doi: 10.1007/978-94-007-4719-7

Berdiev, B. K., Xia, J., McLean, L. A., Markert, J. M., Gillespie, G. Y., Mapstone, T. B., et al. (2003). Acid-sensing ion channels in malignant gliomas. J. Biol. Chem. 278, 15023–15034. doi: 10.1074/jbc.M300991200

Bevensee, M. O., and Boron, W. F. (2013). "Control of intracellular pH," in Seldin and Giebisch's The Kidney 5th Edn., Chapter 52, eds R. J. Alpern, O. W. Moe, and M. Caplan (Oxford: Academic Press), 1773–1835.

Blough, M. D., Al-Najjar, M., Chesnelong, C., Binding, C. E., Rogers, A. D., Luchman, H. A., et al. (2012). DNA hypermethylation and 1p Loss silence NHE-1 in oligodendroglioma. Ann. Neurol. 71, 845–849. doi: 10.1002/ana.23610

Bomben, V. C., and Sontheimer, H. (2010). Disruption of transient receptor potential canonical channel 1 causes incomplete cytokinesis and slows the growth of human malignant gliomas. Glia 58, 1145–1156. doi: 10.1002/glia.20994

Bomben, V. C., and Sontheimer, H. W. (2008). Inhibition of transient receptor potential canonical channels impairs cytokinesis in human malignant gliomas. Cell Prolif. 41, 98–121. doi: 10.1111/j.1365-2184.2007.00504.x

Bomben, V. C., Turner, K. L., Barclay, T. T., and Sontheimer, H. (2011). Transient receptor potential canonical channels are essential for chemotactic migration of human malignant gliomas. J. Cell. Physiol. 226, 1879–1888. doi: 10.1002/jcp.22518

Bosi, A., Micheli, A., Pietrosanti, S., and Olivieri, G. (1991). Effect of pH shifts on radiosensitivity of human lymphocytes irradiated in the G2 stage. Mutat. Res. 250, 325–329. doi: 10.1016/0027-5107(91)90188-T

Brelidze, T. I., and Magleby, K. L. (2004). Protons block BK channels by competitive inhibition with K+ and contribute to the limits of unitary currents at high voltages. J. Gen. Physiol. 123, 305–319. doi: 10.1085/jgp.200308951

Bubien, J. K., Ji, H. L., Gillespie, G. Y., Fuller, C. M., Markert, J. M., Mapstone, T. B., et al. (2004). Cation selectivity and inhibition of malignant glioma Na+ channels by Psalmotoxin 1. Am. J. Physiol. Cell Physiol. 287, C1282–C1291. doi: 10.1152/ajpcell.00077.2004

Busco, G., Cardone, R. A., Greco, M. R., Bellizzi, A., Colella, M., Antelmi, E., et al. (2010). NHE1 promotes invadopodial ECM proteolysis through acidification of the peri-invadopodial space. FASEB J. 24, 3903–3915. doi: 10.1096/fj.09-149518

Charles, N. A., Holland, E. C., Gilbertson, R., Glass, R., and Kettenmann, H. (2011). The brain tumor microenvironment. Glia 59, 1169–1180. doi: 10.1002/glia.21136

Chesler, M. (2003). Regulation and modulation of pH in the brain. Physiol. Rev. 83, 1183–1221. doi: 10.1152/physrev.00010.2003

Chigurupati, S., Venkataraman, R., Barrera, D., Naganathan, A., Madan, M., Paul, L., et al. (2010). Receptor channel TRPC6 is a key mediator of Notch-driven glioblastoma growth and invasiveness. Cancer Res. 70, 418–427. doi: 10.1158/0008-5472.CAN-09-2654

De Groot, J. F., Liu, T. J., Fuller, G., and Yung, W. K. A. (2005). The excitatory amino acid transporter-2 induces apoptosis and decreases glioma growth In vitro and In vivo. Cancer Res. 65, 1934–1940. doi: 10.1158/0008-5472.CAN-04-3626

Ding, X., He, H., Lu, Y., and Wang, Y. (2012). Ionic Channels in the Therapy of Malignant Glioma, Shanghai: InTech.

Doliñska, M., Dybel, A., Zabłocka, B., and Albrecht, J. (2003). Glutamine transport in C6 glioma cells shows ASCT2 system characteristics. Neurochem. Int. 43, 501–507. doi: 10.1016/S0197-0186(03)00040-8

Dringen, R., Peters, H., Wiesinger, H., and Hamprecht, B. (1995). Lactate transport in cultured glial cells. Dev. Neurosci. 17, 63–69. doi: 10.1159/000111275

Endeward, V., Musa-Aziz, R., Cooper, G. J., Chen, L. M., Pelletier, M. F., Virkki, L. V., et al. (2006). Evidence that aquaporin 1 is a major pathway for CO2 transport across the human erythrocyte membrane. FASEB J. 20, 1974–1981. doi: 10.1096/fj.04-3300com

Ernest, N. J., Logsdon, N. J., McFerrin, M. B., Sontheimer, H., and Spiller, S. E. (2010). Biophysical properties of human medulloblastoma cells. J. Membr. Biol. 237, 59–69. doi: 10.1007/s00232-010-9306-x

Fasciglione, G. F., Marini, S., D'alessio, S., Politi, V., and Coletta, M. (2000). pH- and temperature-dependence of functional modulation in metalloproteinases. A

comparison between neutrophil collagenase and gelatinases A and B. Biophys. J. 79, 2138–2149. doi: 10.1016/S0006-3495(00)76461-7

Frantz, C., Karydis, A., Nalbant, P., Hahn, K. M., and Barber, D. L. (2007). Positive feedback between Cdc42 activity and H+ efflux by the Na-H exchanger NHE1 for polarity of migrating cells. J. Cell Biol. 179, 403–410. doi: 10.1083/jcb.200704169

Froberg, M. K., Gerhart, D. Z., Enerson, B. E., Manivel, C., Guzman-Paz, M., Seacotte, N., et al. (2001). Expression of monocarboxylate transporter MCT1 in normal and neoplastic human CNS tissues. Neuroreport 12, 761–765. doi: 10.1097/00001756-200103260-00030

Gerard, V., Rouzaire-Dubois, B., Dilda, P., and Dubois, J. M. (1998). Alterations of ionic membrane permeabilities in multidrug-resistant neuroblastoma x glioma hybrid cells. J. Exp. Biol. 201, 21–31.

Gerard, V., Rouzaire-Dubois, B., and Dubois, J. M. (1994). Contribution of a H+ pump in determining the resting potential of neuroblastoma cells. J. Membr. Biol. 137, 119–125. doi: 10.1007/BF00233481

Gerevich, Z., Zadori, Z. S., Koles, L., Kopp, L., Milius, D., Wirkner, K., et al. (2007). Dual effect of acid pH on purinergic P2X3 receptors depends on the histidine 206 residue. J. Biol. Chem. 282, 33949–33957. doi: 10.1074/jbc.M705840200

Gioia, M., Fasciglione, G. F., Monaco, S., Iundusi, R., Sbardella, D., Marini, S., et al. (2010). pH dependence of the enzymatic processing of collagen I by MMP-1 (fibroblast collagenase), MMP-2 (gelatinase A), and MMP-14 ectodomain. J. Biol. Inorg. Chem. 15, 1219–1232. doi: 10.1007/s00775-010-0680-8

Gleize, V., Boisselier, B., Marie, Y., Poea-Guyon, S., Sanson, M., and Morel, N. (2012). The renal v-ATPase a4 subunit is expressed in specific subtypes of human gliomas. Glia 60, 1004–1012. doi: 10.1002/glia.22332

Glitsch, M. (2011). Protons and Ca2+: ionic allies in tumor progression? Physiology 26, 252–265. doi: 10.1152/physiol.00005.2011

Glunde, K., Dussmann, H., Juretschke, H. P., and Leibfritz, D. (2002). Na(+)/H(+) exchange subtype 1 inhibition during extracellular acidification and hypoxia in glioma cells. J. Neurochem. 80, 36–44. doi: 10.1046/j.0022-3042.2001.00661.x

Grillon, E., Farion, R., Fablet, K., De Waard, M., Tse, C. M., Donowitz, M., et al. (2011). The spatial organization of proton and lactate transport in a rat brain tumor. PLoS ONE 6:e17416. doi: 10.1371/journal.pone.0017416

Grobben, B., De Deyn, P. P., and Slegers, H. (2002). Rat C6 glioma as experimental model system for the study of glioblastoma growth and invasion. Cell Tissue Res. 310, 257–270. doi: 10.1007/s00441-002-0651-7

Hegde, M., Roscoe, J., Cala, P., and Gorin, F. (2004). Amiloride kills malignant glioma cells independent of its inhibition of the sodium-hydrogen exchanger. J. Pharmacol. Exp. Ther. 310, 67–74. doi: 10.1124/jpet.103.065029

Hertel, C., and Staehelin, M. (1983). Reappearance of beta-adrenergic receptors after isoproterenol treatment in intact C6-cells. J. Cell Biol. 97, 1538–1543. doi: 10.1083/jcb.97.5.1538

Hjelmeland, A. B., Wu, Q., Heddleston, J. M., Choudhary, G. S., Macswords, J., Lathia, J. D., et al. (2011). Acidic stress promotes a glioma stem cell phenotype. Cell Death Differ. 18, 829–840. doi: 10.1038/cdd.2010.150

Huang, W. C., Swietach, P., Vaughan-Jones, R. D., Ansorge, O., and Glitsch, M. D. (2008). Extracellular acidification elicits spatially and temporally distinct Ca2+ signals. Curr. Biol. 18, 781–785. doi: 10.1016/j.cub.2008.04.049

Hub, J. S., and De Groot, B. L. (2006). Does CO2 permeate through aquaporin-1? Biophys. J. 91, 842–848. doi: 10.1529/biophysj.106.081406

Ihnatko, R., Kubes, M., Takacova, M., Sedlakova, O., Sedlak, J., Pastorek, J., et al. (2006). Extracellular acidosis elevates carbonic anhydrase IX in human glioblastoma cells via transcriptional modulation that does not depend on hypoxia. Int. J. Oncol. 29, 1025–1033.

Innamaa, A., Jackson, L., Asher, V., Van Schalkwyk, G., Warren, A., Keightley, A., et al. (2013). Expression and effects of modulation of the K2P potassium channels TREK-1 (KCNK2) and TREK-2 (KCNK10) in the normal human ovary and epithelial ovarian cancer. Clin. Transl. Oncol. 15, 910–918. doi: 10.1007/s12094-013-1022-4

Irani, D. N. (2008). Cerebrospinal Fluid in Clinical Practice. Philadelphia: Elsevier Health Sciences.

Isom, L. L., Cragoe, E. J. Jr., and Limbird, L. E. (1987a). Alpha 2-adrenergic receptors accelerate Na+/H+ exchange in neuroblastoma X glioma cells. J. Biol. Chem. 262, 6750–6757.

Isom, L. L., Cragoe, E. J. Jr., and Limbird, L. E. (1987b). Multiple receptors linked to inhibition of adenylate cyclase accelerate Na+/H+ exchange in neuroblastoma x glioma cells via a mechanism other than decreased cAMP accumulation. J. Biol. Chem. 262, 17504–17509.

Jakubovicz, D. E., Grinstein, S., and Klip, A. (1987). Cell swelling following recovery from acidification in C6 glioma cells: an in vitro model of postischemic brain edema. Brain Res. 435, 138–146. doi: 10.1016/0006-8993(87)91594-0

Jakubovicz, D. E., and Klip, A. (1989). Lactic acid-induced swelling in C6 glial cells via Na+/H+ exchange. Brain Res. 485, 215–224. doi: 10.1016/0006-8993(89)90564-7

Kapoor, N., Bartoszewski, R., Qadri, Y. J., Bebok, Z., Bubien, J. K., Fuller, C. M., et al. (2009). Knockdown of ASIC1 and epithelial sodium channel subunits inhibits glioblastoma whole cell current and cell migration. J. Biol. Chem. 284, 24526–24541. doi: 10.1074/jbc.M109.037390

Kapoor, N., Lee, W., Clark, E., Bartoszewski, R., McNicholas, C. M., Latham, C. B., et al. (2011). Interaction of ASIC1 and ENaC subunits in human glioma cells and rat astrocytes. Am. J. Physiol. Cell Physiol. 300, C1246–C1259. doi: 10.1152/ajpcell.00199.2010

Kato, Y., Lambert, C. A., Colige, A. C., Mineur, P., Noel, A., Frankenne, F., et al. (2005). Acidic extracellular pH induces matrix metalloproteinase-9 expression in mouse metastatic melanoma cells through the phospholipase D-mitogen-activated protein kinase signaling. J. Biol. Chem. 280, 10938–10944. doi: 10.1074/jbc.M411313200

Kempski, O., Staub, F., Jansen, M., and Baethmann, A. (1990). Molecular mechanisms of glial cell swelling in acidosis. Adv. Neurol. 52, 39–45.

Kempski, O., Staub, F., Jansen, M., Schodel, F., and Baethmann, A. (1988). Glial swelling during extracellular acidosis in vitro. Stroke 19, 385–392. doi: 10.1161/01.STR.19.3.385

Kislin, K. L., McDonough, W. S., Eschbacher, J. M., Armstrong, B. A., and Berens, M. E. (2009). NHERF-1: modulator of glioblastoma cell migration and invasion. Neoplasia 11, 377–387.

Lakka, S. S., Gondi, C. S., Yanamandra, N., Olivero, W. C., Dinh, D. H., Gujrati, M., et al. (2004). Inhibition of cathepsin B and MMP-9 gene expression in glioblastoma cell line via RNA interference reduces tumor cell invasion, tumor growth and angiogenesis. Oncogene 23, 4681–4689. doi: 10.1038/sj.onc.1207616

Liu, X. Y., Zhang, S. Z., Ma, X. Y., Wang, H., Wu, B. H., Sun, H. L., et al. (2011). Knockdown of ASIC2a subunit aggravates injury of rat C6 glioma cells in acidosis. J. Physiol. Biochem. 67, 275–281. doi: 10.1007/s13105-010-0060-4

Lomneth, R., Medrano, S., and Gruenstein, E. I. (1990). The role of transmembrane pH gradients in the lactic acid induced swelling of astrocytes. Brain Res. 523, 69–77. doi: 10.1016/0006-8993(90)91636-U

Lucien, F., Brochu-Gaudreau, K., Arsenault, D., Harper, K., and Dubois, C. M. (2011). Hypoxia-induced invadopodia formation involves activation of NHE-1 by the p90 ribosomal S6 kinase (p90RSK). PLoS ONE 6:e28851. doi: 10.1371/journal.pone.0028851

Lui, C. P., Fung, K. P., Kong, S. K., Choy, Y. M., and Lee, C. Y. (1995). Effect of hyperthermia on intracellular pH in human U-87 MG glioblastoma cells. Oncology 52, 492–497. doi: 10.1159/000227517

Lust, W. D., Schwartz, J. P., and Passonneau, J. V. (1975). Glycolytic metabolism in cultured cells of the nervous system. I. Glucose transport and metabolism in the C-6 glioma cell line. Mol. Cell. Biochem. 8, 169–176. doi: 10.1007/BF01792767

Mac, M., and Nalecz, K. A. (2003). Expression of monocarboxylic acid transporters (MCT) in brain cells. Implication for branched chain alpha-ketoacids transport in neurons. Neurochem. Int. 43, 305–309. doi: 10.1016/S0197-0186(03)00016-0

Magalhaes, M. A., Larson, D. R., Mader, C. C., Bravo-Cordero, J. J., Gil-Henn, H., Oser, M., et al. (2011). Cortactin phosphorylation regulates cell invasion through a pH-dependent pathway. J. Cell Biol. 195, 903–920. doi: 10.1083/jcb.201103045

Martin, C., Pedersen, S. F., Schwab, A., and Stock, C. (2011). Intracellular pH gradients in migrating cells. Am. J. Physiol. Cell Physiol. 300, C490–C495. doi: 10.1152/ajpcell.00280.2010

Mashima, T., Sato, S., Sugimoto, Y., Tsuruo, T., and Seimiya, H. (2009). Promotion of glioma cell survival by acyl-CoA synthetase 5 under extracellular acidosis conditions. Oncogene 28, 9–19. doi: 10.1038/onc.2008.355

Matsuda, J. J., Filali, M. S., Collins, M. M., Volk, K. A., and Lamb, F. S. (2010). The ClC-3 Cl-/H+ antiporter becomes uncoupled at low extracellular pH. J. Biol. Chem. 285, 2569–2579. doi: 10.1074/jbc.M109.018002

Matsuda, J. J., Filali, M. S., Volk, K. A., Collins, M. M., Moreland, J. G., and Lamb, F. S. (2008). Overexpression of CLC-3 in HEK293T cells yields novel currents that are pH dependent. Am. J. Physiol. Cell Physiol. 294, C251–C262. doi: 10.1152/ajpcell.00338.2007

McCoy, E., and Sontheimer, H. (2007). Expression and function of water channels (aquaporins) in migrating malignant astrocytes. Glia 55, 1034–1043. doi: 10.1002/glia.20524

McLean, L. A., Roscoe, J., Jorgensen, N. K., Gorin, F. A., and Cala, P. M. (2000). Malignant gliomas display altered pH regulation by NHE1 compared with nontransformed astrocytes. Am. J. Physiol. Cell Physiol. 278, C676–C688.

Meuth, S. G., Herrmann, A. M., Ip, C. W., Kanyshkova, T., Bittner, S., Weishaupt, A., et al. (2008). The two-pore domain potassium channel TASK3 functionally impacts glioma cell death. J. Neurooncol. 87, 263–270. doi: 10.1007/s11060-008-9517-5

Miranda-Goncalves, V., Honavar, M., Pinheiro, C., Martinho, O., Pires, M. M., Pinheiro, C., et al. (2013). Monocarboxylate transporters (MCTs) in gliomas: expression and exploitation as therapeutic targets.Neurooncology 15, 172–188. doi: 10.1093/neuonc/nos298

Morelli, M. B., Nabissi, M., Amantini, C., Farfariello, V., Ricci-Vitiani, L., Di Martino, S., et al. (2012). The transient receptor potential vanilloid-2 cation channel impairs

glioblastoma stem-like cell proliferation and promotes differentiation. Int. J. Cancer 131, E1067–E1077. doi: 10.1002/ijc.27588

Mountian, I., Chou, K. Y., and Van Driessche, W. (1996). Electrolyte transport mechanisms involved in regulatory volume increase in C6 glioma cells. Am. J. Physiol. 271, C1041–C1048.

Nabissi, M., Morelli, M. B., Santoni, M., and Santoni, G. (2013). Triggering of the TRPV2 channel by cannabidiol sensitizes glioblastoma cells to cytotoxic chemotherapeutic agents. Carcinogenesis 34, 48–57. doi: 10.1093/carcin/bgs328

Nakada, M., Okada, Y., and Yamashita, J. (2003). The role of matrix metalloproteinases in glioma invasion. Front. Biosci. 8:e261–269. doi: 10.2741/1016

Nakao, K., Shirakawa, H., Sugishita, A., Matsutani, I., Niidome, T., Nakagawa, T., et al. (2008). Ca2+ mobilization mediated by transient receptor potential canonical 3 is associated with thrombin-induced morphological changes in 1321N1 human astrocytoma cells. J. Neurosci. Res. 86, 2722–2732. doi: 10.1002/jnr.21711

Neve, K. A., Kozlowski, M. R., and Rosser, M. P. (1992). Dopamine D2 receptor stimulation of Na+/H+ exchange assessed by quantification of extracellular acidification. J. Biol. Chem. 267, 25748–25753.

Nunnari, J. M., Repaske, M. G., Brandon, S., Cragoe, E. J. Jr., and Limbird, L. E. (1987). Regulation of porcine brain alpha 2-adrenergic receptors by Na+,H+ and inhibitors of Na+/H+ exchange. J. Biol. Chem. 262, 12387–12392.

Philippe, J. M., Dubois, J. M., Rouzaire-Dubois, B., Cartron, P. F., Vallette, F., and Morel, N. (2002). Functional expression of V-ATPases in the plasma membrane of glial cells. Glia 37, 365–373. doi: 10.1002/glia.10041

Putney, L. K., and Barber, D. L. (2004). Expression profile of genes regulated by activity of the Na-H exchanger NHE1. BMC Genomics 5:46. doi: 10.1186/1471-2164-5-46

Raghunand, N., and Gillies, R. J. (2000). pH and drug resistance in tumors. Drug Resist. Updat. 3, 39–47. doi: 10.1054/drup.2000.0119

Raghunand, N., Mahoney, B., Van Sluis, R., Baggett, B., and Gillies, R. J. (2001). Acute metabolic alkalosis enhances response of C3H mouse mammary tumors to the weak base mitoxantrone. Neoplasia 3, 227–235. doi: 10.1038/sj.neo.7900151

Reichert, M., Steinbach, J. P., Supra, P., and Weller, M. (2002). Modulation of growth and radiochemosensitivity of human malignant glioma cells by acidosis. Cancer 95, 1113–1119. doi: 10.1002/cncr.10767

Rooj, A. K., McNicholas, C. M., Bartoszewski, R., Bebok, Z., Benos, D. J., and Fuller, C. M. (2012). Glioma-specific cation conductance regulates migration and cell cycle progression. J. Biol. Chem. 287, 4053–4065. doi: 10.1074/jbc.M111.311688

Ross, S. B., Fuller, C. M., Bubien, J. K., and Benos, D. J. (2007). Amiloride-sensitive Na+ channels contribute to regulatory volume increases in human glioma cells. Am. J. Physiol. Cell Physiol. 293, C1181–C1185. doi: 10.1152/ajpcell.00066.2007

Schnier, J. B., Nishi, K., Harley, W. R., and Gorin, F. A. (2008). An acidic environment changes cyclin D1 localization and alters colony forming ability in gliomas. J. Neurooncol. 89, 19–26. doi: 10.1007/s11060-008-9591-8

Shrode, L. D., and Putnam, R. W. (1994). Intracellular pH regulation in primary rat astrocytes and C6 glioma cells.Glia 12, 196–210. doi: 10.1002/glia.440120305

Sin, W. C., Zhang, Y., Zhong, W., Adhikarakunnathu, S., Powers, S., Hoey, T., et al. (2004). G protein-coupled receptors GPR4 and TDAG8 are oncogenic and overexpressed in human cancers. Oncogene 23, 6299–6303. doi: 10.1038/sj.onc.1207838

Sontheimer, H. (2008). An unexpected role for ion channels in brain tumor metastasis. Exp. Biol. Med. 233, 779–791. doi: 10.3181/0711-MR-308

Staub, F., Baethmann, A., Peters, J., Weigt, H., and Kempski, O. (1990). Effects of lactacidosis on glial cell volume and viability. J. Cereb. Blood Flow Metab. 10, 866–876. doi: 10.1038/jcbfm.1990.143

Staub, F., Mackert, B., Kempski, O., Haberstok, J., Peters, J., and Baethmann, A. (1994). Swelling and damage to nerves and glial cells by acidosis. Anasthesiol. Intensivmed. Notfallmed. Schmerzther. 29, 203–209. doi: 10.1055/s-2007-996719

Stock, C., Gassner, B., Hauck, C. R., Arnold, H., Mally, S., Eble, J. A., et al. (2005). Migration of human melanoma cells depends on extracellular pH and Na+/H+ exchange. J. Physiol. 567, 225–238. doi: 10.1113/jphysiol.2005.088344

Stock, K., Kumar, J., Synowitz, M., Petrosino, S., Imperatore, R., Smith, E. S., et al. (2012). Neural precursor cells induce cell death of high-grade astrocytomas through stimulation of TRPV1. Nat. Med. 18, 1232–1238. doi: 10.1038/nm.2827

Stoop, R., Surprenant, A., and North, R. A. (1997). Different sensitivities to pH of ATP-induced currents at four cloned P2X receptors. J. Neurophysiol. 78, 1837–1840.

Stuwe, L., Muller, M., Fabian, A., Waning, J., Mally, S., Noel, J., et al. (2007). pH dependence of melanoma cell migration: protons extruded by NHE1 dominate protons of the bulk solution. J. Physiol. 585, 351–360. doi: 10.1113/jphysiol.2007.145185

Taraboletti, G., D'ascenzo, S., Giusti, I., Marchetti, D., Borsotti, P., Millimaggi, D., et al. (2006). Bioavailability of VEGF in tumor-shed vesicles depends on vesicle burst induced by acidic pH. Neoplasia 8, 96–103. doi: 10.1593/neo.05583

Tomsig, J. L., Gruenstein, E., and Dimlich, R. V. (1991). Inhibition of lactate-induced swelling by dichloroacetate in human astrocytoma cells. Brain Res. 568, 92–100. doi: 10.1016/0006-8993(91)91383-C

Traynelis, S. F., and Cull-Candy, S. G. (1990). Proton inhibition of N-methyl-D-aspartate receptors in cerebellar neurons. Nature 345, 347–350. doi: 10.1038/345347a0

Vandenberg, R. J., Mitrovic, A. D., and Johnston, G. A. (1998). Serine-O-sulphate transport by the human glutamate transporter, EAAT2. Br. J. Pharmacol. 123, 1593–1600. doi: 10.1038/sj.bjp.0701776

Vila-Carriles, W. H., Kovacs, G. G., Jovov, B., Zhou, Z. H., Pahwa, A. K., Colby, G., et al. (2006). Surface expression of ASIC2 inhibits the amiloride-sensitive current and migration of glioma cells. J. Biol. Chem. 281, 19220–19232. doi: 10.1074/jbc.M603100200

Vlashi, E., Lagadec, C., Vergnes, L., Matsutani, T., Masui, K., Poulou, M., et al. (2011). Metabolic state of glioma stem cells and nontumorigenic cells. Proc. Natl. Acad. Sci. U.S.A. 108, 16062–16067. doi: 10.1073/pnas.1106704108

Volk, C., Albert, T., and Kempski, O. S. (1998). A proton-translocating H+-ATPase is involved in C6 glial pH regulation. Biochim. Biophys. Acta 1372, 28–36. doi: 10.1016/S0005-2736(98)00044-3

Volk, C., Kempski, B., and Kempski, O. S. (1997). Inhibition of lactate export by quercetin acidifies rat glial cells in vitro. Neurosci. Lett. 223, 121–124. doi: 10.1016/S0304-3940(97)13420-6

Watkins, S., and Sontheimer, H. (2011). Hydrodynamic cellular volume changes enable glioma cell invasion. J. Neurosci. 31, 17250–17259. doi: 10.1523/JNEUROSCI.3938-11.2011

Watkins, S., and Sontheimer, H. (2012). Unique biology of gliomas: challenges and opportunities. Trends Neurosci. 35, 546–556. doi: 10.1016/j.tins.2012.05.001

Webb, B. A., Chimenti, M., Jacobson, M. P., and Barber, D. L. (2011). Dysregulated pH: a perfect storm for cancer progression. Nat. Rev. Cancer 11, 671–677. doi: 10.1038/nrc3110

Weng, X. C., Zheng, J. Q., Li, J., and Xiao, W. B. (2007). Underlying mechanism of ASIC1a involved in acidosis-induced cytotoxicity in rat C6 glioma cells. Acta Pharmacol. Sin. 28, 1731–1736. doi: 10.1111/j.1745-7254.2007.00708.x

Willoughby, D., Masada, N., Crossthwaite, A. J., Ciruela, A., and Cooper, D. M. (2005). Localized Na+/H+ exchanger 1 expression protects Ca2+-regulated adenylyl cyclases from changes in intracellular pH. J. Biol. Chem. 280, 30864–30872. doi: 10.1074/jbc.M414355200

Wykoff, C. C., Beasley, N. J., Watson, P. H., Turner, K. J., Pastorek, J., Sibtain, A., et al. (2000). Hypoxia-inducible expression of tumor-associated carbonic anhydrases. Cancer Res. 60, 7075–7083. doi: 10.1016/S0002-9440(10)64048-5

Xu, L., Fukumura, D., and Jain, R. K. (2002). Acidic extracellular pH induces vascular endothelial growth factor (VEGF) in human glioblastoma cells via ERK1/2 MAPK signaling pathway: mechanism of low pH-induced VEGF. J. Biol. Chem. 277, 11368–11374. doi: 10.1074/jbc.M108347200

Ye, Z. C., and Sontheimer, H. (1999). Glioma cells release excitotoxic concentrations of glutamate. Cancer Res. 59, 4383–4391.

AUTOCRINE REGULATION OF GLIOMA CELL PROLIFERATION VIA PH_E-SENSITIVE K^+ CHANNELS

by

AVINASH HONASOGE, KATHERINE A. SHELTON, AND HARALD SONTHEIMER

American Journal of Physiology – Cell Physiology
306(5):C493-505

ABSTRACT

Since the seminal studies of Otto Warburg in the 1920s it has been widely recognized that cancers grow glycolytically even in the presence of oxygen. This generates an abundance of protons in a gradient across most solid tumors with an acidic core and an alkaline rim. Whether and how this proton gradient may also serve in an autocrine fashion on these tumors is unclear. Here we demonstrate that human glioma cells form spheroids which act as a viable three-dimensional tumor model, forming physiologically relevant extracellular pH (pH_e) and cell proliferation gradients. Using fluorescent cell cycle trackers we determined that the rate of cell proliferation is directly dependent on pH_e, and that cells adjust their growth rate according to their position within the pH gradient. We further show that glioma cells sense pH via H^+-sensitive K^+ channels that translate changes in pH into changes in membrane voltage. These channels are tonically active and blocked by acidic pH_e, quinine, and ruthenium red. Blockade of this K^+ conductance either by acidic pH_e or drug inhibition depolarized both glioma cells and tumor spheroids and prevented them from passing through the hyperpolarization-dependent G_1-to-S phase cell cycle checkpoint, thereby inhibiting cell division. In this way, pH_e directly determines the proliferative state of glioma cells.

Keywords: glioma, pH, cell cycle, potassium channel

INTRODUCTION

Over the past 100 years, certain hallmarks of cancer activity have been identified. These tend to be employed (to varying degrees) by cancers throughout the body. One such hallmark is increased glycolysis with increased tumor invasiveness even in the presence of ample oxygen, termed the Warburg Effect (12). The result of this phenomenon is fairly clear: a corresponding hyperacidity of the tumor interstitium due to increased proton production from glycolysis. Cancer cells must then develop mechanisms to overcome this inhospitable environment (11, 34).

Gliomas are archetypal of this effect. They represent an unfortunate intersection between destruction and prevalence, being both the most common and most deadly primary brain cancer. Prognosis for a grade IV glioma, known as glioblastoma multiforme (GBM), is grim, with a median survival of 14 months with the best current treatment (36). GBM lethality is mediated by a unique combination of rapid invasion and aggressive destruction of the surrounding brain (31). It has been previously demonstrated that like other aggressive cancers, gliomas lean disproportionately on glycolytic mechanisms versus oxidative phosphorylation for their ATP production (8, 27), which can lead to increased extracellular acidosis (12). Additionally, they possess other proton-extruding mechanisms including the Na^+/H^+ antiporter NHE1 (23) and surface expression of a vacuolar H^+ ATPase (V-ATPase) (29). The combination, then, of increased glycolysis, proton-extruding proteins, and finally tumor core necrosis leads to marked interstitial/extracellular pH (pH_e) heterogeneity and hyperacidification (9, 10). This phenomenon is either specific to

or heightened in transformed cells versus their non-transformed counterparts, as evidenced by the reversed pH_i versus pH_e gradients of typical glioma cells (pH_i 7.35, pH_e 6.75) and astrocytes (pH_i 7.0, pH_e 7.30) (34).

Recent studies have shown that glial cells both respond to and elicit changes in proton concentrations and brain function. For instance, glial cells in the brainstem are exquisitely sensitive to small alterations in pH_e and in turn regulate breathing through ATP release (14). Additionally, pH is indirectly involved in depolarization-induced alkalinization (DIA), in which an increase in extracellular potassium ($[K^+]_o$) from neuronal activity leads to downstream astrocyte alkalinization and extracellular acidification, which then decreases neuronal excitability (28). Since glioma cells are exposed to even larger proton gradients in the tumor microenvironment, we reasoned that they too might rely on pH_e as a signal.

There is some evidence to show that pH_e can have a profound impact on glioma cell physiology. For instance, prior studies have shown expression of the acid-sensing ion channels (ASICs) in glioma cells and that these channels are involved in cell migration (30). C6 mouse glioma cells, used as a model of glial cells at large, swell upon extracellular acidification in a Na^+-dependent manner, implicating NHE1 in postischemic brain edema (19). Next, VEGF expression is induced in cultured glioma cells upon application of acidic pH_e (37). Finally, acidic pH_e can promote a more stem-like phenotype for glioma cells in a reversible manner (17).

In light of these findings we set out to examine the effect of pH on glioma physiology. To this end we used glioma tumor spheroids, which were capable of reproducing the pH_e heterogeneity previously described *in vivo* (9, 10), thus allowing us to map the dependence of a glioma cell's physiology on its microenvironment. We show that the interstitial spheroid pH can predict glioma cell proliferation, and that changes in pH are sensed by ion channels which transduce pH changes to changes in membrane potential. We discuss how this serves as a feedback mechanism for these tumors to regulate their growth in a self-made acidic environment.

MATERIALS AND METHODS

Cell culture

U251-MG and D54 human glioma cells were derived from WHO grade IV glioblastoma multiforme tumors. The D54 cells were a gift from Dr. D. Bigner (Duke University). Cultured cortical astrocytes were obtained from P5-8 mouse pups and passaged once before being plated on coverslips. All cells were incubated in variants of DMEM/F12 media (Invitrogen) with 7% fetal bovine serum (FBS).

Tumor Spheroid Formation

U251-MG human glioma cells were plated in 200 µl of DMEM/F12 media with 7% FBS at a starting concentration of between 5×10^3 and 1.5×10^4 cells/well into agarose-coated 96-well plates. The plates were coated with 50 µl/well of autoclaved 1.5% wt/vol agarose-containing DMEM/F12 and cooled until the agarose was hardened. Initial spheroid formation occurred two days after plating; the spheroids were grown in an incubator in bicarbonate-buffered DMEM/F12 at 37 C and 10% CO_2 for at least one week. After one week, spheroids were between 100 and 500 µm in diameter.

Paraffin Embedding

Spheroids >1 week old were collected and fixed with 4% paraformaldehyde in phosphate buffered saline (PBS), dehydrated in EtOH, and embedded in Histogel blocks (Thermo Scientific) using cryomolds. This Histogel was processed to paraffin and then embedded in a paraffin block. 7 µm sections were cut using a Leica

microtome and placed on positively-charged glass slides (Fisher Scientific 12-550-17).

Immunocytochemistry

The paraffin sections of tumor spheroid were deparaffinized using CitriSolv (Fisher 22-143-975), rehydrated, and then washed with PBS. The spheroids were then blocked and permeabilized in PBS-containing 0.3% Triton-X and 10% normal goat serum (NGS) before being stained overnight at 4 C with rabbit anti-Ki67 antibody (1:1000, AbCam 15580) in a 1:2 dilution of blocking buffer (BB) in PBS. After washing in PBS, the slides were then stained with Alexa Fluor 488 goat anti-rabbit secondary antibody (1:500, Invitrogen A-11008) in the diluted BB for two hours at room temperature, washed, and incubated for 5 minutes in PBS with 1 mg/ml 4',6-dianidino-2-phenylindole (DAPI) (1:1000, Thermo 62248), before being mounted with Aqua-Poly/Mount (Polysciences 18606) and a coverglass. Images were acquired using a Zeiss Axiovert 200M microscope with a 20x air objective and Axiovision Rel. 4.6 software. Ki67 staining was visualized using a FITC filter set, while DAPI staining was visualized using a DAPI filter set.

pH Recordings of Spheroids

Spheroids >1 week old were pre-incubated in sulfate- and phosphate-free (SPF) baths (for composition, see *Electrophysiology* section of methods) of varying pH for 2 hours at 37 C before being placed in a solution with 20 μM of the cell-impermeant pH indicator dye seminaphtharhodafluor-5F 5-(and-6-)-carboxylic acid (SNARF-5F, Invitrogen S-23922) on the stage of an Olympus FV1000 Confocal

Microscope with 405, 473, and 559 nm diode lasers. After 30 minutes in this SNARF-5F solution, the fluorophore was excited with the 473 nm diode laser and images captured with two bandpass filters: 490-590 nm and 655-755 nm. A ratio of the long/short wavelength provided the pH of the bath and spheroid interstitium, and was calibrated using a linear regression of the pH 6.0, 7.4, and 8.8 baths (r^2 = 0.9999).

Voltage Dye Recordings of Spheroids

Spheroids >1 week old were pre-incubated in 2 μM of bis-(1,3-dibutylbarbituric acid) trimethine oxonol ($DiBAC_4(3)$, Sigma D8189) and 2 μM of CellTracker Orange (Invitrogen C2927) for 45 minutes at 37 C in SPF 7.4 bath (for composition, see *Electrophysiology* section of methods) and were then washed once with SPF 7.4 bath. Spheroids were then placed in SPF 7.4 bath and excited at two wavelengths, 473 nm ($DiBAC_4(3)$) and 559 nm (CellTracker Orange), and captured using two bandpass filters: 490-540 nm and 575-675 nm. Results were normalized to the CellTracker Orange dye.

Confocal Microscopy and Image Analysis

Confocal images were captured with an Olympus FV1000 Confocal Microscope using a 20x air objective. Images were captured in z-stacks of 5 μm section thickness through the spheroid with Olympus Fluoview ASW 3.1. The images were then analyzed using WCIF ImageJ. For both the pH_e and V_m recordings, raw images were blurred with a 10 pixel radius mean filter, false colored with ImageJ lookup tables and saved as TIFF files. The Ki67-stained spheroids were

analyzed by comparing the ratio of Ki67/DAPI mean fluorescent intensity in the core and the rim of the tumor. Core and rim were delineated by marked changes in cellularity and laminar composition between the two phases, and were selected via ImageJ as elliptical and annular sections, respectively.

Electrophysiology

U251-MG and D54 human glioma cells were whole-cell patch-clamped from 3-5 day old coverslips using standard techniques. Patch pipettes were pulled to 3-5 MΩ from thin-walled borosilicate glass (World Precision Instruments TW150F-4) using an upright puller (Narashige Instruments PP-830). Signals were captured with an Axopatch 200A amplifier (Molecular Devices), converted using a Digidata 1320A (Molecular Devices), and recorded using pClamp 8 (Molecular Devices). Cells were 80% compensated for capacitance and series resistance but omitted if the series resistance was >12 MΩ, indicating poor whole-cell access. Voltage-clamped cells were held at -40 mV until step protocols were administered at 20 mV increments. Current-clamp was used to monitor cell voltage in I=0 mode, without injection of additional current; changes in V_m were calculated using an average of at least two reversible barrel applications of either drug or different pH_e bath and correcting for baseline drift over time. Standard pipette solution was as follows (in mM) and was adjusted to pH 7.2 via NaOH: 140 KCl, 10 EGTA, 10 HEPES sodium salt. Standard sulfate- and phosphate-free (SPF) bath solutions were as follows (in mM) and were adjusted to their respective pH with either HCl or NaOH: 130 NaCl, 5 KCl, 1 $CaCl_2$, and either 15 MES + 15 HEPES (pH 6.0), 30 HEPES (pH 7.4), or 15 Tris +

15 HEPES (pH 8.8). Osmolarity for the pipette and bath solutions were 305 and 320 mOsm, respectively, and adjusted via addition of glucose.

Cell Proliferation and Viability

To assess cell proliferation, D54 human glioma cells were plated at a starting concentration of $1x10^4$ cells/well into 12-well plates in quadruplicate and incubated overnight at 37 C and 5% CO_2 in DMEM/F12 media with 7% FBS. The first batch of cells was collected and counted through a Multisizer 3 Coulter Counter (Beckman-Coulter). This was set as Day 0, and the remaining plated cells were incubated in DMEM/F12 with an additional 5.97 mM, 18.88 mM, and 59.72 mM $NaHCO_3$ for pH media 6.7, 7.2, and 7.7 respectively. The media were adjusted to 365 mOsm using D-mannitol. Quinine and ruthenium red were applied at concentrations of 100 μM and 20 μM respectively. The media were replaced daily to minimize changes in pH or of the drug potency.

To assess cell viability, D54 cells were plated in 10-cm dishes at a concentration of $4x10^5$ cells/dish in 10 mL of DMEM/F12 media with 7% FBS and allowed to adhere overnight. The next day, the media were replaced with the respective pH and drug-conditioned media and allowed to incubate at 37 C and 5% CO_2 for the next two days. The cells were then collected and stained with trypan blue, a diazo dye that enters cell with compromised plasma membranes. These cells were counted using a hemacytometer and the percent viable was calculated for each condition.

Cell Cycle

D54 human glioma cells were plated in 10-cm dishes at concentrations ranging from $4x10^5$ to $1x10^6$ cells/dish in 10 mL of DMEM/F12 media with 7% FBS and allowed to adhere overnight. The next day, the media were replaced with the respective pH and drug-conditioned media and allowed to incubate at 37 C and 5% CO_2 for the next two days. These cells were then harvested and resuspended in cold PBS before being dehydrated with cold EtOH. After being spun down, the cells were then resuspended in a PI staining solution of 0.02 mg/ml PI (Invitrogen P21493), 0.2 mg/ml DNAse-free RNAse (Invitrogen AM2286), and 0.1% v/v Triton X-100 (Sigma T-8787) for 30 minutes. These preparations were then analyzed using a LSR II cell sorter (BD Biosciences).

Statistics

Statistics were performed using GraphPad Prism 5.0 and are shown as mean ± SEM. $n \geq 3$ for all experiments with * = $p < .05$, ** = $p < .01$, and *** = $p < .001$.

RESULTS

Glioma cells organically evolve gradients of pH_e and cell proliferation in vitro

Prior studies have demonstrated a proclivity of gliomas to acidify heterogeneously, but generally with increased proton concentration towards the tumor core. The cause of this acidification is multifaceted, and includes heterogeneous expression of acid extruders, poor access to nutrients, and a mix of cell populations (18). We wondered if tumor acidification could organically evolve from a clonal population of cells and in the presence of ample nutrients. Previous studies demonstrated a pH_e gradient in rat gliomas *in vivo* (9, 10) and in glioma spheroids *in vitro* (1). To gain sufficient pH_e resolution, we elected to analyze spheroid pH_e gradients using 20 μM of the cell-impermeant ratiometric pH indicator dye 5-(and 6)-Carboxylic Acid (SNARF-5F). U251 human glioma cells, which quickly aggregate, were grown to form spheroids with $\sim 10^4$ cells and analyzed via confocal microscopy for pH_e differences. We compared pH_e gradients from spheroids bathed for two hours in acidic, neutral, and alkaline pH-buffered media to both determine if the core acidification was saturable and how well the proton gradients dissipated (Fig. 1A-C). In the span of the ~100 μm diameter spheroids, glioma cells experienced a wide range of proton concentrations, with an increased concentration focused in the core of the spheroids. The spheroids all acidified below pH_e 6.0, regardless of incubating medium (Fig. 1D-E; pH_e 5.3-5.9; n = 3 each). Consequently, the proton concentration gradient was significantly steeper in the alkaline pH media solutions, where maximally there was an order of magnitude change in proton

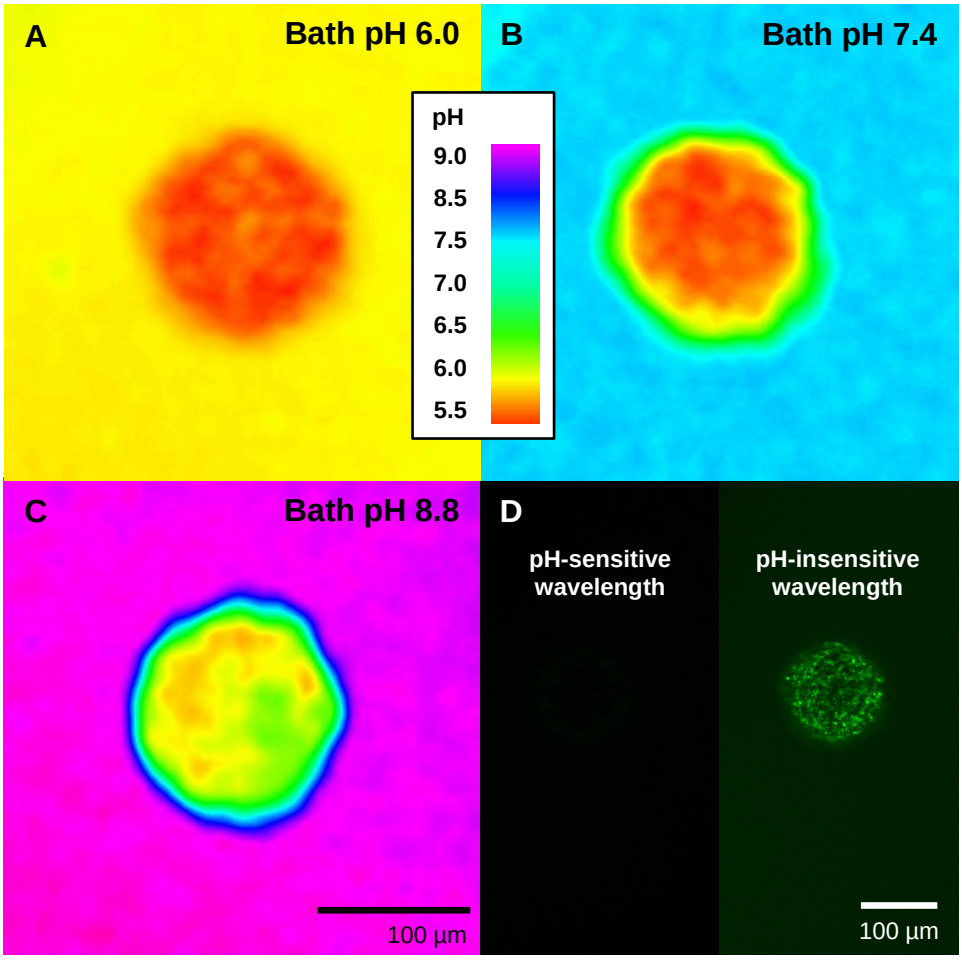

Fig. 1. Quantification of tumor spheroid acidification. *A-C,* >1 week old U251 human glioma spheroids were pre-incubated and then placed for confocal imaging in baths with 20 µM cell-impermeant SNARF-5F pH indicator dye of pH 6.0, 7.4, and 8.8, respectively. Shown are representative z-sections at 20x through the middle of the spheroids. *D,* Representative pH 6.0 bathed spheroid showing full diffusion of SNARF-5F.

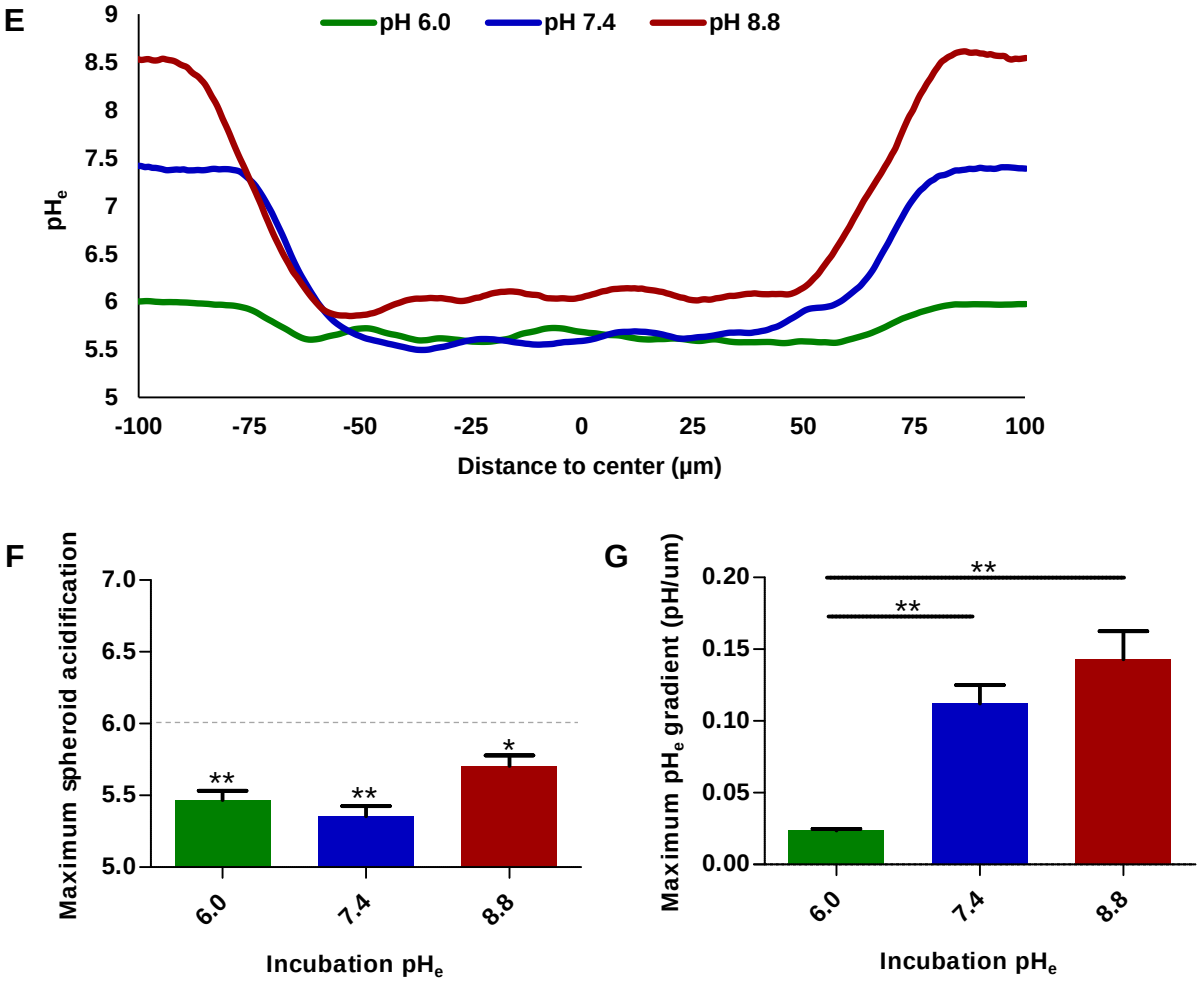

Fig. 1 cont'd. Quantification of tumor spheroid acidification. *E,* Line graphs through the center of the representative spheroids shows that they create standing pH_e gradients that can acidify to ≈pH_e 6.0 regardless of bathing medium. *F-G,* Quantification of the maximum acidity (one-tailed t-test for H_0 $pH_e < 6.0$, n=3) and maximum gradient of acidification (one-way ANOVA with Tukey-Kramer post-test, n=3), respectively.

concentration every 7 microns into the spheroid core (Fig. 1F). Thus, glioma cells *in situ* are capable of reconstituting and experiencing a wide range of proton concentrations over short lengths, and this pH_e heterogeneity is slow to dissipate.

We further hypothesized that this acidification inversely corresponded to tumor cell proliferation. Paraffin sections of one week-old tumor spheroids were immunostained for Ki67, a protein specifically expressed during all active phases of the cell cycle, but absent at rest (G_0 phase). These spheroids demonstrated a rim of Ki67 expression (Fig. 2A-B) which was decreased in the spheroid core relative to nuclear DAPI staining (Fig. 2C). Thus, the cell proliferation gradient mimicked that of pH_e within these spheroids, with greater proliferation and higher pH_e away from the tumor core.

Glioma cells proliferate in alkaline pH_e

We next sought to directly test the relationship between cell proliferation and interstitial acidity. The functional consequence of protons on the many pH-dependent processes in glioma cells remains largely unknown. To this end, we cultured D54 human glioma cells, whose growth curves have been well-characterized (5, 16, 22) in a CO_2/HCO_3^- media buffering system that set pH_e to 6.7 (acidic), 7.2 (neutral), and 7.7 (alkaline). Glioma cells displayed a strong preference for alkaline pH_e, even at supraphysiological levels (Fig. 2E). Cell counts using the Beckman Coulter Counter revealed exponential growth at alkaline and neutral pH_e conditions with stagnation at acidic pH_e. By Day 3, there was no significant difference between cell counts at pH_e 7.7 and 7.2, but 66% fewer cells in acidic pH_e

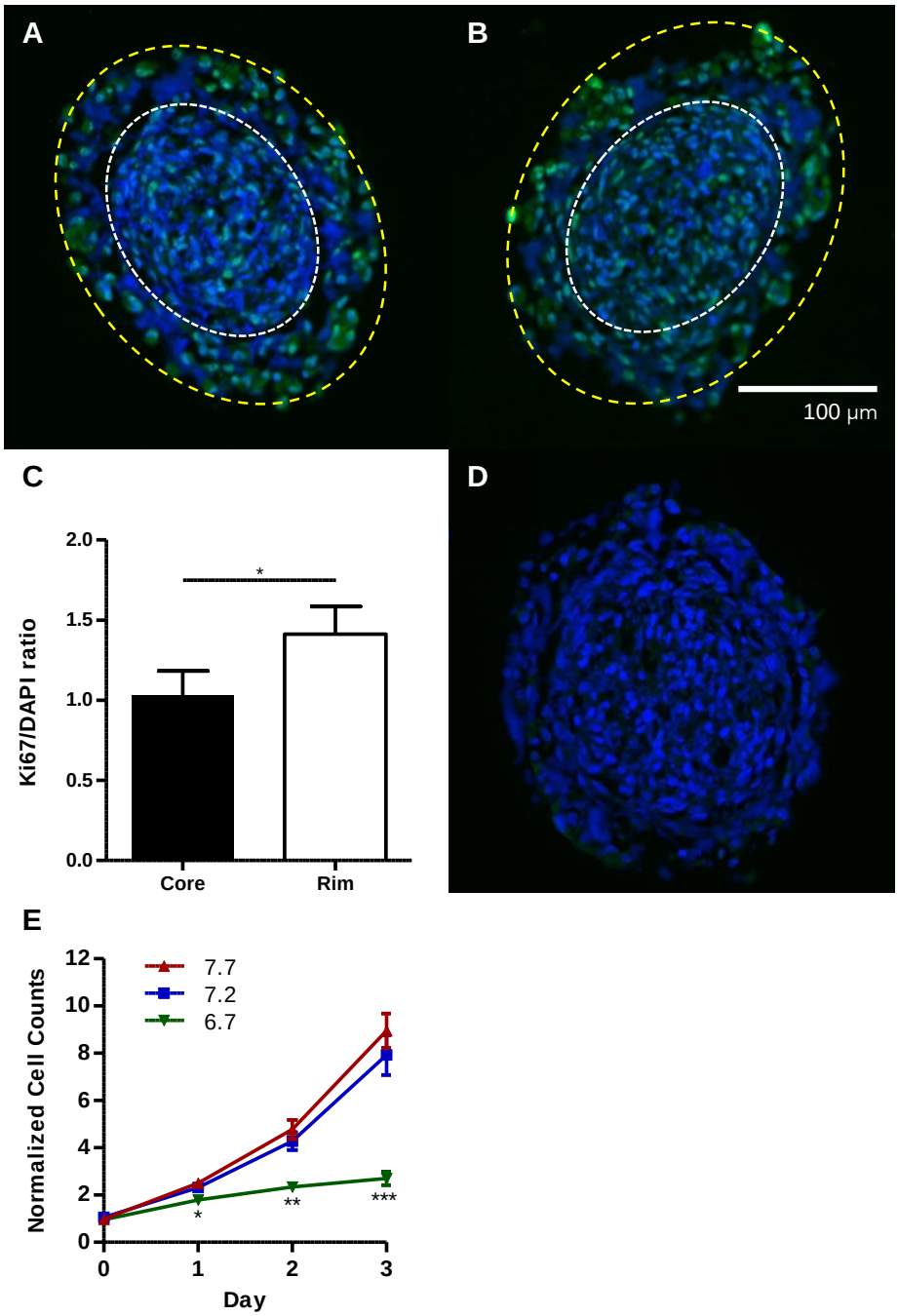

Fig. 2. Human glioma spheroids evolve pH_e and proliferation gradients. *A-B*, >1 week old U251 human glioma spheroids that were paraffin embedded, cross-sectioned, and stained for Ki67 (green) and DAPI (blue). White dotted line encapsulates the core of the spheroid while the area between the yellow and white dotted lines encapsulates the spheroidal rim. Sections were visualized at 20x. *C*, Ki67 staining normalized to DAPI shows more proliferation of the rim glioma cells (two-tailed paired t-test, n=7). *D,* Control spheroid without Ki67 primary antibody. *E*, Quantification of Coulter Counter data with cells cultured at varying pH_e levels with media changed daily (two-tailed t-tests versus pH_e 7.2 as control, n≥6).

compared to neutral pH_e ($n \geq 6$; $p = 0.38$ and $p < 0.001$, respectively). Thus, extracellular proton concentrations control glioma cell growth.

pH_e-*dependence of* V_m *in human glioma cells*

We hypothesized that pH_e affects this glioma cell growth via a transmembrane chemosensor capable of translating extracellular protons to intracellular signaling, and surmised that pH_e-sensitive ion channels could act as this transducer. To test this, D54 glioma cells studied in whole-cell patch-clamp showed large pH_e-sensitive changes in both current density and membrane potential (Fig. 3). Cells were placed in a bath of pH_e 7.4 with barrel-applied isotonic solutions of pH_e 6.0, 7.4, and 8.8, buffered accordingly. In voltage-clamp (Fig. 3A-C), there was a moderate decrease in current density switching from pH_e 7.4 to 6.0 (-3.69 ± .34 pA/pF at +100 mV), while there was an increase in current density switching from pH_e 7.4 to 8.8 (+11.5 ± 6.3 pA/pF at +100 mV). In current-clamp (Fig. 3D-E), acidic pH_e induced large depolarizations (+13.5 ± 0.92 mV), while alkaline pH_e induced large hyperpolarizations (-28.8 ± 6.8 mV). These changes in membrane potential were sustained, reversible, and additive, and occurred with or without physiological levels (60 nM) of calcium in the pipette solution (data not shown). At pH_e 6.0 there was an additional transient strong depolarization followed by a plateau phase; this transient depolarization is reflective of previously-described ASIC channels (35) and was blocked by a 10 μM application of benzamil (Fig. 3F), a potent amiloride analog and ASIC blocker, while leaving the plateau phase untouched. We repeated these experiments in U251 glioma cells with similar effects (Fig. 3D). By contrast, cultured

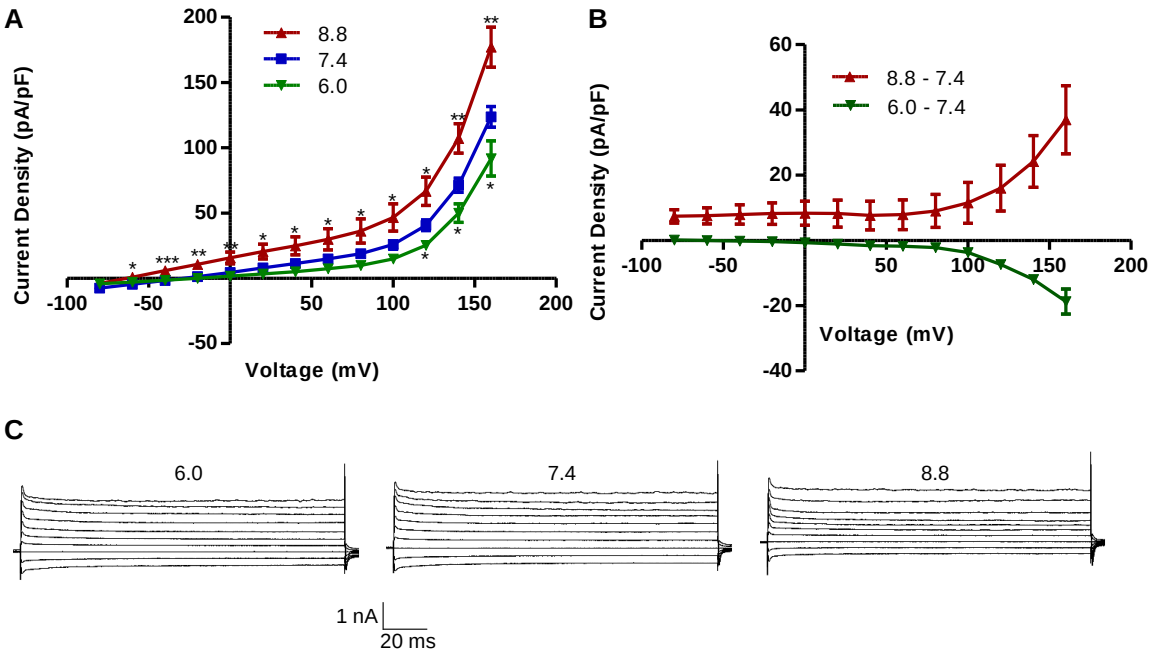

Fig. 3. Glioma cells display a pH_e-sensitive whole-cell conductance. *A*, Voltage-clamp recordings from D54 human glioma cells in different pH_e bath solution. *B*, pH_e-sensitive currents after barrel-applying pH_e 6.0 or 8.8 from a control of pH_e 7.4. *C*, Representative traces of whole-cell currents from D54 glioma cells in pHe 6.0, 7.4, and 8.8 bath solutions.

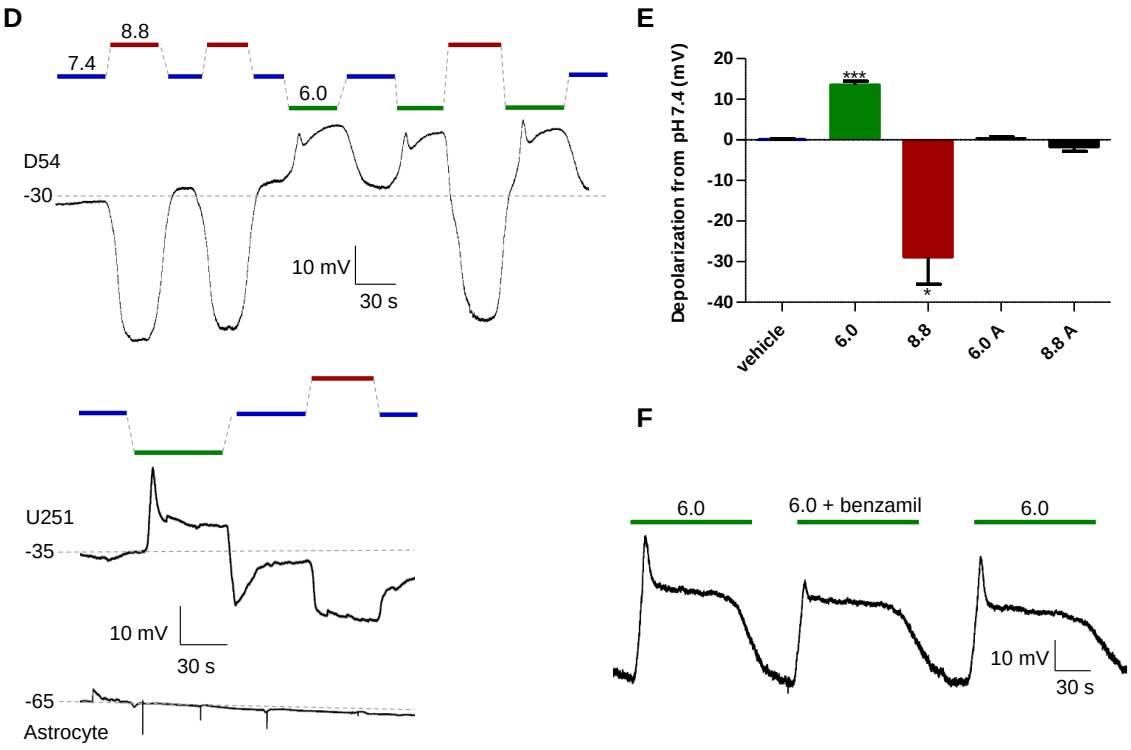

Fig. 3 cont'd. Glioma cells display a pH_e-sensitive whole-cell conductance. *D*, Whole-cell current-clamp recordings from representative D54 and U251 human glioma cells, along with cultured cortical astrocytes. *E*, Quantification of pH_e-sensitive current-clamp depolarizations and hyperpolarizations in D54 glioma cells and cortical astrocytes. *F*, Representative current-clamp trace of D54 glioma cell with reversible ASIC blockade using 10 μM benzamil.

astrocytes did not show any significant pH_e-sensitive changes in membrane potential (+0.328 ± 0.34 and -1.67 ± 1.2 mV for acidic and alkaline pH_e shifts, respectively; Fig. 3E). Thus, pH_e changes translate into changes in transmembrane current density of malignant but not normal glial cells.

pH_e-modulated V_m in glioma cells is K^+-dependent

To determine the ion(s) responsible for these pH_e-sensitive changes in glioma cells, we first repeated the current-clamp findings in normal (5 mM) and high (25 mM) $[K^+]_o$ conditions (Fig. 4). We hypothesized that these biophysical changes were especially dependent on the Nernst potential for potassium (E_K), with channels opening at high pH_e (and driving the cell towards E_K) and closing at low pH_e (and driving the cell away from E_K). Consistent with this hypothesis, the hyperpolarizations induced by high pH_e were largely ablated by high $[K^+]_o$ relative to the control baseline (-0.402 ± 2.0 mV, Fig. 4A-B), which shifts E_K from -87 mV to -49 mV, while the acidic pH_e-dependent depolarizations remained intact (+20.22 ± 1.4 mV). We additionally stepped from each pH_e condition to its respective high $[K^+]_o$ (Fig. 4C) and found that the majority of the conductance at pH_e 8.8 was K^+-mediated (35.4 ± 1.3 mV depolarization) as opposed to at pH_e 6.0 (4.47 ± 0.30 mV depolarization; $p < 0.001$ versus pH_e 8.8). Thus, extracellular protons evoke large shifts in the basal K^+ permeability of glioma cells.

pH_e modulations of V_m are inhibited by K^+ channel blockers

Next, we sought to pharmacologically inhibit this pH_e-sensitive permeability (Fig. 5). For this purpose we assayed a variety of inhibitors previously known to inhibit

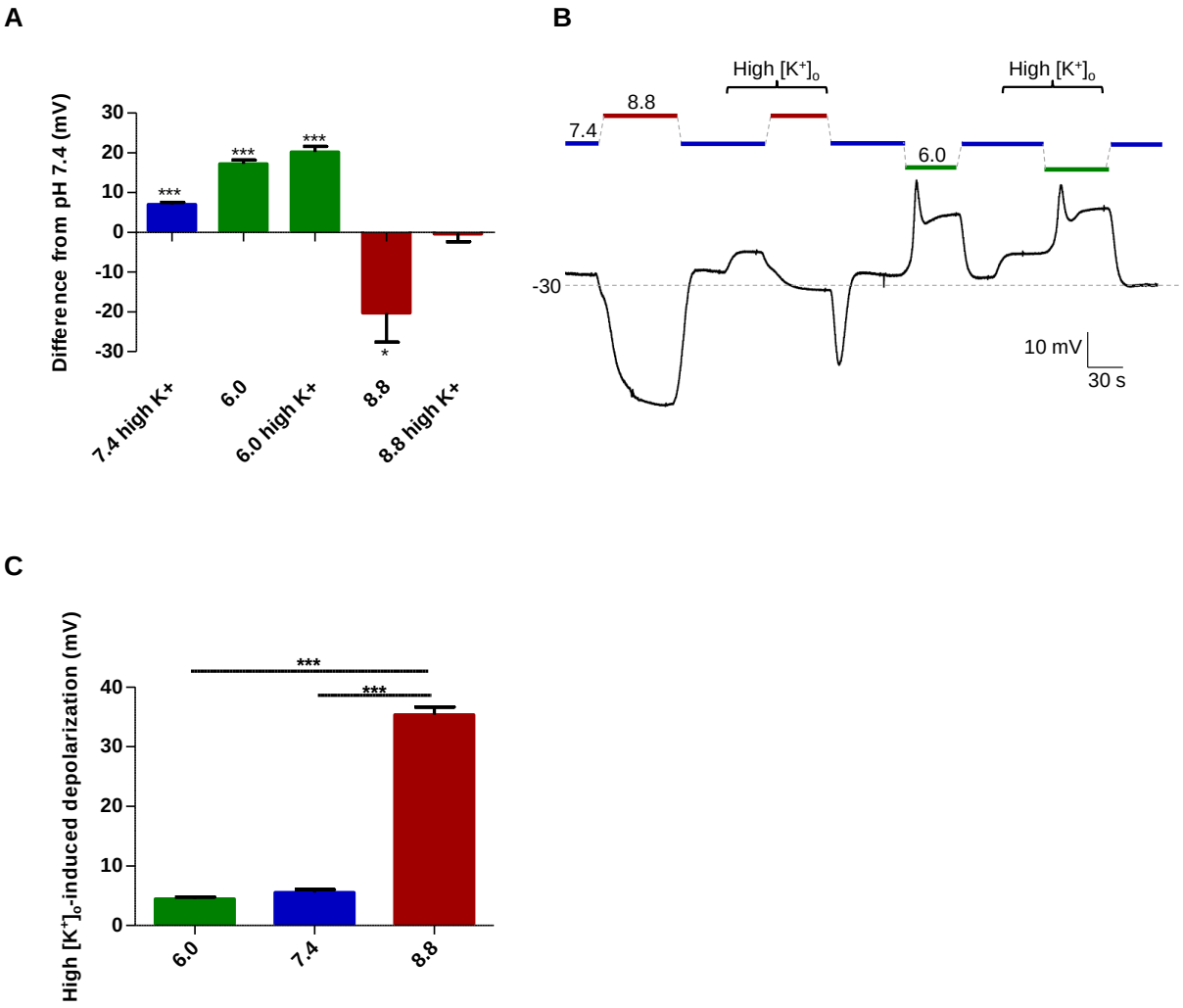

Fig. 4. The pH_e-sensitive conductance is $[K^+]_o$-dependent. *A*, Quantification of pH_e-dependent changes in current-clamp in either normal (5 mM) or high (25 mM) $[K^+]_o$ in D54 glioma cells (n=6, two-tailed t-test versus pH_e 7.4 with normal $[K^+]_o$). *B*, Representative current-clamp trace of D54 glioma cell switched to high $[K^+]_o$ bath of varying pH_e. *C*, Depolarizations in current-clamp mode from each pH_e condition induced by a step to high (25 mM) $[K^+]_o$ (n=5, one-way ANOVA with Tukey-Kramer post-test).

pH_e-sensitive K^+ channels (21). We first tested drugs in current-clamp, where our most robust V_m response was from 1 mM quinine HCl (Fig. 5A). When bath applied, quinine completely prevented the acid-induced depolarizations and turned the alkaline-induced hyperpolarizations into slight depolarizations. To isolate quinine-sensitive current density and voltage changes, D54 glioma cells were pre-incubated in bath solutions of varying pH_e for at least two hours prior to recording. We captured larger pH_e-sensitive currents in voltage-clamp (Fig. 5C-D) at alkaline pH_e (+1.56 ± 0.71 pA/pF at pH_e 6.0 and +33.6 ± 8.6 pA/pF at pH_e 8.8 at +100 mV). Additionally, quinine depolarized cells incubated in alkaline pH_e to a far greater extent than acidic pH_e in current-clamp (Fig. 5B; +0.100 ± 0.23 mV at pH_e 6.0 and +50.1 ± 2.62 mV at pH_e 8.8), consistent with the hypothesis that this quinine-sensitive channel contributes to the pH_e-sensitive V_m.

However, we did not find that cells at pH_e 6.0 were depolarized at a baseline. In our current-clamp experiments where cells were pre-incubated at pH_e 6.0 prior to patching, the average resting membrane potential was -39.83 ± 1.03 mV (n=5); yet these cells were also completely resistant to subsequent quinine depolarization (Fig 5B). It is therefore possible that some cells at this low pH_e re-adjusted their V_m by closing Cl^- conductance (E_{Cl} = 0 mV in our experiments) to compensate for the closed K^+ channels, thus allowing them to maintain a less-depolarized V_m but still leaving them incapable of further subsequent depolarization.

This aforementioned conductance is markedly different from the prior-described tonic ASIC current in D54 glioma cells (20), which was not significantly

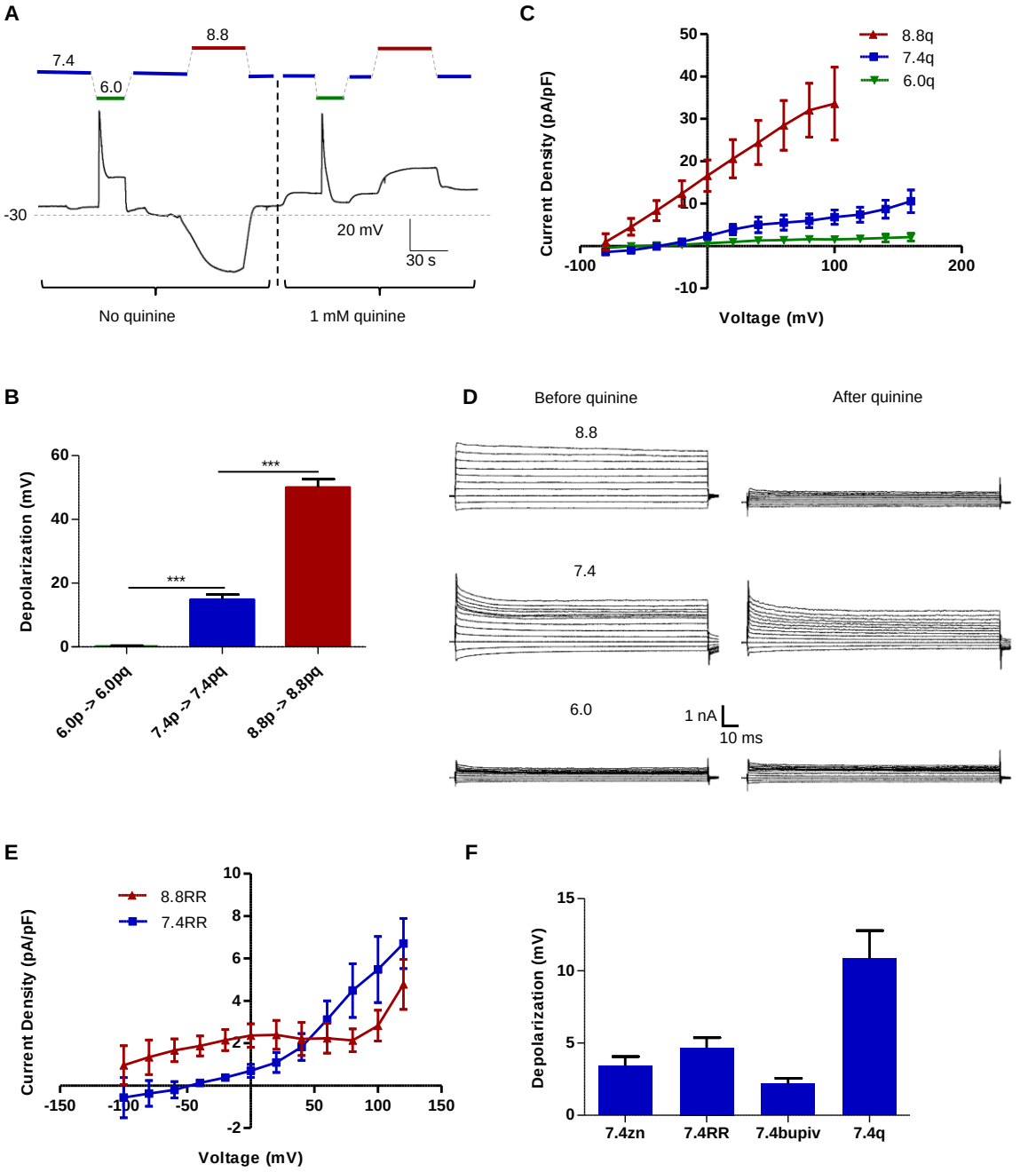

Fig. 5. Inhibition of the pH_e-sensitive K^+ conductance. *A*, Current-clamp trace of D54 glioma cells tracking V_m while modulating both pH_e and 1 mM quinine via barrel application. *B*, Quantification of quinine-induced depolarizations with cells bathed in different pH_e conditions. *C*, Quinine-sensitive currents from voltage-clamp recordings of D54 glioma cells. *D*, Representative voltage-clamp traces before and after 1 mM quinine application. *E*, Ruthenium red-sensitive currents from voltage-clamp recordings of D54 glioma cells. *F*, Drug-induced depolarizations from 100 µM zinc (zn), 200 µM ruthenium red (RR), 1 mM bupivacaine (bupiv), and 1 mM quinine (q).

changed when the cells were incubated in different pH_e baths. In conclusion, glioma cells express pH_e-sensitive K^+ currents that translate pH changes into changes in V_m and these are blocked by both quinine and acidic pH_e.

Quinine depolarizes glioma spheroids

Since isolated glioma cells demonstrate a pH_e-dependence of V_m, we next tested if this held up when cells formed three-dimensional tumors (Fig. 6). U251 glioma spheroids were loaded with the slow-response voltage-sensitive dye $DiBAC_4(3)$. This bis-oxonol potentiometric dye enters and fluoresces within depolarized cells, but is excluded from the mitochondrial membrane due to its negative charge. Additionally, it sacrifices speed for sensitivity, allowing even small changes in membrane potential to be accounted for. As this is a non-ratiometric V_m indicator, we co-loaded and normalized cells to the fluorescent labeler CellTracker Orange (F_{norm}). Under control conditions and in the absence of any drug, we noticed a gradient of V_m that mimicked those of both pH_e and cell proliferation (Fig. 6A-D); the rim of the spheroid displayed an alkaline environment rich in hyperpolarized and prolific cells, while the core contained cells of depolarized potentials and limited proliferation.

From here, we hypothesized that if this V_m gradient is caused by a pH_e gradient, application of quinine should disrupt that relationship. To test this, we pre-incubated these spheroids for two hours in 1 mM quinine HCl along with the co-loaded V_m and cell tracking dyes, allowing ample time for diffusion of drug beyond the tumor rim. Our prediction was that quinine would homogenize cellular V_m,

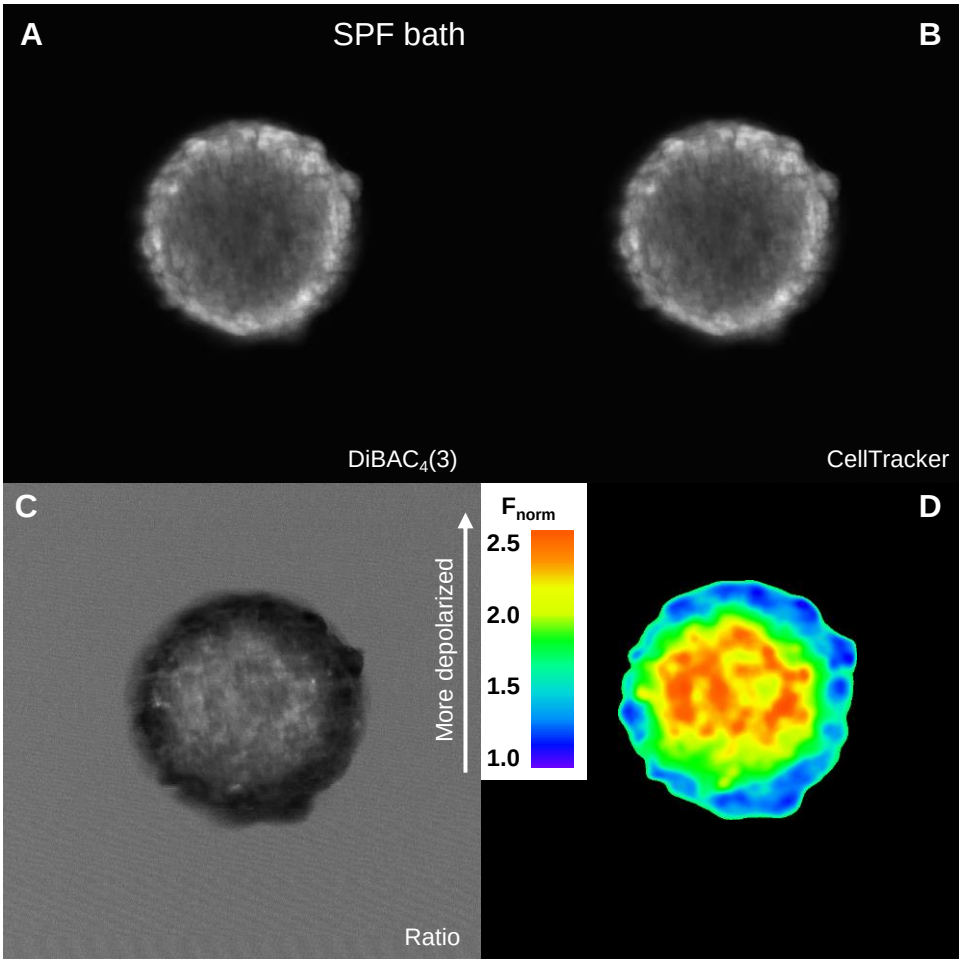

Fig. 6. Quinine depolarizes glioma spheroids. *A-D,* Confocal cross-section image of a U251 glioma spheroid co-loaded with the voltage-sensitive dye $DiBAC_4(3)$ (*A*) and the cell tracking dye CellTracker Orange (*B*). The images were then normalized to the CellTracker dye (*C*) and then falsely colored (*D*).

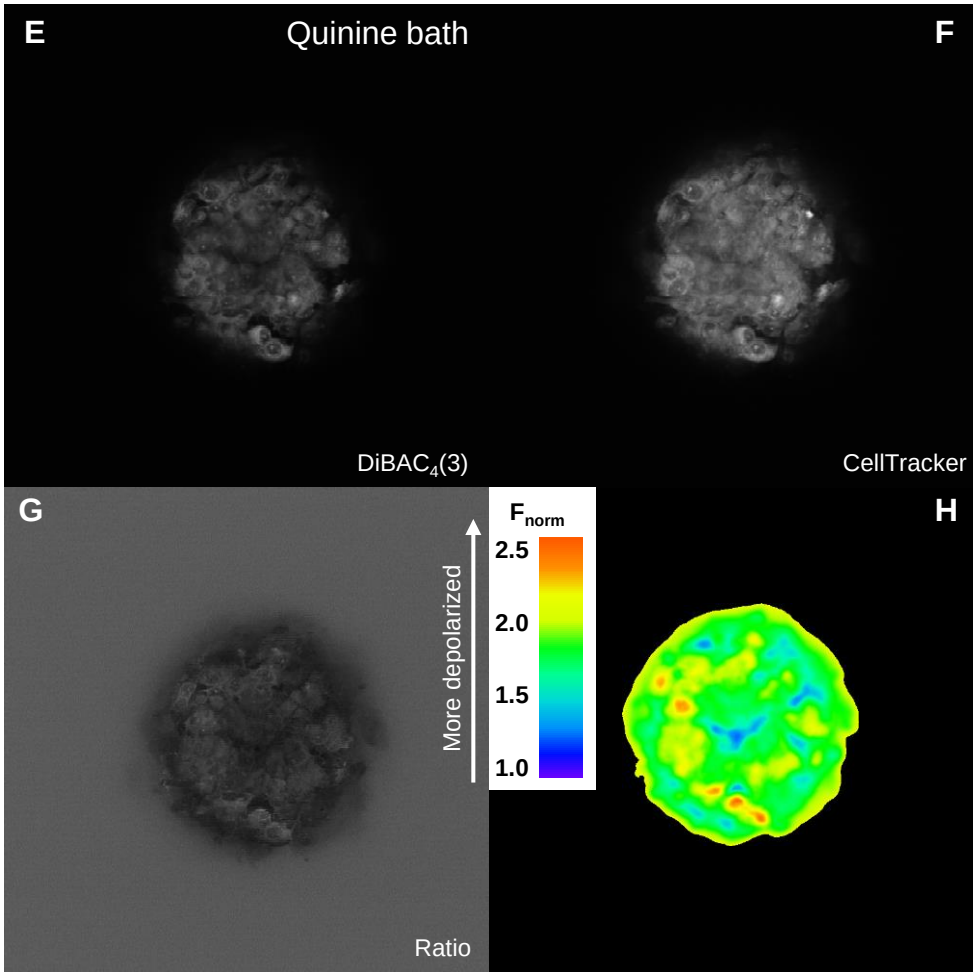

Fig. 6 cont'd. Quinine depolarizes glioma spheroids. *E-H*, Confocal imaging of a U251 spheroid pre-incubated for 2 hours with 1 mM quinine, showing the voltage-sensitive channel (*E*), cell tracker channel (*F*), normalization to the cell tracking dye (*G*), and ratiometric coloring (*H*).

clamping all quinine-affected cells to a similarly depolarized state in a similar manner as the prior current-clamp experiments (Fig. 5B). Consistent with this hypothesis, Fig. 6E-H shows a pronounced depolarization of the rim tumor spheroid cells, while the core cells remain similarly depolarized as before. This parallels quinine's effect on the monolayer glioma cells demonstrated prior – at acidic pH_e, the quinine shows little depolarization effect, and that effect size grows in conjunction with a more alkaline pH_e. Thus, gliomas demonstrate exquisite sensitivity to the pH_e environment directly surrounding them, and modulate their V_m accordingly.

pH_e-sensitive K^+ conductance affects glioma cell proliferation

Given that the less-proliferating cells of the core sat both at a more depolarized state and in a more acidic pH_e environment, we wanted to establish a possible link between a glioma cell's pH_e environment, its V_m, and its proliferative state. To do this, we repeated the Coulter Counter studies with the additional manipulation of pharmacologic inhibition from 100 μM quinine (Fig. 7). We hypothesized that in acidic pH_e conditions, cell proliferation should be low and quinine application should have no additional effect. On the other hand, in alkaline pH_e conditions, cell proliferation should be high, but this should be blocked by the strong depolarization from quinine. Quinine was chronically applied and media replaced daily over the course of the experiment; and consistent with our hypothesis quinine showed a larger effect at higher pH_e (Fig. 7A). At pH_e 6.7, there was no significant decrease in cell counts at Day 2 relative to control (95.7% of control; p =

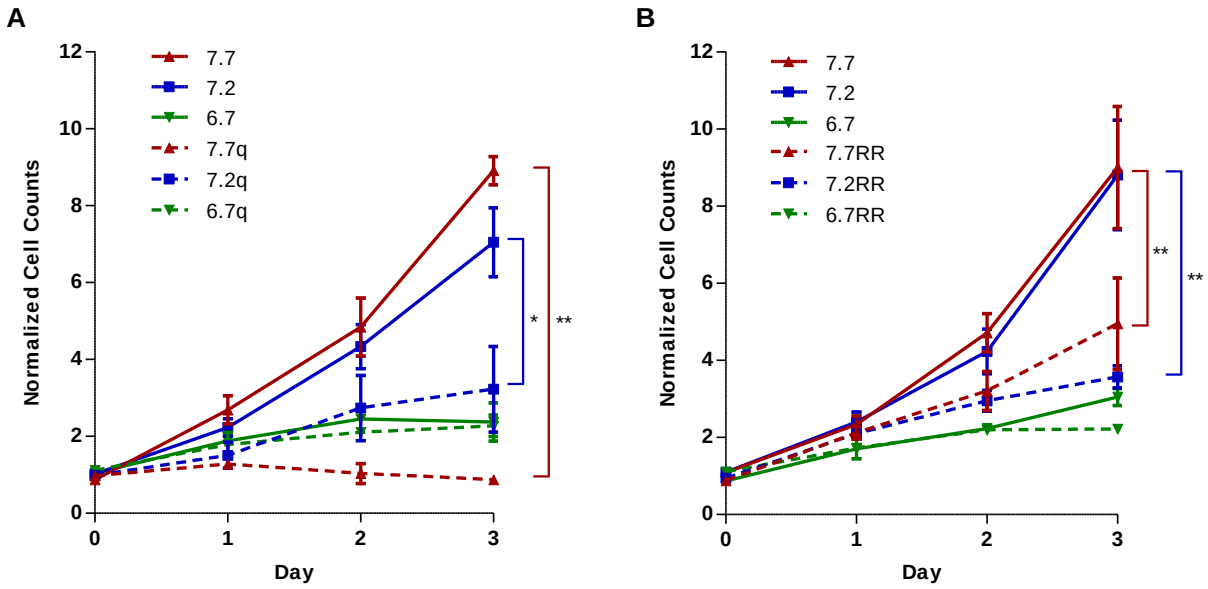

Fig. 7. pH_e-sensitive conductance modulates glioma cell cycle. *A-B*, Coulter Counter results comparing drug inhibition of proliferation at different pH_e levels. Drug conditions were compared to their respective pH_e controls at Day 2 (n≥3; two-sample t-tests).

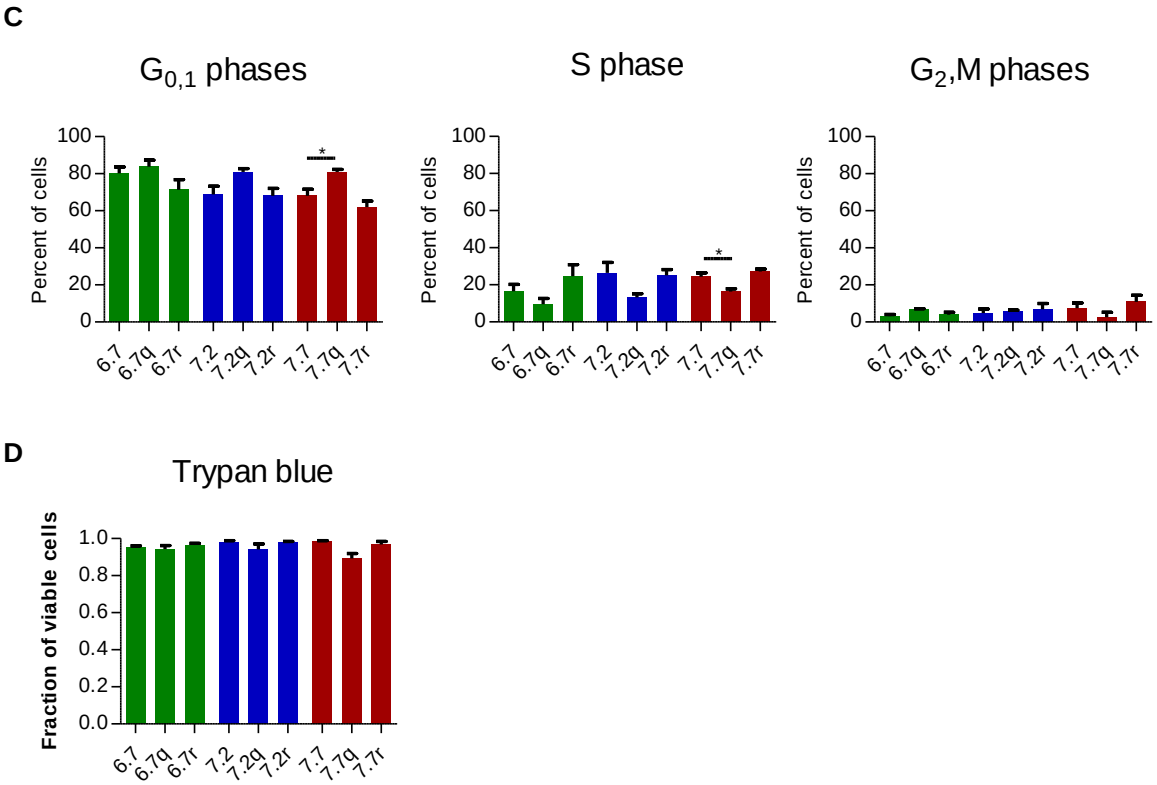

Fig. 7 cont'd. pH_e-sensitive conductance modulates glioma cell cycle. *C*, Percentage of cells in different phases of the cell cycle as quantified by propidium iodide intensity via FACS. Cells were kept in 10-cm dishes for two days without media change. Statistics compared the drug conditions with their drug-free counterparts (n≥3; two-sample t-tests). *D*, Trypan blue staining for cell viability after 2 days in each condition. Drug columns were compared to their respective drug-free pH_e control (n=3; two-sample t-tests). Drug concentrations for all experiments were 100 µM quinine and 20 µM RR. Media were changed daily for the Coulter Counter studies.

0.90); contrastingly, there was a significant reduction in cell counts both at pH_e 7.2 (45.8% of control; $p < 0.05$) and pH_e 7.7 (9.7% of control; $p < 0.01$). We additionally used a second inhibitor from our screen of K^+-channel blockers (ruthenium red, 20 μM; Fig. 5F) that yielded us pH_e-sensitive results similar to those of quinine (Fig. 7B).

A decrease in cell count could be due to either a decrease in cell proliferation or a decrease in cell viability. To separate these phenomena, we first tested cell viability with a trypan blue stain (Fig. 7D). Trypan blue is a membrane-impermeant dye that is only incorporated in cells with compromised membranes. We found no significant difference in trypan blue inclusion between control and drug conditions at any pH_e ($p > 0.05$) indicating that the drugs might instead be having the bulk of their effect on cell proliferation. Thus, the K^+ channel inhibitors that demonstrated pH_e-dependent depolarization of glioma cells also showed a pH_e-dependent effect physiologically, with a greater growth inhibition at more alkaline pH_e.

pH_e-sensitive K^+ conductance affects glioma cell G_1-to-S phase transition

Prior studies have especially implicated K^+ channels as necessary for membrane hyperpolarization during the G_1-to-S phase transition of the cell cycle (4, 26). We thus performed a complete cell cycle analysis using a propidium iodide stain and fluorescence-activated cell sorting (FACS). Propidium iodide incorporates in DNA and a cell's fluorescent intensity is dependent on the number of copies of DNA contained in that cell, thus allowing a more complete picture of cell cycle status from a larger population of cells. If this pH_e-sensitive K^+ conductance provided a

necessary hyperpolarization from G_1-to-S phase, we would expect a clustering of cells in the G_1-phase of the cell cycle with pharmacologic inhibition, especially at higher pH_e. In agreement with this hypothesis, we found that glioma cells were significantly increased in the $G_{0/1}$-phases (81.0 ± 1.3% versus 68.1 ± 3.4%; $p < 0.05$) and significantly decreased in the S-phase at pH_e 7.7 (16.4 ± 1.4% versus 24.3 ± 2.1%; $p < 0.05$) in quinine versus control conditions (Fig. 7C). In conclusion, the aforementioned pH_e-sensitive, quinine-sensitive K^+ glioma cell conductance specifically affects the G_1-to-S phase transition of the glioma cell cycle.

DISCUSSION

In light of the wide-held notion that cancers in general exhibit the Warburg effect (12), whereby tumors grow anaerobically and extrude lactate and protons even in the presence of O_2, we asked whether this establishes a pH_e gradient across a tumor mass and whether this could result in altered cellular growth across the tumor.

Using glioma spheroids as a tumor model system, we were able to show that a homogeneous tissue mass, which presumably originated by clonal expansion from a single cell, is able to establish and maintain a pH_e gradient where the core is highly acidic and the rim is alkaline. Importantly, we show that cells grown in this gradient adjust their rate of proliferation proportionally, with lowest growth in the acidic core and highest growth on the alkaline rim. Furthermore, using single-cell electrophysiology we were able to identify a pH_e-sensitive K^+ conductance that likely acts as an environmental pH sensor, translating changes in extracellular pH into changes in membrane voltage.

Spheroids were pre-incubated in the bulk pH_e solution 2 hours prior to recording. Regarding the maintenance of this pH gradient, it is likely that several factors are at play: 1) cell coupling and bulk cellular presence forming a barrier for molecular clearance; 2) a gradient of protein expression compartmentalizing proton formation, uptake, and extrusion and maintaining a proton flux steady-state (15); and 3) carbonic anhydrases acting as catalysts of "facilitated diffusion" by accelerating the clearance of acid from the spheroidal core (33). It is also very likely

these data would be recapitulated even in a bicarbonate-buffered environment. Work in colon carcinoma spheroids has demonstrated a role for carbonic anhydrase 9 in facilitating the diffusion of the pH gradient within the tumor spheroids, and thus the most likely differences between a HEPES environment and a bicarbonate one would be the rate of diffusion of protons and the subsequent steepness of the gradient (33). The actual formation of the spheroidal pH_e gradient occurred in bicarbonate-buffered DMEM/F12 media.

These findings are a significant extension of prior observations in the literature (1, 6, 32). The presence of pH gradients across gliomas has been previously shown; however, these studies often included inputs from both the tumor cells themselves and the surrounding stroma or failed to afford the same cellular resolution of interstitial pH as our voltage-sensitive dye experiments. Furthermore, core tissue necrosis has often been ascribed to a loss of nutrient supply in the core (7). Our studies occur in the absence of vasculature yet in the presence of ample media-derived nutrients and thus we can directly ascribe the graded growth pattern to the endogenously generated pH environment.

Acid-mediated depolarization of glioma cells might contribute to the current model of tumor core necrosis which already includes nutritive exhaustion, cytokine release, and reactive oxygen species production (7). While these many mechanisms of core necrosis occur simultaneously *in vivo*, here we show an acid-induced cell cycle arrest that is independent of oxygen and nutrient levels, as even in the presence of ample nutrients and cultured in a monolayer, glioma cells showed

markedly attenuated growth at acidic pH_e. Conversely, these cells are capable of thriving in supraphysiologically alkaline pH_e conditions, and may in fact rely on this alkaline pH_e to allow them to hyperpolarize and pass the G_1-to-S checkpoint of the cell cycle.

Our results fit with prior studies characterizing glioma cells as relatively depolarized compared to other glial cells (25). This is characteristic of highly proliferative cells; however, there still exist cell cycle checkpoints that require transient changes in V_m (2). As a result, it appears glioma cells are depolarized *en masse* yet cannot proliferate if clamped to this depolarized potential. In this vein, we found an inhibitor of the pH_e-dependent hyperpolarization in quinine that forcibly depolarized glioma cells in a pH_e-dependent manner. Application of this drug combined with a varied pH_e allowed us to isolate the input of this pH_e-sensitive K^+ conductance from the other pH_e-dependent cell cycle machinery at play. Incidentally, quinine has served as treatment for malaria for centuries, is inexpensive, and is well-tolerated in high doses in humans, making it therapeutically relevant.

While our studies were able to unequivocally identify a K^+ conductance as a pH_e sensor for glioma cells, we were not able to definitively implicate any specific underlying channel(s). However, several candidates, especially those of the two-pore potassium (K_2P) channel family, fit our observation of a pH_e-sensitive basal K^+ conductance and will serve as targets in future studies (21). The most likely candidates given the sensitivities to quinine and ruthenium red are TASK-1 and

TASK-3, and both of these have been previously implicated in glioma cell physiology (24). Importantly, the kinetics, pharmacology, activation properties, and ion permeability of the here-observed K^+ conductance are a poor fit for previously-shown pH_e-sensitive glioma channels including ASICs and TRPs. Our resultant K^+ conductance was not cation-nonspecific, unlike many of the pH_e-sensitive ASIC channels (3). Additionally, the K^+ conductance was modulated by the same pathophysiological range of pH_e created by the glioma, and unlike many of the ASIC and TRP channels does not rely on extremely high acidity levels ($pH_e < 5.0$) to be activated (13, 35). Finally, it is very possible that a residual conductance usually masked by the large quinine-sensitive basal current is unmasked in the quinine-bathed conditions. Glioma cells express many channels, and several of them have demonstrated pH-sensitivity including ClC-3, TRP channels, and P2X receptors (18).

Given the nature of our assay, we were able to only study tumor growth. In the brain, however, there exists a balance of growth and tumor invasion. Hence it is possible that our observed pH_e-dependent growth mediates an important switch between the growth and invasion phases of the tumor – that tumor growth is favored by alkaline pH_e, as observed, whereas tumor invasion may be aided by acidic pH_e. Recently, for instance, studies have highlighted the idea of "acid-mediated invasion" of solid tumors, with the most acidic tumor edge being most predisposed to invasion (6). In our study, then, we sought to isolate the role of proton concentration on the tumor cell cycle independent of its role in tumor invasion. Future studies should replicate our findings in an environment where both growth and invasion are amendable to study, for example growth in cultured tissue slices.

In spite of some of the limitations pointed out above, our findings suggest that gliomas possess an environmental sensor for pH and adjust their growth rate accordingly in a feed-back manner. In light of this, it may be possible to disrupt this sensor, as we have done using quinine, and this in turn may be sufficient to disrupt tumor growth *in vivo.* Finally, while our studies were done in gliomas, it is possible that other solid tumors behave the same way and that our observed pH_e-dependent growth gradient may apply more broadly to other systemic cancers.

GRANTS

This research was funded by the following grants from the National Institutes of Health: R01 NS031234 and R01 NS036692 for HS, P30 NS047466 for the UAB Neuroscience Molecular Detection Core, and 5P30 AR048311 and 3P30 AI027767-22S1 for the UAB Comprehensive Flow Cytometry Core.

ACKNOWLEDGEMENTS

We would like to thank the UAB Neuroscience Molecular Detection Core, namely Terry L. Lewis, Gretta Jordan, and Jamie McNaught for their help with the spheroid paraffin embedding and sectioning. We would also like to thank the UAB Comprehensive Flow Cytometry Core and Enid Keyser for their help with the cell cycle analysis.

DISCLOSURES

The authors report no conflicts of interest, financial or otherwise.

AUTHOR CONTRIBUTIONS

AH, KAS, and HS conceived and planned the experiments; AH and KAS performed the experiments and analyzed the data; AH, KAS, and HS interpreted the results; AH prepared the figures; AH drafted the manuscript; AH and HS edited, revised, and approved the final manuscript.

LIST OF REFERENCES

1. Acker H, Carlsson J, Holtermann G, Nederman T, and Nylen T. Influence of glucose and buffer capacity in the culture medium on growth and pH in spheroids of human thyroid carcinoma and human glioma origin. *Cancer research* 47: 3504-3508, 1987.

2. Becchetti A. Ion channels and transporters in cancer. 1. Ion channels and cell proliferation in cancer. *American journal of physiology Cell physiology* 301: C255-265, 2011.

3. Berdiev BK, Xia J, McLean LA, Markert JM, Gillespie GY, Mapstone TB, Naren AP, Jovov B, Bubien JK, Ji HL, Fuller CM, Kirk KL, and Benos DJ. Acid-sensing ion channels in malignant gliomas. *The Journal of biological chemistry* 278: 15023-15034, 2003.

4. Chittajallu R, Chen Y, Wang H, Yuan X, Ghiani CA, Heckman T, McBain CJ, and Gallo V. Regulation of Kv1 subunit expression in oligodendrocyte progenitor cells and their role in G1/S phase progression of the cell cycle. *Proceedings of the National Academy of Sciences of the United States of America* 99: 2350-2355, 2002.

5. Cuddapah VA, Habela CW, Watkins S, Moore LS, Barclay TT, and Sontheimer H. Kinase activation of ClC-3 accelerates cytoplasmic condensation during mitotic cell rounding. *American journal of physiology Cell physiology* 302: C527-538, 2012.

6. Estrella V, Chen T, Lloyd M, Wojtkowiak J, Cornnell HH, Ibrahim-Hashim A, Bailey K, Balagurunathan Y, Rothberg JM, Sloane BF, Johnson J, Gatenby RA, and Gillies RJ. Acidity generated by the tumor microenvironment drives local invasion. *Cancer research* 73: 1524-1535, 2013.

7. Festjens N, Vanden Berghe T, and Vandenabeele P. Necrosis, a well-orchestrated form of cell demise: signalling cascades, important mediators and concomitant immune response. *Biochimica et biophysica acta* 1757: 1371-1387, 2006.

8. Flavahan WA, Wu Q, Hitomi M, Rahim N, Kim Y, Sloan AE, Weil RJ, Nakano I, Sarkaria JN, Stringer BW, Day BW, Li M, Lathia JD, Rich JN, and Hjelmeland AB. Brain tumor initiating cells adapt to restricted nutrition through preferential glucose uptake. *Nat Neurosci* 16: 1373-1382, 2013.

9. Garcia-Martin ML, Herigault G, Remy C, Farion R, Ballesteros P, Coles JA, Cerdan S, and Ziegler A. Mapping extracellular pH in rat brain gliomas in vivo by 1H magnetic resonance spectroscopic imaging: comparison with maps of metabolites. *Cancer research* 61: 6524-6531, 2001.

10. Garcia-Martin ML, Martinez GV, Raghunand N, Sherry AD, Zhang S, and Gillies RJ. High resolution pH(e) imaging of rat glioma using pH-dependent relaxivity.

Magnetic resonance in medicine : official journal of the Society of Magnetic Resonance in Medicine / Society of Magnetic Resonance in Medicine 55: 309-315, 2006.

11. Gatenby RA, and Gillies RJ. A microenvironmental model of carcinogenesis. *Nature reviews Cancer* 8: 56-61, 2008.

12. Gatenby RA, and Gillies RJ. Why do cancers have high aerobic glycolysis? *Nature reviews Cancer* 4: 891-899, 2004.

13. Glitsch M. Protons and Ca2+: ionic allies in tumor progression? *Physiology (Bethesda, Md)* 26: 252-265, 2011.

14. Gourine AV, Kasymov V, Marina N, Tang F, Figueiredo MF, Lane S, Teschemacher AG, Spyer KM, Deisseroth K, and Kasparov S. Astrocytes control breathing through pH-dependent release of ATP. *Science (New York, NY)* 329: 571-575, 2010.

15. Grillon E, Farion R, Fablet K, De Waard M, Tse CM, Donowitz M, Remy C, and Coles JA. The spatial organization of proton and lactate transport in a rat brain tumor. *PloS one* 6: e17416, 2011.

16. Haas BR, and Sontheimer H. Inhibition of the Sodium-Potassium-Chloride Cotransporter Isoform-1 reduces glioma invasion. *Cancer research* 70: 5597-5606, 2010.

17. Hjelmeland AB, Wu Q, Heddleston JM, Choudhary GS, MacSwords J, Lathia JD, McLendon R, Lindner D, Sloan A, and Rich JN. Acidic stress promotes a glioma stem cell phenotype. *Cell death and differentiation* 18: 829-840, 2011.

18. Honasoge A, and Sontheimer H. Involvement of tumor acidification in brain cancer pathophysiology. *Frontiers in Physiology* 4: 2013.

19. Jakubovicz DE, Grinstein S, and Klip A. Cell swelling following recovery from acidification in C6 glioma cells: an in vitro model of postischemic brain edema. *Brain research* 435: 138-146, 1987.

20. Kapoor N, Bartoszewski R, Qadri YJ, Bebok Z, Bubien JK, Fuller CM, and Benos DJ. Knockdown of ASIC1 and epithelial sodium channel subunits inhibits glioblastoma whole cell current and cell migration. *The Journal of biological chemistry* 284: 24526-24541, 2009.

21. Lotshaw DP. Biophysical, pharmacological, and functional characteristics of cloned and native mammalian two-pore domain K+ channels. *Cell biochemistry and biophysics* 47: 209-256, 2007.

22. McFerrin MB, Turner KL, Cuddapah VA, and Sontheimer H. Differential role of IK and BK potassium channels as mediators of intrinsic and extrinsic apoptotic cell death. *American journal of physiology Cell physiology* 303: C1070-1078, 2012.

23. McLean LA, Roscoe J, Jorgensen NK, Gorin FA, and Cala PM. Malignant gliomas display altered pH regulation by NHE1 compared with nontransformed astrocytes. *American journal of physiology Cell physiology* 278: C676-688, 2000.

24. Meuth SG, Herrmann AM, Ip CW, Kanyshkova T, Bittner S, Weishaupt A, Budde T, and Wiendl H. The two-pore domain potassium channel TASK3 functionally impacts glioma cell death. *Journal of neuro-oncology* 87: 263-270, 2008.

25. Olsen ML, and Sontheimer H. Mislocalization of Kir channels in malignant glia. *Glia* 46: 63-73, 2004.

26. Ouadid-Ahidouch H, and Ahidouch A. K+ channel expression in human breast cancer cells: involvement in cell cycle regulation and carcinogenesis. *The Journal of membrane biology* 221: 1-6, 2008.

27. Oudard S, Boitier E, Miccoli L, Rousset S, Dutrillaux B, and Poupon MF. Gliomas are driven by glycolysis: putative roles of hexokinase, oxidative phosphorylation and mitochondrial ultrastructure. *Anticancer research* 17: 1903-1911, 1997.

28. Pappas CA, and Ransom BR. Depolarization-induced alkalinization (DIA) in rat hippocampal astrocytes. *Journal of neurophysiology* 72: 2816-2826, 1994.

29. Philippe JM, Dubois JM, Rouzaire-Dubois B, Cartron PF, Vallette F, and Morel N. Functional expression of V-ATPases in the plasma membrane of glial cells. *Glia* 37: 365-373, 2002.

30. Rooj AK, McNicholas CM, Bartoszewski R, Bebok Z, Benos DJ, and Fuller CM. Glioma-specific cation conductance regulates migration and cell cycle progression. *The Journal of biological chemistry* 287: 4053-4065, 2012.

31. Sontheimer H. A role for glutamate in growth and invasion of primary brain tumors. *Journal of neurochemistry* 105: 287-295, 2008.

32. Staub F, Baethmann A, Peters J, Weigt H, and Kempski O. Effects of lactacidosis on glial cell volume and viability. *Journal of cerebral blood flow and metabolism : official journal of the International Society of Cerebral Blood Flow and Metabolism* 10: 866-876, 1990.

33. Swietach P, Patiar S, Supuran CT, Harris AL, and Vaughan-Jones RD. The role of carbonic anhydrase 9 in regulating extracellular and intracellular ph in three-dimensional tumor cell growths. *J Biol Chem* 284: 20299-20310, 2009.

34. Webb BA, Chimenti M, Jacobson MP, and Barber DL. Dysregulated pH: a perfect storm for cancer progression. *Nature reviews Cancer* 11: 671-677, 2011.

35. Wemmie JA, Price MP, and Welsh MJ. Acid-sensing ion channels: advances, questions and therapeutic opportunities. *Trends in neurosciences* 29: 578-586, 2006.

36. Westphal M, and Lamszus K. The neurobiology of gliomas: from cell biology to the development of therapeutic approaches. *Nature reviews Neuroscience* 12: 495-508, 2011.

37. Xu L, Fukumura D, and Jain RK. Acidic extracellular pH induces vascular endothelial growth factor (VEGF) in human glioblastoma cells via ERK1/2 MAPK signaling pathway: mechanism of low pH-induced VEGF. *The Journal of biological chemistry* 277: 11368-11374, 2002.

CLC-3 ACTS AS A PLASMA MEMBRANE Cl^-/H^+ ANTIPORTER IN HUMAN GLIOMAS

by

AVINASH HONASOGE, KENNETH T. HOLT, VIVIAN Y. LIN,
AND HARALD SONTHEIMER

Submitted to *The Journal of General Physiology*

Format adapted for dissertation

ABSTRACT

Glioblastoma multiforme (GBM) is a highly aggressive and deadly primary brain cancer. It relies heavily on ion channels to shrink and expand in the confined brain space. One channel of major focus in glioma literature is ClC-3, a putative Cl^- channel highly expressed in GBM that is necessary for glioma cell migration and proliferation. Interestingly, GBM cells uniquely possess surface expression of ClC-3, a protein usually largely confined intracellularly to vesicles and endosomes and recently shown to act as a Cl^-/H^+ antiporter. We thus wondered if glioma ClC-3 surface expression resulted in H^+ movement and pH_i regulation in addition to its previously-described role as a Cl^- channel. Simultaneous perforated-patch and pH_i-sensitive fluorescent dye recordings revealed an electrogenic, chloride-dependent movement of protons in glioma cells. We next found that in Na^+ and K^+-free conditions, these glioma cells contained a pH_e-dependent reversal potential (E_{rev}), which is uncoupled at acidic pH_e, consistent with previously-described ClC-3 currents. ClC-3 knockdown glioma cells showed reduced pH_e-dependence of E_{rev}, reduced $[K^+]_o$-driven electrogenic movement of protons, and disrupted pH_i dynamics. Taken together, these data suggest endogenous surface expression of a mammalian Cl^+/H^+ antiporter and a novel role for ClC-3 in human glioma pathophysiology.

Keywords: ClC-3, glioma, pH, Cl^-/H^+ exchange, chloride transporter

INTRODUCTION

Gliomas are primary tumors of the brain that are highly invasive, prolific, and resistant to treatment; namely, the WHO Grade IV tumor GBM has a median survival of just over a year (Stupp et al., 2005). These tumor cells display striking ability to migrate and proliferate, due largely to an enhanced ability to volume regulate. Chloride and potassium channels help flux salt across the plasma membrane, which combined with water transport through aquaporins allows isotonic adjustment of cytoplasm (Watkins and Sontheimer, 2012). This chloride flux in particular aids in two aspects of glioma cell physiology: cell shrinkage and expansion squeezes glioma cells through the interstitium (Ransom et al., 2001; Watkins and Sontheimer, 2011), while premitotic condensation pushes them through the cell cycle (Cuddapah et al., 2012).

Of chloride channels, the best studied in gliomas are members of the CLC family. These proteins exist in mammalian cells as strict chloride channels, Cl^-/H^+ antiporters, or sometimes even both (Mindell, 2008). The channel members are usually expressed on the plasma membrane and flux chloride ions for cell migration, proliferation, salt balance, Cl^- homeostasis, and setting the membrane potential. Members that antiport Cl^- and H^+ are generally confined to intracellular compartments and serve to either acidify vesicles or neutralize the electric charge buildup of protons contained within those vesicles (Stauber et al., 2012). Functionally, this translates to pH and Cl^- regulation of vesicles (Stobrawa et al., 2001; Riazanski et al., 2011), governing debris degradation in lysosomes (Graves et

al., 2008), and bone resorption by osteoclasts (Lange et al., 2006). Interestingly, it appears that several of the CLC proteins falling into this antiporter subgroup (CLC-2, CLC-3, and CLC-5) are actually expressed on the glioma cell surface (Olsen et al., 2003). CLC-3 in particular has been shown to affect chloride flux and govern glioma cell movement and division, but the potential of these channels to alter pH in glioma cells has not been studied.

pH homeostasis is vital to the survival of all cells. Through a combination of buffering and transport, free protons are usually limited to submicromolar concentrations intracellularly. As a result, only small deviations in intracellular pH (pH_i) are required to effect drastic changes in cell physiology. Solid tumors are ripe for study in this regard, as their highly glycolytic metabolisms (known as the Warburg effect) makes them potent interstitial acidifiers (Gatenby and Gillies, 2004). This poses a special problem for tumor cells mired in a self-created acidic environment: how can they thrive despite themselves?

Gliomas face this same conundrum with the added wrinkle of a cramped and stagnant microenvironment of the brain. GBMs encounter proton concentrations far more heterogeneous than the average brain due in part to the Warburg effect, in which cancer cells choose glycolysis over oxidative phosphorylation even in normoxic conditions, leading to an overproduction of protons (Vander Heiden et al., 2009). To adapt, they have evolved several proton transport mechanisms beyond their astrocytic counterparts, most notably the Na^+/H^+ exchanger NHE1 (McLean et al., 2000), which provide additional methods of proton extrusion.

We thus wondered if CLC antiporters, which are highly expressed on glioma cells and especially on lamellipodia (McFerrin and Sontheimer, 2006), flux protons in addition to chloride, and if this antiport might make CLC proteins relevant as pH_i regulators in addition to their previously explored roles in chloride movement. As CLC antiporters are electrogenic, we were able to use electrophysiological methods with simultaneous fluorescence imaging to test both if glioma cell pH_i regulation was electrogenic and if it depended on chloride. In cation-free conditions, we found currents similar to those in previously published CLC overexpression models (Matsuda et al., 2008; Matsuda et al., 2010). Knockdown of a highly expressed CLC protein in gliomas, ClC-3, significantly ablated these currents. Using $[K^+]_o$ to change V_m, we drove protons out of glioma cells in a ClC-3-dependent manner. Finally, using confocal microscopy, we determined that ClC-3 regulated the lagging-leading edge pH_i gradient of glioma cells. Therefore we propose that ClC-3 acts as a functional Cl^-/H^+ antiporter on the surface of glioma cells, and in doing so couples chloride movement with pH_i regulation.

MATERIALS AND METHODS

Electrophysiology

For all recordings, patch pipettes were pulled to 4- to 6-MΩ from thin-walled borosilicate glass using an upright puller, and an Axopatch 200B (Molecular Devices) amplifier stimulated the cells with data converted to digital signal by a Digidata 1440A (Molecular Devices). The tips were then lowered and suction applied to form a GΩ seal. For whole-cell patch clamp recordings, both the bath solutions and the patch pipette were Na^+- and K^+-free (see *Solutions* section). Cells were either: 1) held at -40 mV and stepped in 20 mV increments from -160 to +100 mV, or 2) held at 0 mV and ramped from -200 to +120 mV, depending on the experiment. Individual steps or ramps from different bath conditions were analyzed for E_{rev}. A 3M KCl agar salt bridge connected the bath to the ground electrode to stabilize recordings. Cells were compensated to 80% for capacitance and series resistance.

For the simultaneous perforated-patch/fluorescence imaging recordings, glioma cells on coverslips were loaded with BCECF AM dye (Teflabs, 0062) and visualized with a Zeiss Axiovert 200M microscope. Pipettes were filled with lightly buffered 1 mM HEPES pipette solution (see *Solutions* section) containing 120 μg/ml amphotericin B (Sigma, A9528). Cells were placed in a continuously barrel-applied SPF bath containing 1 mM amiloride HCl (Sigma, A7410). At least 5 minutes were required for sufficient break-in (cell resistance < 500 MΩ and series resistance < 30 MΩ) by the ionophore to allow electrical access to the cell. The cells were held at a

-40 mV baseline and left uncompensated as any amount of compensation caused ringing oscillations and/or seal rupture. Any cells with series resistance >30 MΩ 15 minutes post-GΩ seal were discarded.

Fluorescence imaging

To measure simultaneous fluorescence for the perforated-patch recordings, cells were loaded with 2 μM BCECF AM, a dual-excitation, single-emission ratiometric pH-sensitive dye. Light from an X-Cite 120Q mercury arc lamp (Lumen Dynamics) was fed through a liquid light guide and into a filter wheel (Lambda 10-2 filter wheel, Sutter Instruments) mounted on the back of the microscope. This wheel held excitation filters of 440/20 and 495/10 nm. After passing through this filter, light reflected onto the coverslip and emissions were collected through a 515 nm cutoff dichroic mirror and 540/60 emissions filter mounted in a cube in the filter turret underneath the stage, and then was collected by a cooled CCD camera (CoolSNAP HQ^2, Photometrics). Cells were excited by 400 ms exposures at each excitation wavelength and images were captured every 10 s. The 495/440 emission ratio was calibrated using high $[K^+]_o$/nigericin bath solution standards at pH 6.5, 7.2, and 7.9 and found to be linear over this range ($R^2 = 0.9357$).

Immunostaining visualization, V_m-dependent pH_i experiments, and pH_i gradient experiments were all performed on an Olympus Fluoview FV1000 confocal microscope equipped with 4 diode lasers at 405, 473, 559, and 635 nm. For the immunostaining experiments, cells were visualized using a 40x air objective (NA 0.75, Olympus), excited with the diode lasers and light collected with bandpass

filters at the following wavelengths: DAPI 405 ex, 430-455 em; phalloidin 559 ex, 575-620 em; ClC-3 635 ex, 655-755 em. For the pH_i experiments, glioma cells were loaded with 2 μM carboxy SNARF-1 AM (Molecular Probes, C1271), a single-excitation, dual-emission ratiometric pH_i-sensitive dye. Cells were excited using a 559 nm diode laser and light was collected using 575-620 nm and 655-755 nm bandpass filters through a 40x water immersion objective (NA 0.8, Olympus). The ratio of long/short emission wavelengths was found to linearly correspond to pH_i using high $[K^+]_o$/nigericin bath solution standards at pH 7.4, 8.1, and 8.8 (R^2 = 0.9987).

For the V_m-dependent pH_i experiments, different SPF bath solutions were flowed at room temperature into a chamber containing glioma cells on coverslips using a Dynamax peristaltic pump (Rainin, RP-1). The flow rate was 1.6 mL/min except during condition changes, when the chamber was flushed with the new bath solution at 3.75 mL/min for one minute.

For the pH_i gradient experiments, 100 μl of cells at a concentration of 1-3x10^5 cells/ml were loaded into the channel of μ-slides (Ibidi, 80106), with an additional 600 μl of DMEM/F12 media added to each well, and allowed to adhere overnight. The next day, 40 μl of MEM containing carboxy SNARF-1 AM (4 μM in DMSO) and EGF (10 ng/ml in dH_2O with 0.2% BSA) was injected into one end of the channel to provide both a loading of pH_i-sensitive dye and to induce chemotaxis. Cells were incubated in this solution for 1 hour prior to imaging. Next, we used

confocal microscopy to detect pH_i through a 40x water immersion lens using an upright microscope.

pH_i analysis

For the V_m-dependent pH_i experiments, cells were imaged every 20 s at 800 x 800 resolution. Images were analyzed using ImageJ by taking a ratio of the long to short wavelength channels and placing regions of interest on all cells that remained within their selected regions for the duration of the experiment (~30 minutes). Cell pH_i was averaged across the last 5 recordings from each bath condition.

For the pH_i gradient experiments, each μ-slide contained at least 10 ROI imaged at 1024 x 1024 resolution. Then, three ROI were chosen at both the lagging and leading edges within each cell that demonstrated clear directionality, while taking care to avoid the nucleus, as described prior (Martin et al., 2011). The mean values of the carboxy SNARF-1 ratios from the three regions were averaged to form one leading and one lagging pH_i value per cell.

Cell culture

D54 and U251 cells are glioma cell lines derived from WHO grade IV GBM tumors. The D54 cells were gifted to us from Dr. D. Bigner of Duke University. These cells were cultured in DMEM/F12 media (Life Technologies, 11330) with 7% FBS. The Jx22 and Jx14 cells are from patient-derived primary brain tumors xenografted into and passaged by flank injections of nude, athymic mice as previously described (Giannini et al., 2005; Sarkaria et al., 2007). Before tumor

lysates were created, these xenolines were cultured as gliospheres in Neurobasal A media (Life Technologies, 10888022) lacking FBS to prevent cell attachment.

Knockdown of ClC-3

To constitutively knock down ClC-3, a pGIPZ lentiviral vector containing either a hairpin sequence targeting CLCN3 or a scrambled negative control (Open Biosystems) was transfected into D54 human glioma cells as previously described (Cuddapah et al., 2012). These cells were also stably transfected with EGFP as previously described (Habela et al., 2008). Both scrambled and knockdown cells were maintained on puromycin at 10 μg/ml.

Immunostaining

Cells were cultured on round 12-mm coverslips (Fisher) in a 24-well plate for 2 days, washed with pH 7.4 SPF bath solution (see *Solutions* section), and fixed with 4% paraformaldehyde for 10 min. Cells were then blocked and permeabilized in SPF bath solution containing 10% normal goat serum and 0.1% Triton X-100 for 30 min at room temperature, followed by overnight incubation in a rabbit polyclonal anti-ClC-3 antibody (Alomone Labs, 1:250) at 4 °C. After overnight incubation, cells were washed with a 1:3 dilution of the blocking buffer in SPF bath solution and subsequently incubated in Alexa Fluor 633 goat anti-rabbit secondary antibody (Invitrogen, 1:500) for 2 h at room temperature. Cells were washed again with the diluted blocking buffer, then incubated with Alexa Fluor 546 Phalloidin (Invitrogen, 1:50) for 20 min at room temperature. Following further washing with the diluted blocking buffer, cells were incubated with 4′,6-diamidino-2-phenylindole

(DAPI, 1:2000) for 5 min at room temperature. After a final washing, coverslips were mounted onto 3 x 1-inch x 1-mm glass slides (Fisher) with Fluoromount (Sigma) and stored at 4 °C.

Western blot analysis

Cells were lysed using RIPA buffer and the protein was diluted to 15 µg/sample. Sample buffer (60% glycerol, 300 mm Tris, pH 6.8, 12 mm EDTA, 12% SDS, 864 mm 2-mercaptoethanol, 0.05% bromphenol blue) was added to samples loaded into 15-well 4-20% gradient pre-cast SDS-polyacrylamide gels (Bio-Rad), and the protein was separated at 150 mV for 1 hour. Gels were then transferred to polyvinylidene difluoride paper (Millipore) at 100 mV for 1 hour. Blots were blocked with blocking buffer TBS-T (10% nonfat dried milk, Tris-buffered saline, and 0.1% Tween-20) for 1 hour at room temperature, followed by incubation in rabbit anti-ClC-3 antibody (Alpha Diagnostic International, 1:1500 or Alomone labs, 1:250) overnight at 4° C. After a wash in TBS-T the blots were incubated with horseradish peroxidase-conjugated secondary antibodies (Santa Cruz Biotechnology; 1:1500) for 1 hour at room temperature. Blots were developed with Supersignal West Femto (Thermo Scientific) or Western Blotting Luminol Reagent (Santa Cruz) and imaged on a 4000MM Image Station (Eastman Kodak). Glyceraldehyde-3-phosphate dehydrogenase (GAPDH) was used as a loading control and probed for with a mouse anti-GAPDH primary antibody (Abcam, 1:5000).

Solution composition

All remaining chemicals found in solutions were purchased from Sigma Aldrich. Pipette solutions were adjusted to 300 mOsm and contained the following (in mM): 1) CsCl solution 50 CsCl, 50 TEA acetate, 30 HEPES, 10 EGTA, pH 7.2 adjusted with CsOH; 2) TEA Cl solution 40 TEA Cl, 30 MOPS, 10 EGTA, and either 0 or 3 $CaCl_2$, pH 7.2 adjusted with CsOH; 3) perforated-patch solution 140 KCl, 10 EGTA, 9 NaCl, 1 $MgCl_2$, 1 HEPES, 120 µg/ml amphotericin B dissolved in DMSO at 1:500 concentration from stock, pH 7.2 adjusted with NaOH.

Bath solutions were adjusted to 320 mOsm and contained the following (in mM): 1) TEA Cl solution 40 TEA Cl, 30 buffer (MES, HEPES, MOPS, or Tris as appropriate), 1 $CaCl_2$, pH 6.0-8.8 adjusted with Tris; 2) SPF solution 130 NaCl, 30 buffer, 5 KCl, 1 CaCl2, pH 7.4 with NaOH or HCl.

Statistics

All statistics and regressions were performed in GraphPad Prism 6. *, **, ***, and **** indicate $p < 0.05$, 0.01, 0.001, and 0.0001, respectively. All ANOVAs used Tukey's correction for multiple comparisons, and all unpaired t-tests were modified with Welch's correction.

RESULTS

Surface expression of ClC-3 protein on human glioma cells

Human glioma cells have robust expression of several ClC proteins, especially ClC-2, ClC-3, and ClC-5. Three lines of evidence indicate surface expression of ClC protein: 1) immunogold electron microscopy revealed localization of ClC-2, ClC-3, and ClC-5 on the surface of D54 human glioma cells (Olsen et al., 2003); 2) ClC-3 colocalized with phalloidin, a cortical actin protein (Cuddapah and Sontheimer, 2010; Cuddapah et al., 2012); and 3) ClC-3 localized to lipid rafts and was internalized with chlorotoxin application (McFerrin and Sontheimer, 2006). We confirmed ClC-3 protein expression in both human glioma cell lines and patient-derived xenograft tissue (Fig. 1A). Additionally, we found colocalization of ClC-3 with the plasma membrane in D54 human glioma cells (Fig. 1B). Taken together, these results indicate an unusual surface localization profile for ClC-3 on human glioma cells.

Electrogenic and Cl^--dependent pH_i regulation in human glioma cells

We next tested for ClC antiporter surface expression electrophysiologically. As all previously described proton regulators in human glioma cells are non-electrogenic (Honasoge and Sontheimer, 2013), we hypothesized that changes in pH_i driven by changes in voltage would suggest a role for pH_i regulation by the ClC family. To test this, we simultaneously voltage-clamped human glioma cells while measuring pH_i with an intracellular pH-sensitive dye, BCECF AM, in a manner previously employed on rat astrocytes (Bevensee et al., 1997). Electrical access was

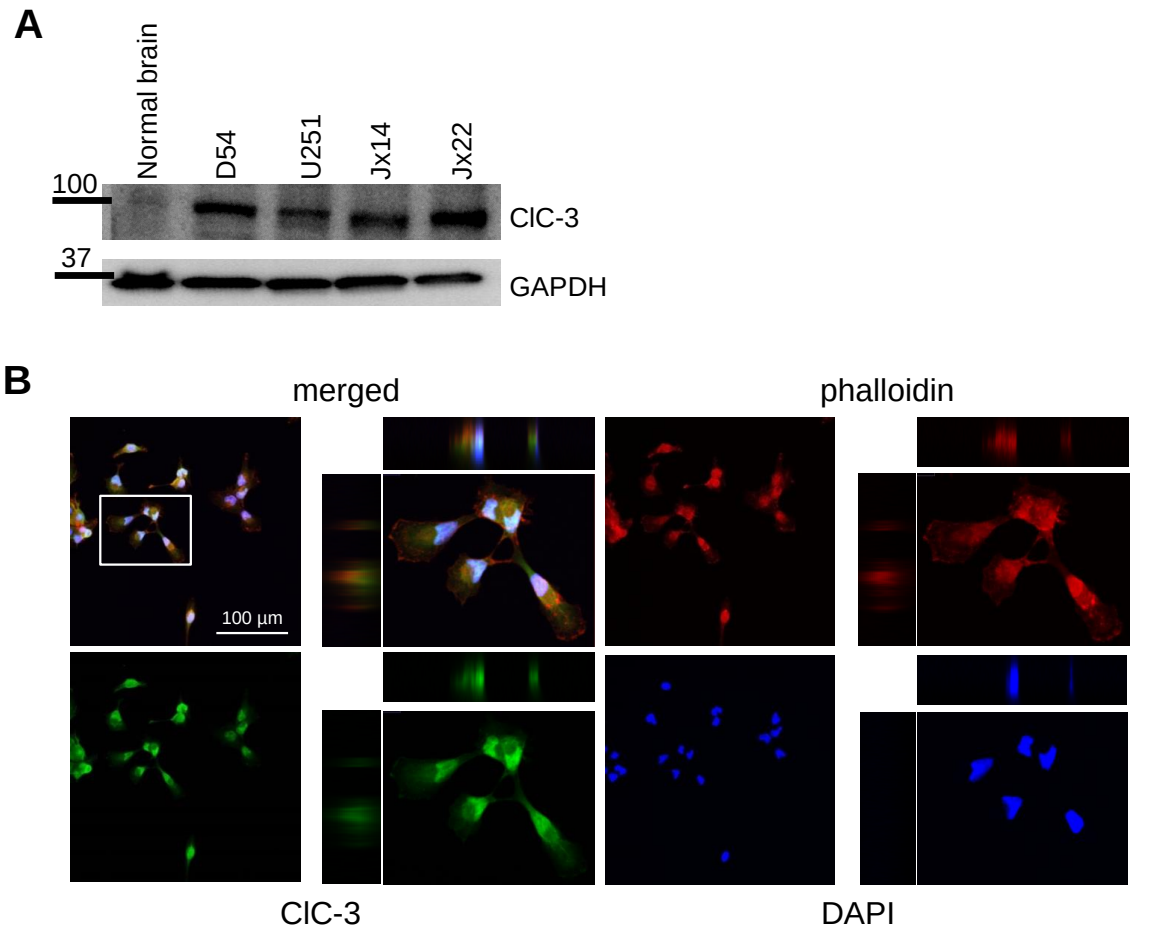

Fig. 1. Expression of ClC-3 protein in human glioma cells. *A,* Western blot demonstrating ClC-3 expression on two human glioma cell lines (D54 and U251) and two patient-derived human glioma xenografts (Jx14 and Jx22) passaged in the flanks of mice. *B*, Three-view immunostaining showing ClC-3 expression (green) in the D54 human glioma cell line and colocalization with phalloidin (red), which binds to cortical actin. DAPI (blue) was used to stain cell nuclei.

obtained via perforated-patch with a lightly-buffered pipette solution containing amphotericin B (120 μg/ml) to limit ionic diffusion. The cells were plated on coverslips and placed in a HCO_3^--free bath containing 1 mM amiloride HCl to block the sodium-proton exchanger NHE1 and allow chronic acidification. Upon depolarization to +60 mV for 5 minutes, the perforated-patched cells resisted the amiloride-induced acidification versus control cells in the same field of view (Fig. 2, 0.014±0.006 pH/min difference; $p < 0.05$). Replacement of chloride with gluconate in the bath solution eliminated the effect ($p = 0.47$). Thus, in the presence of chronic acidification, there exists an electrogenic transport of protons through glioma cells that is chloride-dependent.

Human glioma cells have pH_e-dependent currents in Na^+ and K^+-free conditions

Ion transport in the CLC family is both complex and incompletely understood, owing to the "broken transporter" nature of several of the family members that leads to unusual stoichiometries (Accardi and Picollo, 2010). If the ClC proteins indeed have surface expression on human glioma cells, we should be able to isolate their currents by whole-cell patch clamp electrophysiology and test these characteristics. To this end, we used bath and pipette solutions lacking Na^+ and K^+ ions and including TEA as both a cation replacement and to block residual chloride-independent conductance (Fig. 3). We also included 200 μM 5-nitro-2-(3-phenylpropylamino) benzoic acid (NPPB) in an attempt to inhibit any additional chloride leak currents and maximize the input of protons on E_{rev}. Glioma cells were patched and the pipette solution allowed to dialyze before voltage ramps were

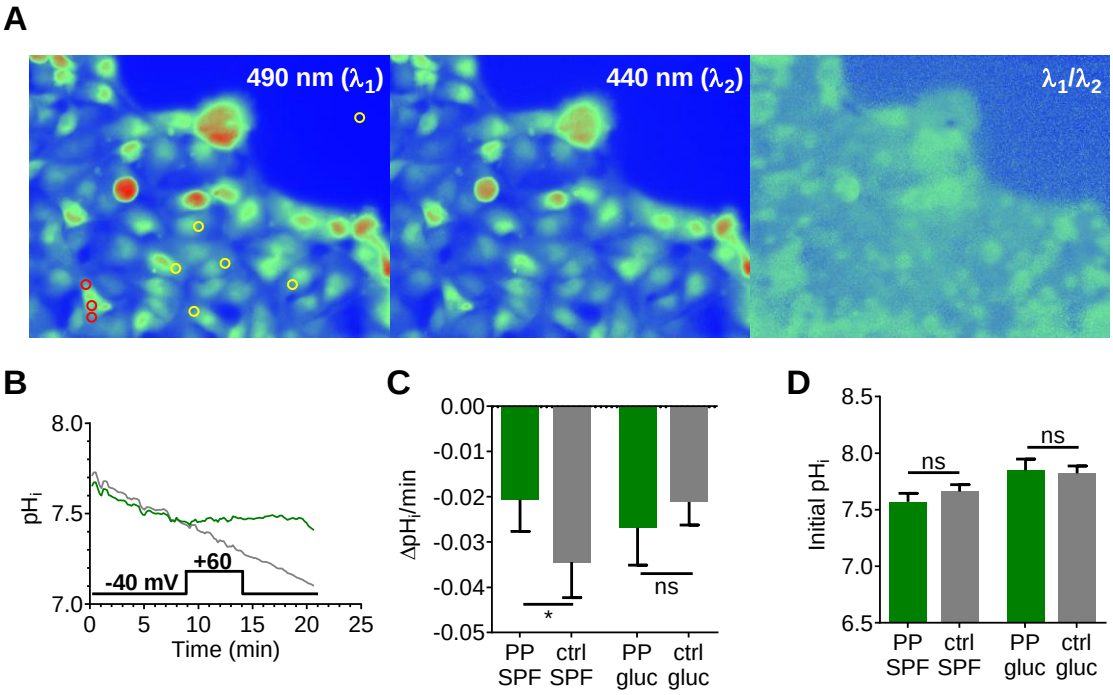

Fig. 2. Electrogenic movement of protons in human glioma cells. A, Representative field of view of D54 human glioma cells on a coverslip. Cells were loaded with 2 µM BCECF-AM dye and ratiometrically imaged with simultaneous voltage clamp recording of a perforated-patched cell (red ROI) and monitoring of several more control cells (yellow ROI). B, Smoothed pHi traces from the averaged perforated-patched (PP, green) and control (ctrl, gray) cells from the field of view in A. 1 mM amiloride was constantly present in the bath solution and provided a chronic acid load on all cells. The PP cell was stepped from -40 to +60 mV and held for 5 mins. C, Comparison of PP and ctrl cells showed a decreased acidification rate in chloride-containing SPF bath ($t = 2.48$, $p = 0.031$) but not low chloride gluconate bath ($t = 0.763$, $p = 0.47$). D, Initial pHi of PP and ctrl cells was not different in either SPF ($t = 1.36$, $p = 0.20$) or gluconate ($t = 0.29$, $p = 0.78$) bath conditions. $n \geq 7$ cells for each condition. Bars represent mean ± s.e.m.

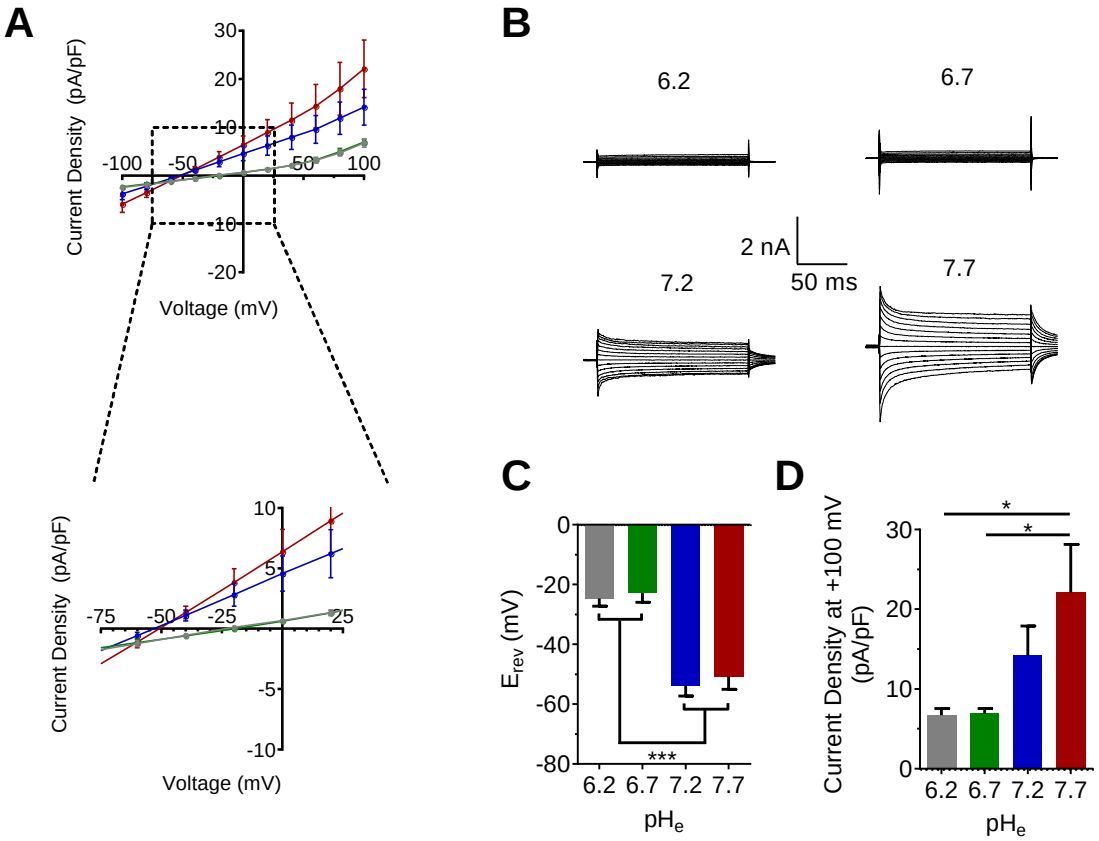

Fig. 3. pH$_e$-dependent E$_{rev}$ and current density in human glioma cells. *A,* I-V curves of whole-cell patch-clamped D54 human glioma cells at different pH$_e$ with a zoomed inset to show E$_{rev}$ at pH$_e$ 6.2 (gray), 6.7 (green), 7.2 (blue), and 7.7 (red). *B,* Representative traces of D54 glioma cells stepped from -160 to +100 mV (+20 mV steps). *C*, Quantification of E$_{rev}$ at varying pH$_e$. E$_{rev}$ was calculated from a linear extrapolation of the two voltage steps straddling zero current and determining the x-intercept of that line (one-way ANOVA, $F_{3,19} = 22.67$, $p < 0.0001$). *D,* Quantification of the current density at +100 mV (one-way ANOVA, $F_{3,19} = 3.855$, $p = 0.026$) $n \geq 5$ cells for all conditions. Bars represent mean ± s.e.m.

applied while altering the proton concentration in a physiological range (pH_e 6.2-7.7). We first found that shifts in pH_e were capable of producing shifts in E_{rev}, hinting at proton permeation. The largest shift was between pH_e 6.7 and 7.2, where a 0.5 pH unit change (Nernstian shift of 30 mV) moved E_{rev} by 30.9±4.8 mV (Fig. 3c, $p < 0.0001$, one-way ANOVA). The same logarithmic jumps from 6.2 to 6.7 and 7.2 to 7.7 failed to move E_{rev} similarly (-1.86±5.05 mV and -2.84±4.82 mV, respectively; $p > 0.05$). These results are consistent with prior overexpression studies of human ClC-3 in particular, which possesses three properties: 1) it permeates protons (Matsuda et al., 2008); 2) its Cl^-/H^+ antiport activity is uncoupled at acidic pH_e (Matsuda et al., 2010); and 3) it is gated by acidic pH_e (Matsuda et al., 2008; Matsuda et al., 2010). Finally, conductance at +100 mV was smallest at the most acidic pH_e. Taken together, there exists evidence that the ClC-3 on glioma cells permeates protons.

Knockdown of ClC-3 in human glioma cells ablates their proton-dependent properties

To determine if ClC-3 was responsible for the proton permeation in human glioma cells, we used an inducible ClC-3 shRNA knockdown of D54 human glioma cells tied to eGFP and compared it to a scrambled shRNA control (Fig. 5). Immunostaining and Western blot confirmed downregulation of both ClC-3 protein and surface expression (Fig. 4). Again using Na^+ and K^+-free conditions, knockdown of ClC-3 significantly ablated the pH_e-dependence of E_{rev} in glioma cells especially at the most alkaline pH_e (Fig. 5b, $p < 0.05$), consistent with a decrease in reliance on the E_{rev} of H^+ and resembling the signature ClC-3 currents described prior. Thus, it

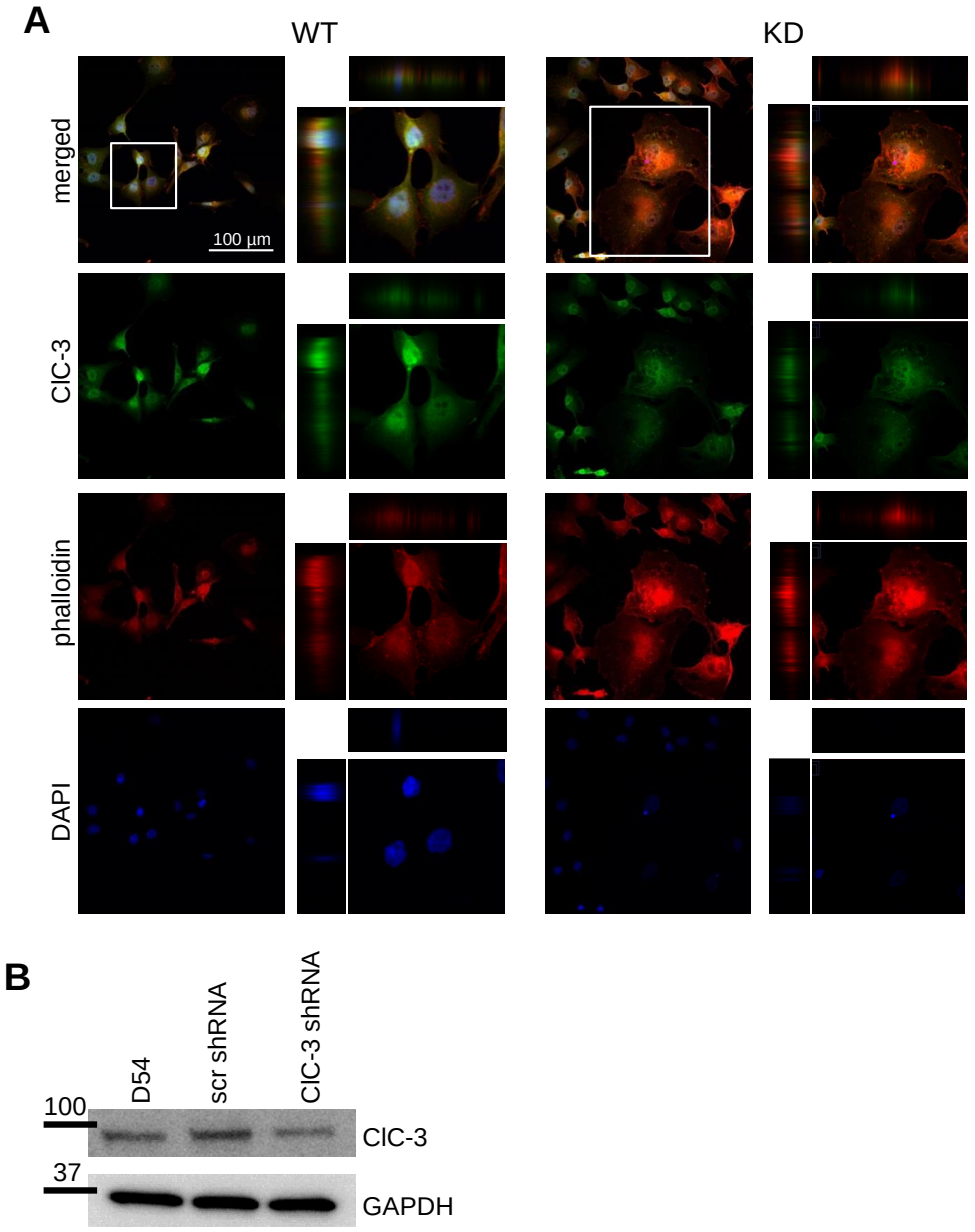

Fig. 4. Knockdown of ClC-3 protein in human glioma cells. *A*, Three-view immunostaining of ClC-3 WT and KD human glioma cells for ClC-3 (green), cortical actin (phalloidin, red), and cell nuclei (DAPI, blue). The cells containing knockdown shRNA were notably flatter and more spread out than their scrambled shRNA counterparts. *B*, Western blot demonstrating ClC-3 protein knockdown in D54 human glioma cells expressing a ClC-3 targeting shRNA construct (KD) versus D54 cells with scrambled (scr) shRNA (WT) or no construct.

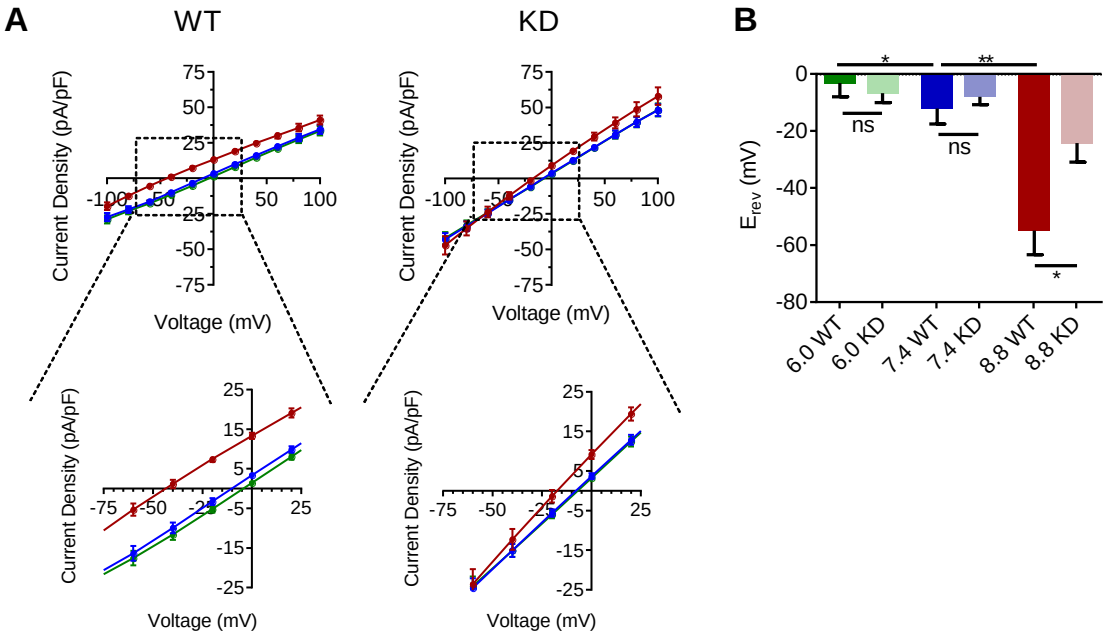

Fig. 5. ClC-3 determines pH_e-dependence of glioma cells. *A,* I-V plots of whole-cell patch-clamped wild-type (WT) and knockdown (KD) D54 human glioma cells with zoomed insets to show E_{rev} at pH_e 6.0 (green), 7.4 (blue), and 8.8 (red). *B*, Comparison of E_{rev} between pH_e groups for both WT and KD. WT cells showed their most leftward-shifted E_{rev} at pH_e 8.8 (RM one-way ANOVA between pH_e 6.0, 7.4, and 8.8, $F_{1.084, 7.588} = 28.79$, $p = 0.0007$), an effect that was diminished in the KD cells (t-test between WT and KD in each column, $t = 2.819$ at pH_e 8.8, $p = 0.015$). $n \geq 7$ cells for each condition. Bars represent mean ± s.e.m.

appears that the pH_e-dependence of E_{rev} of human glioma cells is also dependent on ClC-3 expression.

$[K^+]_o$-stimulated ClC-3-dependent alkalinization of human glioma cells

We next attempted to electrogenically regulate the pH_i of glioma cells without disrupting the cell membrane and postulated that any electrogenically active pH_i regulation depended on ClC-3 (Fig. 6). To enhance potential pH_i shifts, we took advantage of two biophysical properties of these glioma cells. Firstly, from our prior experiments, we found the largest conductance and most leftward-shifted E_{rev} of ClC-3 at the most alkaline pH_e of 8.8, consistent with H^+ permeation of the cell membrane. We combined this knowledge with the well-characterized K^+ permeation of the glioma cell membrane (Weaver et al., 2006; Turner et al., 2014) to hyper- and depolarize the cells by altering $[K^+]_o$ while maximizing potential pH_i shifts by placing the cells in pH_e 8.8 bath, thus maximizing conductance (Fig. 6a). A previous study showed that glioma cells are most hyperpolarized at alkaline pH_e largely due to an opening of pH_e-dependent K^+ channels, which also maximized our influence on the cell V_m at pH_e 8.8 (Honasoge et al., 2013). In tandem, by opening ClC-3 maximally at an alkaline pH_e and by altering $[K^+]_o$, we were able to detect changes in pH_i on populations of glioma cells without patch pipette intervention (Fig. 6b).

These changes were detected by perfusing coverslips coated with D54 human glioma cells and taking the ratio of two wavelengths of the loaded carboxy SNARF-1 AM dye. Starting in a baseline bath solution with 5 mM $[K^+]_o$, cells were

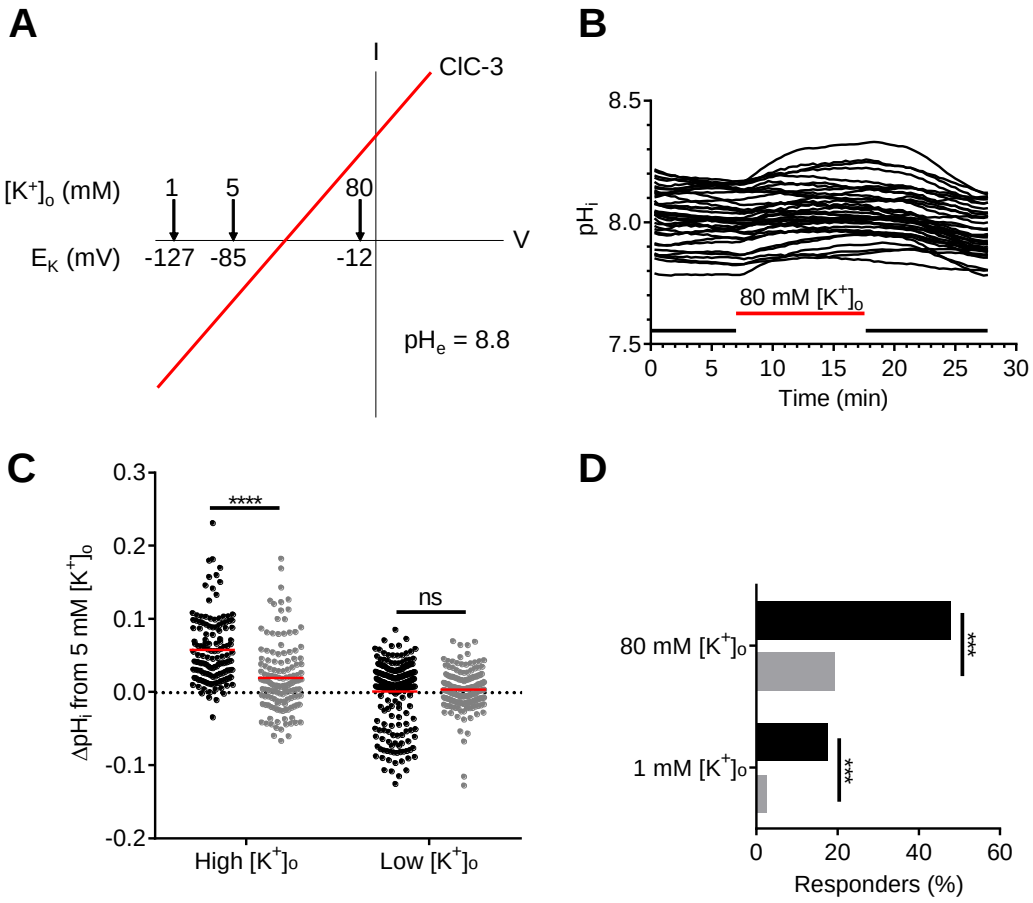

Fig. 6. ClC-3 is electrogenically driven by altered $[K^+]_o$. *A,* Schematic of conditions allowing maximal $[K^+]_o$-induced hyper- and depolarizations in human glioma cells. *B,* Representative plot monitoring the pH_i of all cells within the field of view of a D54 human glioma cells on a coverslip. *C,* Quantification of pH_i shifts from baseline for both ClC-3 wild-type (black) and knockdown (gray) D54 glioma cells to 80 mM $[K^+]_o$ ($t = 7.038$, $p < 0.0001$) and 1 mM $[K^+]_o$ ($t = 0.692$, $p = 0.4895$) conditions. *D,* Percentage of cells that shifted more than +0.05 or -0.05 pH_i units when moved to 80 mM $[K^+]_o$ or 1 mM $[K^+]_o$, respectively ($p < 0.001$ for each WT versus KD, Fisher's exact test). $n \geq 138$ cells for all four conditions. Bars represent mean ± s.e.m.

either next exposed to high $[K^+]_o$ (80 mM) or low $[K^+]_o$ (1 mM) and then re-perfused with 5 mM $[K^+]_o$. We hypothesized that the high $[K^+]_o$ condition would depolarize the cells, electrogenically stimulating ClC-3 and causing an efflux of H^+ with a rise in pH_i. Consistent with this hypothesis, control glioma cells with scrambled shRNA significantly raised their pH_i at high $[K^+]_o$ (Fig. 6c, 0.057±0.004 pH units), an effect that was diminished in the ClC-3 knockdown cells (0.019±0.004 pH units, $p < 0.0001$ versus control, two-way ANOVA). When averaged, we saw no significant low $[K^+]_o$-induced acidification in either wild-type or knockdown cells (Fig. 6c, $p > 0.05$, two-way ANOVA). We next analyzed both high $[K^+]_o$ and low $[K^+]_o$ groups for "large" responders, defined as $\Delta pH_i > \pm 0.05$ from medium $[K^+]_o$ to high and low $[K^+]_o$, respectively (Fig. 6d). Knockdown of ClC-3 significantly decreased the percentage of large responders with both 80 mM $[K^+]_o$ (47.8% versus 19.4%) and 1 mM $[K^+]_o$ (17.7% versus 2.74%) stimulations ($p < 0.001$ for each, Fisher's exact test). This decrease of pH_i by low $[K^+]_o$ represents uphill movement of protons against their gradient, from an alkalinized extracellular environment to a relatively acidic intracellular one. Thus, ClC-3 electrogenically moves H^+ ions across the membrane of human glioma cells and can be stimulated either via voltage clamp or by altering $[K^+]_o$.

Glioma cells contain pH_i gradients that are enhanced by ClC-3 knockdown

Highly migratory cells are capable of creating pH_i gradients that aid in their orientation and migration. For instance, melanoma cells localize NHE1 to their leading edge, causing focal intracellular alkalinization which then can regulate both

the cytoskeleton and cell adhesion (Martin et al., 2011; Ludwig et al., 2013). Knockdown of NHE1 in these cells disrupted the pH_i gradient and consequently the cell's orientation and migration. We wondered if glioma cells possess similar intracellular pH gradients and if ClC-3 would affect them. It has been prior demonstrated that ClC-3 knockdown decreases glioma cell migration (Cuddapah and Sontheimer, 2010), and it is possible a component of that impaired migration is an altered pH_i gradient. Additionally, given that ClC-3 selectively localizes to the leading edge of glioma cells (McFerrin and Sontheimer, 2006), we hypothesized that a knockdown of ClC-3 might specifically alter leading edge pH_i. To test these hypotheses we plated cells into μ-slide capillaries and loaded one well with both epidermal growth factor (EGF) to serve as a chemoattractant and carboxy SNARF-1 AM to monitor pH_i (Fig. 7a). Using carboxy SNARF-1 allowed us to ratiometrically monitor pH_i and despite potential uneven loading of cells across the gradient (Fig. 7a). Analyzed cells were those that demonstrated clear directionality. We first found human glioma cells possess a pH_i gradient (Fig. 7b) similar to the one found prior in melanoma cells (Martin et al., 2011). Next, we compared each edge separately (Fig. 7c) and found no difference in lagging edge pH_i but a significant increase in leading edge pH_i in knockdown versus wild-type ClC-3 glioma cells ($p < 0.0001$, one-way ANOVA). Thus, ClC-3 specifically affects leading edge pH_i in glioma cells.

We further hypothesized that since the pH_i alterations were limited to the leading edge, any covariation between leading and lagging edge pHi could be disrupted in ClC-3 knockdown cells. To test this, we analyzed plots comparing

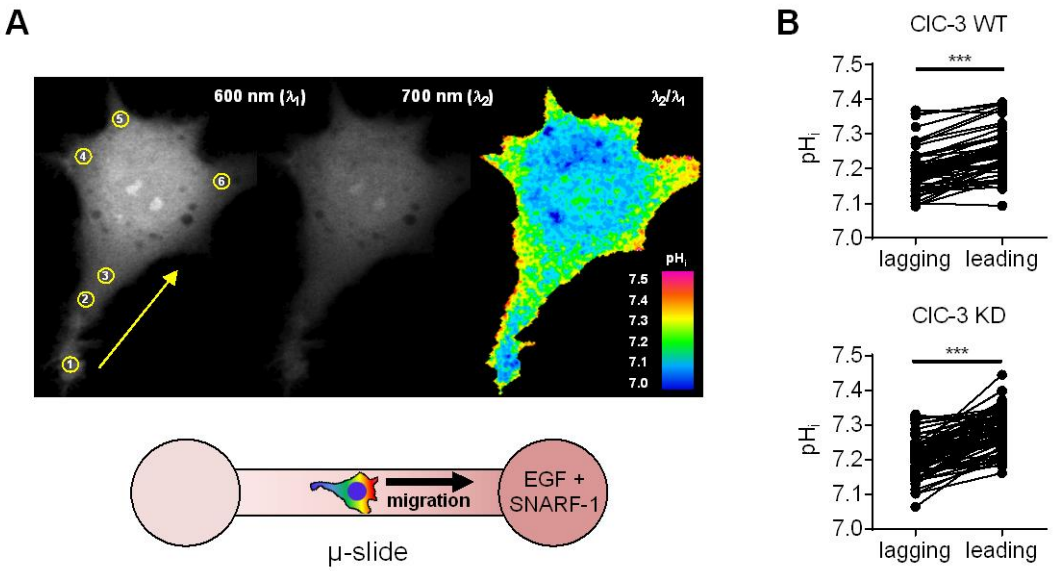

Fig. 7. Disruption of leading edge pH_i and pH_i covariation in ClC-3 knockdown glioma cells. *A,* Representative D54 human glioma cell possessing clear leading-lagging directionality. Cells were imaged after a 1-hour incubation in a μ-slide gradient where one well contained EGF-enriched minimal essential media that also had 2 μM SNARF-1 AM dye to monitor pH_i. Three ROI were chosen at each edge and averaged. *B,* Paired comparison of leading and lagging edges for both ClC-3 WT ($t = 11.47$, $p < 0.0001$) and KD ($t = 13.07$, $p < 0.0001$) cells.

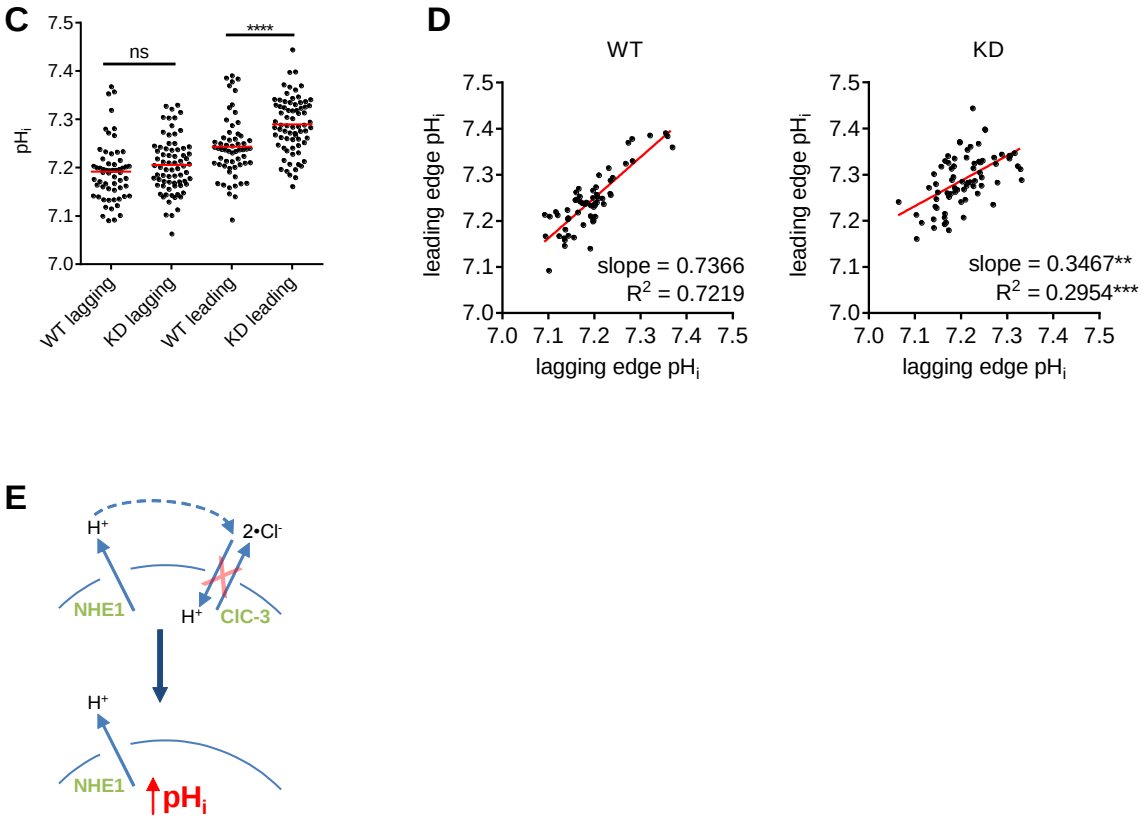

Fig. 7 cont'd. Disruption of leading edge pH_i and pH_i covariation in ClC-3 knockdown. *C,* Quantification of pH_i for WT and KD cells shows a difference in the leading ($t = 4.340$, $p < 0.0001$) but not lagging ($t = 1.296$, $p = 0.20$) edge. *D,* Correlation of leading and lagging edge pH_i in ClC-3 WT and KD cells. KD cells possessed both a shallower slope ($F_{1,129} = 7.024$, $p = 0.009$, ANCOVA) and a lower r value ($z = 3.62$, $p = 0.0001$, Fisher's r-to-Z transformation). *E,* Proposed mechanism for ClC-3-mediated acidification of the leading edge of glioma cells. $n \geq 60$ cells for each condition. Bars represent mean ± s.e.m.

leading and lagging edge pH_i in each cell (Fig. 7d). In the control cells, each marginal increase of pH by one unit at the lagging edge corresponded to a 0.88 ±0.07 unit pH increase at the leading edge. In contrast, the knockdown cells had only a 0.55 ±0.10 pH unit increase at the leading edge over that same span, a significantly shallower slope ($p < 0.01$, ANCOVA). Additionally, while both sets of data fit linear regressions ($p < 0.0001$ for each line), the correlation of lagging to leading edge was significantly less in the ClC-3 knockdown cells ($p < 0.001$, Fisher's r-to-Z transformation). These data suggest that ClC-3 acidifies glioma cells specifically at the leading edge. In Fig. 7e we propose a mechanism for this phenomenon in which ClC-3 utilizes the gradient generated by NHE1 and other proton extruders to increase the driving force of Cl^- extrusion at the leading edge of the cell. Knockdown of ClC-3 clamps the leading edge of cells to an abnormally high pH_i due to less shunting of the proton gradient, thus also preventing covariation of the leading edge with the lagging edge.

DISCUSSION

Robust pH regulation serves as one of the defining characteristics of cancer cells and separates them from their non-tumor counterparts; the self-created environment of inhospitably high proton concentrations would severely curb tumor cell physiology were it not for the many upregulated proton transporters and pumps. Here, we are proposing that a highly-expressed chloride channel on glioma cells functions as an additional proton pathway through the cell membrane. Using electrophysiological intervention and genetic manipulation combined with simultaneous pH_i imaging, we demonstrate that human glioma cells possess electrogenic transport of protons through the ClC-3 chloride antiporter. This is a novel finding for several reasons. First, we described endogenous cell-surface expression of a ClC transporter, ClC-3, that is usually confined to intracellular compartments. We believe this is one of the first demonstrations of high steady-state ClC-3 surface expression in mammalian cells. Next, we showed that ClC-3 moves both chloride and protons in a voltage-driven manner. Finally, we demonstrated that ClC-3 H^+ movement serves a biological purpose as it can affect the pH_i of glioma cells, especially at the leading edge.

An outstanding question is why glioma cells in particular are capable of such high surface expression of ClC-3. Endosomes can carry adhesive proteins that direct cell migration to the cell surface (Ulrich and Heisenberg, 2009; Schiefermeier et al., 2011), and rapid membrane turnover at the leading edge is a hallmark of fast migrating cells (Howes et al., 2010). Usually, any surface ClC-3 is rapidly

internalized into endosomes, relying upon a clathrin-interacting N-terminus; these endosomes can then be recycled to the surface or trafficked into lysosomes and result in only 6% surface expression (Zhao et al., 2007). As glioma cells are rapidly migrating, it is possible that the endosomal recycling (and thus surface localization) of ClC-3 protein is enhanced. Additionally, increased $[Ca^{2+}]_i$ also caused translocation of hClC-3 to the cell membrane in a mammalian transfection model (Huang et al., 2001); as glioma cells have high resting $[Ca^{2+}]_i$ (Manning et al., 2000), this could serve to increase steady-state surface ClC-3 expression.

It is unclear what other roles this novel proton pathway could play. For instance, it might intertwine chloride-dependent and electrogenic glioma processes with pH_i regulation in a previously-undescribed manner. Proton and chloride transport are vital aspects of cancer cell migration and invasiveness, and their regulators both localize to the invadopodia. This could result in three possible roles for ClC-3: 1) ClC-3 moves chloride and protons in directions where both movements are beneficial; 2) ClC-3 works in tandem with proton transporters to shuttle protons out of an acidic cell at the cost of cell swelling; 3) ClC-3 acidifies tumor cells as a byproduct of chloride extrusion for a shrinking cell and relies on proton transporters such as NHE1 to re-alkalinize the cytoplasm. The particular role ClC-3 plays might be dependent on the current state of the cell (e.g. whether it needs to swell or shrink, acid load levels, and V_m), but in our examination of migrating tumor cells through a gradient in a two-dimensional environment (Figure 7) we saw them favor this last option. Future studies will attempt to force glioma cells into other

states by acidifying and alkalinizing the cell with concurrent volume stresses and seeing if ClC-3 drives simultaneous chloride and proton movement.

Finally, it is possible that this H^+ flux through ClC-3 has direct implications for glioma cell proliferation. ClC-3 knockdown glioma cells have impaired pre-mitotic condensation (PMC), a cell shrinkage immediately prior to M-phase (Cuddapah et al., 2012). In addition, glioma cells have slower proliferation at more acidic pH_e (Honasoge et al., 2013), in part due to blockade of pH_e-sensitive K^+ channels, which clamps the V_m to a depolarized potential and prevents cells from passing the G_1-to-S checkpoint of the cell cycle. Consistent with our proposed mechanism in Figure 7, a knockdown of ClC-3 would prevent shunting of H^+ back into the cell, thus acidifying pH_e which in turn could block pH_e-sensitive K^+ channels, thus preventing proliferation and exacerbating the impaired cell cycling due to inhibited PMC.

ACKNOWLEDGEMENTS

Funding was provided by the NIH 5RO1NS031234 and 2RO1-NS036692 . The authors declare no competing financial interests.

AUTHOR CONTRIBUTIONS

A.H. and H.S. are responsible for conception and design of the research; A.H., K.T.H, and V.Y.L performed the experiments; A.H., K.T.H., and V.Y.L. analyzed the data; A.H., K.T.H., V.Y.L., and H.S. interpreted the results of the experiments; A.H., K.T.H., and V.Y.L. prepared the figures; A.H., K.T.H., and V.Y.L. drafted the manuscript; A.H. and H.S. edited and revised the manuscript; A.H., K.T.H., V.Y.L., and H.S. approved the final version of the manuscript.

REFERENCES

Accardi, A., and A. Picollo. 2010. CLC channels and transporters: proteins with borderline personalities. *Biochimica et Biophysica Acta (BBA)-Biomembranes*. 1798:1457-1464.

Bevensee, M.O., M. Apkon, and W.F. Boron. 1997. Intracellular pH regulation in cultured astrocytes from rat hippocampus II. Electrogenic Na/HCO3 cotransport. *The Journal of general physiology*. 110:467-483.

Cuddapah, V.A., C.W. Habela, S. Watkins, L.S. Moore, T.-T.C. Barclay, and H. Sontheimer. 2012. Kinase activation of ClC-3 accelerates cytoplasmic condensation during mitotic cell rounding. *American Journal of Physiology-Cell Physiology*. 302:C527-C538.

Cuddapah, V.A., and H. Sontheimer. 2010. Molecular interaction and functional regulation of ClC-3 by Ca2+/calmodulin-dependent protein kinase II (CaMKII) in human malignant glioma. *Journal of biological chemistry*. 285:11188-11196.

Gatenby, R.A., and R.J. Gillies. 2004. Why do cancers have high aerobic glycolysis? *Nature reviews. Cancer*. 4:891-899.

Giannini, C., J.N. Sarkaria, A. Saito, J.H. Uhm, E. Galanis, B.L. Carlson, M.A. Schroeder, and C.D. James. 2005. Patient tumor EGFR and PDGFRA gene amplifications retained in an invasive intracranial xenograft model of glioblastoma multiforme. *Neuro-oncology*. 7:164-176.

Graves, A.R., P.K. Curran, C.L. Smith, and J.A. Mindell. 2008. The Cl-/H+ antiporter ClC-7 is the primary chloride permeation pathway in lysosomes. *Nature*. 453:788-792.

Habela, C.W., M.L. Olsen, and H. Sontheimer. 2008. ClC3 is a critical regulator of the cell cycle in normal and malignant glial cells. *The Journal of Neuroscience*. 28:9205-9217.

Honasoge, A., K.A. Shelton, and H. Sontheimer. 2013. Autocrine regulation of glioma cell proliferation via pHe-sensitive K+ channels. *American journal of physiology. Cell physiology*.

Honasoge, A., and H. Sontheimer. 2013. Involvement of tumor acidification in brain cancer pathophysiology. *Frontiers in Physiology*. 4.

Howes, M.T., M. Kirkham, J. Riches, K. Cortese, P.J. Walser, F. Simpson, M.M. Hill, A. Jones, R. Lundmark, and M.R. Lindsay. 2010. Clathrin-independent carriers form a high capacity endocytic sorting system at the leading edge of migrating cells. *The Journal of cell biology*. 190:675-691.

Huang, P., J. Liu, A. Di, N.C. Robinson, M.W. Musch, M.A. Kaetzel, and D.J. Nelson. 2001. Regulation of human CLC-3 channels by multifunctional Ca2+/calmodulin-dependent protein kinase. *Journal of Biological Chemistry*. 276:20093-20100.

Lange, P.F., L. Wartosch, T.J. Jentsch, and J.C. Fuhrmann. 2006. ClC-7 requires Ostm1 as a β-subunit to support bone resorption and lysosomal function. *Nature*. 440:220-223.

Ludwig, F.T., A. Schwab, and C. Stock. 2013. The Na+/H+-exchanger (NHE1) generates pH nanodomains at focal adhesions. *Journal of cellular physiology*. 228:1351-1358.

Manning, T.J., J.C. Parker, and H. Sontheimer. 2000. Role of lysophosphatidic acid and rho in glioma cell motility. *Cell motility and the cytoskeleton*. 45:185-199.

Martin, C., S.F. Pedersen, A. Schwab, and C. Stock. 2011. Intracellular pH gradients in migrating cells. *American Journal of Physiology-Cell Physiology*. 300:C490-C495.

Matsuda, J.J., M.S. Filali, M.M. Collins, K.A. Volk, and F.S. Lamb. 2010. The ClC-3 Cl−/H+ antiporter becomes uncoupled at low extracellular pH. *Journal of biological chemistry*. 285:2569-2579.

Matsuda, J.J., M.S. Filali, K.A. Volk, M.M. Collins, J.G. Moreland, and F.S. Lamb. 2008. Overexpression of CLC-3 in HEK293T cells yields novel currents that are pH dependent. *American Journal of Physiology-Cell Physiology*. 294:C251-C262.

McFerrin, M.B., and H. Sontheimer. 2006. A role for ion channels in glioma cell invasion. *Neuron glia biology*. 2:39.

McLean, L.A., J. Roscoe, N.K. Jørgensen, F.A. Gorin, and P.M. Cala. 2000. Malignant gliomas display altered pH regulation by NHE1 compared with nontransformed astrocytes. *American Journal of Physiology-Cell Physiology*. 278:C676-C688.

Mindell, J.A. 2008. The chloride channel's appendix. *Nature structural & molecular biology*. 15:781-783.

Olsen, M., S. Schade, S. Lyons, M. Amaral, and H. Sontheimer. 2003. Expression of voltage-gated chloride channels in human glioma cells. *The Journal of neuroscience*. 23:5572-5582.

Ransom, C.B., J.T. O'Neal, and H. Sontheimer. 2001. Volume-activated chloride currents contribute to the resting conductance and invasive migration of human glioma cells. *The Journal of Neuroscience*. 21:7674-7683.

Riazanski, V., L.V. Deriy, P.D. Shevchenko, B. Le, E.A. Gomez, and D.J. Nelson. 2011. Presynaptic CLC-3 determines quantal size of inhibitory transmission in the hippocampus. *Nature neuroscience*. 14:487-494.

Sarkaria, J.N., L. Yang, P.T. Grogan, G.J. Kitange, B.L. Carlson, M.A. Schroeder, E. Galanis, C. Giannini, W. Wu, and E.B. Dinca. 2007. Identification of molecular characteristics correlated with glioblastoma sensitivity to EGFR kinase inhibition through use of an intracranial xenograft test panel. *Molecular cancer therapeutics*. 6:1167-1174.

Schiefermeier, N., D. Teis, and L.A. Huber. 2011. Endosomal signaling and cell migration. *Current opinion in cell biology*. 23:615-620.

Stauber, T., S. Weinert, and T.J. Jentsch. 2012. Cell biology and physiology of CLC chloride channels and transporters. *Comprehensive Physiology*.

Stobrawa, S.M., T. Breiderhoff, S. Takamori, D. Engel, M. Schweizer, A.A. Zdebik, M.R. Bösl, K. Ruether, H. Jahn, and A. Draguhn. 2001. Disruption of ClC-3, a chloride channel expressed on synaptic vesicles, leads to a loss of the hippocampus. *Neuron*. 29:185-196.

Stupp, R., W.P. Mason, M.J. Van Den Bent, M. Weller, B. Fisher, M.J. Taphoorn, K. Belanger, A.A. Brandes, C. Marosi, and U. Bogdahn. 2005. Radiotherapy plus concomitant and adjuvant temozolomide for glioblastoma. *New England Journal of Medicine*. 352:987-996.

Turner, K.L., A. Honasoge, S.M. Robert, M.M. McFerrin, and H. Sontheimer. 2014. A proinvasive role for the Ca2+-activated K+ channel KCa3. 1 in malignant glioma. *Glia*.

Ulrich, F., and C.P. Heisenberg. 2009. Trafficking and cell migration. *Traffic*. 10:811-818.

Vander Heiden, M.G., L.C. Cantley, and C.B. Thompson. 2009. Understanding the Warburg effect: the metabolic requirements of cell proliferation. *Science (New York, N.Y.)*. 324:1029-1033.

Watkins, S., and H. Sontheimer. 2011. Hydrodynamic cellular volume changes enable glioma cell invasion. *The Journal of Neuroscience*. 31:17250-17259.

Watkins, S., and H. Sontheimer. 2012. Unique biology of gliomas: challenges and opportunities. *Trends in neurosciences*. 35:546-556.

Weaver, A.K., V.C. Bomben, and H. Sontheimer. 2006. Expression and function of calcium-activated potassium channels in human glioma cells. *Glia*. 54:223-233.

Zhao, Z., X. Li, J. Hao, J.H. Winston, and S.A. Weinman. 2007. The ClC-3 chloride transport protein traffics through the plasma membrane via interaction of an N-terminal dileucine cluster with clathrin. *Journal of Biological Chemistry*. 282:29022-29031.

SUMMARY AND DISCUSSION

In this thesis, we sought to identify key points of autocrine regulation of glioma cells by their acidic microenvironment. This led to two interesting findings: 1) glioma tumor spheroid proliferation occurs in an outside-out manner due to a steep pH_e gradient setting V_m through pH_e-sensitive K^+ channels, which in turn determines cellular passage through the G_1-to-S checkpoint of the cell cycle (Figure 1); and 2) the prior-described glioma Cl^- channel ClC-3 is actually a Cl^-/H^+ antiporter that can be electrogenically stimulated with or without patch pipette intervention and affects the pH_i gradient in glioma cells in a manner consistent with ClC-3 localization to the leading edge.

The pH_e dependence of proliferation is interesting in both its implications for gliomas and its generalizability across solid tumors. It implies that glioma cells overwhelmingly prefer to grow in more alkaline environments, meaning their autocrine acidification is deleterious to tumor growth. This acid-induced cell cycle shutdown might be part of a larger pathology that has been previously characterized as the "go versus grow" hypothesis of cancer biology (Hatzikirou et al., 2012); that is, tumor cells are either migrating or proliferating, but not both simultaneously. Figure 2 demonstrates how the findings in this thesis might pertain to this hypothesis. Cells in the tumor core are given a proliferation shutdown signal by their built up protons, either enhancing their chemokinesis in a random walk

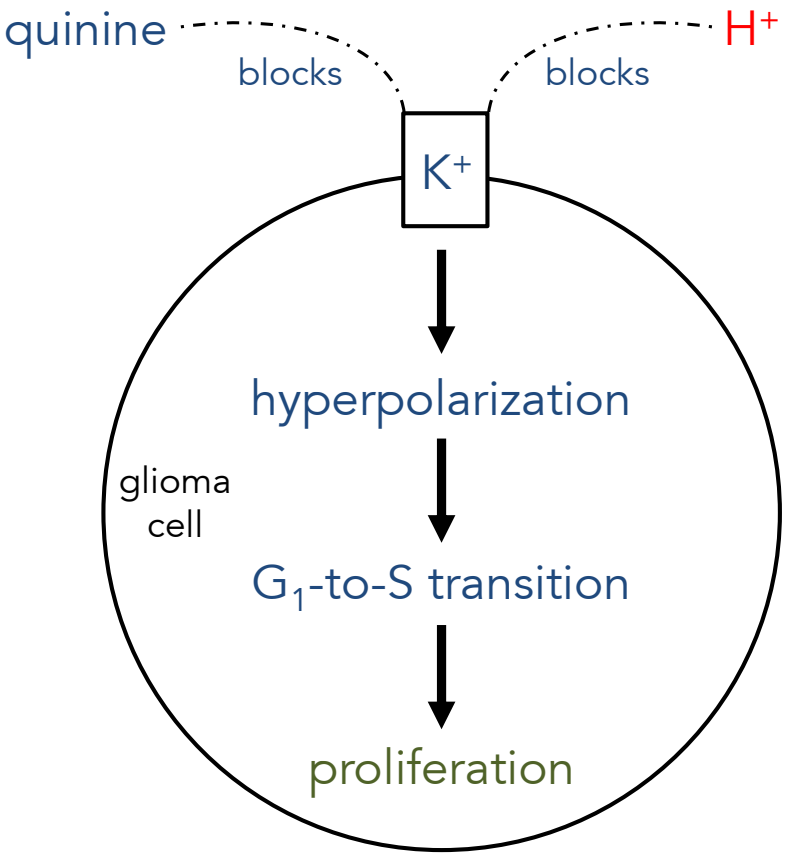

Figure 1. pH_e control of glioma cell proliferation via pH_e-and quinine-sensitive K^+ channels. Schematic depicting how pH_e-sensitive K^+ conductance governs glioma cell proliferation, thus translating the cell's extracellular environment to intracellular signaling. Though the exact K^+ channels are unknown, potential candidates include TASK-1 and TASK-3, members of the two-pore potassium channel (K_2P) family.

fashion or speeding up chemotaxis towards gradients away from the tumor core. In either case, the cells that eventually find themselves in more hospitable (alkaline) environments would be hyperpolarized and switched back to a proliferative state, while the others would continue to try to escape the core. This escape may partially explain the outside-out pattern of tumor growth (McIntyre et al., 2012; Vinci et al., 2012). It is important to note that while more proliferative cells are usually depolarized versus quiescent cells, some still require hyperpolarization to pass through checkpoints of the cell cycle (Becchetti et al., 2014). It is our contention that depolarizing glioma cells either with acidic pH_e or quinine clamps the cells at a depolarized potential and prevents even a transient hyperpolarization.

One major finding of this thesis was that tumor spheroids serve as viable models to study tumor physiology. While tumor spheroids have been prior implicated in the study of proliferation and drug assays, through both fixed and live tissue analysis we found that they can be used much more broadly and that they recapitulate each step of glioma pathophysiology. In our case, we saw identical gradients for pH_e, voltage, and proliferation within the spheroids, and the spheroids responded in a manner consistent with monolayer glioma cell findings.

We were unable to definitively identify any particular pH_e-sensitive K+ channel in this thesis. By far the best two candidates are TASK-1 and TASK-3, members of the two-pore K^+ channel family that function as "leak" basal K^+ conductances, are blocked robustly by quinine, and close to acidic pH_e (Lotshaw, 2007). Additionally, expression of both of these channels has been prior

demonstrated in glioma cell lines (Meuth et al., 2008). Future studies will seek to identify which channel(s) form the pH_e-sensitivity of glioma cells and whether more specific and potent drugs are available for blockade.

The second part of this thesis explored a novel and exciting role for the ClC-3 antiporter in glioma physiology. ClC-3 is overexpressed in gliomas versus normal brain (Olsen et al., 2003; Cuddapah and Sontheimer, 2010); additionally, it is rare to have ClC-3 surface expression save for exogenous overexpressor models (Jentsch, 2007; Zhao et al., 2007; Jentsch, 2008; Stauber et al., 2012). These two properties make ClC-3 an attractive target for glioma chemotherapy. While ClC-3 moving chloride through the glioma cell plasma membrane has been accepted and manipulated (Cuddapah and Sontheimer, 2010; Watkins and Sontheimer, 2011; Cuddapah et al., 2012), its roles in proton movement across the plasma membrane and pH_i regulation in glioma cells had not been hitherto explored. This is partially because it is still unclear whether and how ClC-3 moves protons in *any* model system. This poor elucidation results from the complexity by which the entire CLC protein class transports ions and the dearth of ClC-3 surface expression (Mindell, 2008). For our experiments, we faced the additional hurdle of keeping mammalian cells alive during electrophysiological manipulations that could affect both pH_i and buffering capacity while still detecting potential protonic currents. We thus had to resort to complex measures, for instance simultaneously perforated patching glioma cells with a lightly-buffered pipette solution while ratiometrically imaging a pH_i-sensitive fluorescent dye to observe measurable ClC-3 H^+ movement in a manner previously employed on rat astrocytes (Bevensee et al., 1997). We also attempted to

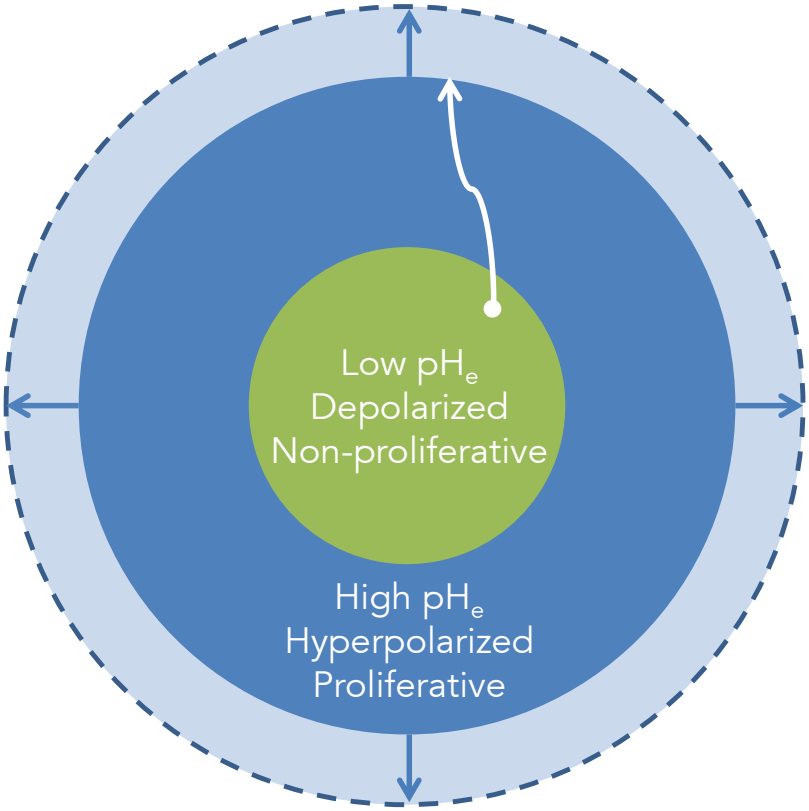

Figure 2. Role of pH_e control of glioma cell proliferation in the go-vs. grow hypothesis of cancer cells. Schematic demonstrating how tumor cells in the acidic core face a microenvironment inhospitable to growth, forcing them to migrate towards the rim of the tumor. At this point, the more alkaline pH_e would allow cell hyperpolarization and passage through the cell cycle.

electrogenically stimulate ClC-3 without electrophysiological intervention by altering $[K^+]_o$, using the glioma cell's basal permeability to K^+ as a driving force for V_m. This modulation allowed us to leave the intracellular composition of glioma cells relatively unperturbed (except for the loaded fluorescent dye) and also allowed us to monitor dozens of cells on a single coverslip simultaneously. It also limited the hyper- and depolarizations to a range that glioma cells could conceivably reach on their own *in vivo*.

As we focused largely on characterizing the antiport properties of ClC-3, future studies will be directed at how this this newfound H^+ movement impacts glioma pathophysiology. In our pH_i gradient experiment, we found hints of ClC-3 specifically affecting the leading edge of migrating glioma cells, possibly shunting proton extrusion from other transporters to drive chloride movement. This model is described in Figure 7 on page 97 entitled "Disruption of leading edge pH_i and pH_i covariation in ClC-3 knockdown glioma cells" and is consistent with other pH_i regulators such as NHE1 localizing to the leading edge of the cell (Martin et al., 2011). We therefore believe there is an entirely new and unexplored physiology that can be assigned to ClC-3 in gliomas, potentially leading to new treatments specifically designed to attack this aspect of ClC-3 permeability and preventing glioma cells from migrating and proliferating. For example, chemotherapy therapy with an NHE1 inhibitor (such as the already clinically accessible amiloride) could prevent shunted H^+ from being extruded in the first place, thereby indirectly blocking Cl^- movement. This could be combined with chlorotoxin, a drug currently in clinical trials that internalizes ClC-3 and in doing so decreases its currents

(Deshane et al., 2003; McFerrin and Sontheimer, 2006), to disrupt a glioma cell's ability to flux chloride at multiple levels.

Finally, it is important to place these findings in the context of brain chemistry. pH regulation and metabolism are dynamic, tightly-controlled, and intertwined processes in the brain, and gliomas may act to disrupt the astrocyte-neuron relationships. All of the players described here in glioma pathophysiology exist in normal brain physiology, thus leaving the brain vulnerable to physiologic hijacking or disruption by glioma cells. As previously mentioned, glioma cells metabolize copious amounts of glucose and secrete lactate and protons, potentially causing local chemical imbalance. Astrocytes are usually responsible for glucose uptake from the bloodstream, converting it to lactate, and shuttling this lactate to neurons that use it as fuel (Chih and Roberts, 2003). Increased extracellular lactate from glioma cells may therefore alter the lactate gradient and prevent astrocytic transport and neuronal uptake of lactate where needed.

Another example of pH-dependent interplay between astrocytes and neurons is known as depolarization-induced alkalinization (DIA): 1) stimulated cortical neurons repolarize by effluxing K^+, thereby increasing $[K^+]_o$; 2) increased $[K^+]_o$ depolarizes astrocytes, which possess an electrogenic Na^+/HCO_3^- co-transporter (NBCe); 3) NBCe is stimulated by this depolarization and promotes the influx of bicarbonate, thereby alkalinizing the astrocyte and acidifying the extracellular space (Brookes and Turner, 1994; Grichtchenko and Chesler, 1994; Pappas and Ransom, 1994; Florence et al., 2012). This extracellular acidification can prevent further

neuronal firing by proton inhibition of ion channels, especially the NMDA glutamate receptor (Traynelis and Cull-Candy, 1990). Additionally, a recent study has shown that the NBCe-dependent bicarbonate influx is responsible for activating astrocytic soluble adenylyl cyclase (sAC), which then increases cyclic AMP (cAMP) levels and promotes lactate formation eventually shuttled to neurons (Choi et al., 2012). Thus, if these sequences of events are disrupted by glioma cells over-acidifying the extracellular space, they can affect the fine balance between neuronal excitation and inhibition.

In conclusion, glioma cells face a pH microenvironment unlike any other cells in the brain. They have tuned their physiology to reflect this via changes in surface expression of pH_e-sensitive ion channels, resulting in pH_e-dependent growth and ion flux. These changes are most likely beneficial to the glioma in facing a hostile microenvironment; however, they also leave glioma cells vulnerable to both physiological and pharmacologic attack provided we find drugs that either modulate pH_e or specifically target the pH_e-sensitive ion channels. Further work must be done to understand additional downstream consequences of this pH_e sensitivity and to find glioma-specific targets for therapy.

GENERAL LIST OF REFERENCES

Accardi, A., and A. Picollo. 2010. CLC channels and transporters: proteins with borderline personalities. *Biochimica et Biophysica Acta (BBA)-Biomembranes*. 1798:1457-1464.

Andrews, R.J., J.R. Bringas, and G. Alonzo. 1994. Cerebrospinal fluid pH and PCO2 rapidly follow arterial blood pH and PCO2 with changes in ventilation. *Neurosurgery*. 34:466-470.

Becchetti, A. 2011. Ion channels and transporters in cancer. 1. Ion channels and cell proliferation in cancer. *American journal of physiology. Cell physiology*. 301:C255-265.

Becchetti, A., A. Arcangeli, and L. Munaron. 2014. Ion Transport in Cell Cycle and Cancer. Frontiers E-books.

Berdiev, B.K., J. Xia, L.A. McLean, J.M. Markert, G.Y. Gillespie, T.B. Mapstone, A.P. Naren, B. Jovov, J.K. Bubien, and H.-L. Ji. 2003. Acid-sensing ion channels in malignant gliomas. *Journal of Biological Chemistry*. 278:15023-15034.

Bevensee, M.O., M. Apkon, and W.F. Boron. 1997. Intracellular pH regulation in cultured astrocytes from rat hippocampus II. Electrogenic Na/HCO3 cotransport. *The Journal of general physiology*. 110:467-483.

Brookes, N., and R.J. Turner. 1994. K (+)-induced alkalinization in mouse cerebral astrocytes mediated by reversal of electrogenic Na (+)-HCO3-cotransport. *American Journal of Physiology-Cell Physiology*. 267:C1633-C1640.

Buckingham, S.C., S.L. Campbell, B.R. Haas, V. Montana, S. Robel, T. Ogunrinu, and H. Sontheimer. 2011. Glutamate release by primary brain tumors induces epileptic activity. *Nature medicine*. 17:1269-1274.

Buckingham, S.C., and S. Robel. 2013. Glutamate and tumor-associated epilepsy: Glial cell dysfunction in the peritumoral environment. *Neurochemistry international*. 63:696-701.

Busco, G., R.A. Cardone, M.R. Greco, A. Bellizzi, M. Colella, E. Antelmi, M.T. Mancini, M.E. Dell'Aquila, V. Casavola, and A. Paradiso. 2010. NHE1 promotes invadopodial ECM proteolysis through acidification of the peri-invadopodial space. *The FASEB Journal*. 24:3903-3915.

Cairns, R.A., I.S. Harris, and T.W. Mak. 2011. Regulation of cancer cell metabolism. Nature Reviews Cancer. 11:85-95.

Campbell, S.L., S.C. Buckingham, and H. Sontheimer. 2012. Human glioma cells induce hyperexcitability in cortical networks. *Epilepsia*. 53:1360-1370.

Chih, C.-P., and E.L. Roberts. 2003. Energy Substrates for Neurons During Neural Activity: A Critical Review of the Astrocyte-Neuron Lactate Shuttle Hypothesis. *Journal of Cerebral Blood Flow & Metabolism*. 23:1263-1281.

Choi, H.B., G.R. Gordon, N. Zhou, C. Tai, R.L. Rungta, J. Martinez, T.A. Milner, J.K. Ryu, J.G. McLarnon, and M. Tresguerres. 2012. Metabolic communication between astrocytes and neurons via bicarbonate-responsive soluble adenylyl cyclase. *Neuron*. 75:1094-1104.

Cohen, A., Y. Ben-Abu, and N. Zilberberg. 2009. Gating the pore of potassium leak channels. *European Biophysics Journal*. 39:61-73.

Cuddapah, V.A., C.W. Habela, S. Watkins, L.S. Moore, T.-T.C. Barclay, and H. Sontheimer. 2012. Kinase activation of ClC-3 accelerates cytoplasmic condensation during mitotic cell rounding. *American Journal of Physiology-Cell Physiology*. 302:C527-C538.

Cuddapah, V.A., and H. Sontheimer. 2010. Molecular interaction and functional regulation of ClC-3 by Ca2+/calmodulin-dependent protein kinase II (CaMKII) in human malignant glioma. *Journal of biological chemistry*. 285:11188-11196.

Deshane, J., C.C. Garner, and H. Sontheimer. 2003. Chlorotoxin inhibits glioma cell invasion via matrix metalloproteinase-2. *Journal of Biological Chemistry*. 278:4135-4144.

Florence, C.M., L.D. Baillie, and S.J. Mulligan. 2012. Dynamic volume changes in astrocytes are an intrinsic phenomenon mediated by bicarbonate ion flux. *PloS one*. 7:e51124.

García-Martín, M.-L., G. Hérigault, C. Rémy, R. Farion, P. Ballesteros, J.A. Coles, S. Cerdán, and A. Ziegler. 2001. Mapping Extracellular pH in rat Brain Gliomas in vivo by H Magnetic Resonance Spectroscopic Imaging: Comparison with maps of metabolites. *Cancer research*. 61:6524-6531.

Garcia-Martin, M.L., G.V. Martinez, N. Raghunand, A.D. Sherry, S. Zhang, and R.J. Gillies. 2006. High resolution pHe imaging of rat glioma using pH-dependent relaxivity. *Magnetic resonance in medicine*. 55:309-315.

Grichtchenko, I., and M. Chesler. 1994. Depolarization-induced alkalinization of astrocytes in gliotic hippocampal slices. *Neuroscience*. 62:1071-1078.

Grillon, E., R. Farion, K. Fablet, M. De Waard, C.M. Tse, M. Donowitz, C. Rémy, and J.A. Coles. 2011. The spatial organization of proton and lactate transport in a rat brain tumor. *PLoS One*. 6:e17416.

Habela, C.W., M.L. Olsen, and H. Sontheimer. 2008. ClC3 is a critical regulator of the cell cycle in normal and malignant glial cells. *The Journal of Neuroscience*. 28:9205-9217.

Hatzikirou, H., D. Basanta, M. Simon, K. Schaller, and A. Deutsch. 2012. 'Go or Grow': the key to the emergence of invasion in tumour progression? *Mathematical Medicine and Biology*. 29:49-65.

Honasoge, A., K.A. Shelton, and H. Sontheimer. 2013. Autocrine regulation of glioma cell proliferation via pHe-sensitive K+ channels. *American journal of physiology. Cell physiology*.

Honasoge, A., and H. Sontheimer. 2013. Involvement of tumor acidification in brain cancer pathophysiology. *Frontiers in Physiology*. 4.

Javaheri, S., A. Clendening, N. Papadakis, and J. Brody. 1984. PH changes on the surface of brain and in cisternal fluid in dogs in cardiac arrest. *Stroke*. 15:553-557.

Jentsch, T.J. 2007. Chloride and the endosomal–lysosomal pathway: emerging roles of CLC chloride transporters. *The Journal of physiology*. 578:633-640.

Jentsch, T.J. 2008. CLC chloride channels and transporters: from genes to protein structure, pathology and physiology. *Critical reviews in biochemistry and molecular biology*. 43:3-36.

Kapoor, N., R. Bartoszewski, Y.J. Qadri, Z. Bebok, J.K. Bubien, C.M. Fuller, and D.J. Benos. 2009. Knockdown of ASIC1 and epithelial sodium channel subunits inhibits glioblastoma whole cell current and cell migration. *Journal of biological chemistry*. 284:24526-24541.

Lagadic-Gossmann, D., L. Huc, and V. Lecureur. 2004. Alterations of intracellular pH homeostasis in apoptosis: origins and roles. *Cell Death & Differentiation*. 11:953-961.

Lopes, C.M., N. Zilberberg, and S.A. Goldstein. 2001. Block of Kcnk3 by Protons EVIDENCE THAT 2-P-DOMAIN POTASSIUM CHANNEL SUBUNITS FUNCTION AS HOMODIMERS. *Journal of Biological Chemistry*. 276:24449-24452.

Lotshaw, D.P. 2007. Biophysical, pharmacological, and functional characteristics of cloned and native mammalian two-pore domain K+ channels. *Cell biochemistry and biophysics*. 47:209-256.

Magalhaes, M.A., D.R. Larson, C.C. Mader, J.J. Bravo-Cordero, H. Gil-Henn, M. Oser, X. Chen, A.J. Koleske, and J. Condeelis. 2011. Cortactin phosphorylation regulates cell invasion through a pH-dependent pathway. *The Journal of cell biology*. 195:903-920.

Martin, C., S.F. Pedersen, A. Schwab, and C. Stock. 2011. Intracellular pH gradients in migrating cells. *American Journal of Physiology-Cell Physiology*. 300:C490-C495.

Matsuda, J.J., M.S. Filali, M.M. Collins, K.A. Volk, and F.S. Lamb. 2010. The ClC-3 Cl−/H+ antiporter becomes uncoupled at low extracellular pH. *Journal of biological chemistry*. 285:2569-2579.

Matsuda, J.J., M.S. Filali, K.A. Volk, M.M. Collins, J.G. Moreland, and F.S. Lamb. 2008. Overexpression of CLC-3 in HEK293T cells yields novel currents that are pH dependent. *American Journal of Physiology-Cell Physiology*. 294:C251-C262.

McFerrin, M.B., and H. Sontheimer. 2006. A role for ion channels in glioma cell invasion. *Neuron glia biology*. 2:39.

McIntyre, A., S. Patiar, S. Wigfield, J.-l. Li, I. Ledaki, H. Turley, R. Leek, C. Snell, K. Gatter, and W.S. Sly. 2012. Carbonic anhydrase IX promotes tumor growth and necrosis in vivo and inhibition enhances anti-VEGF therapy. *Clinical Cancer Research*. 18:3100-3111.

McLean, L.A., J. Roscoe, N.K. Jørgensen, F.A. Gorin, and P.M. Cala. 2000. Malignant gliomas display altered pH regulation by NHE1 compared with nontransformed astrocytes. *American Journal of Physiology-Cell Physiology*. 278:C676-C688.

Meuth, S.G., A.M. Herrmann, C.W. Ip, T. Kanyshkova, S. Bittner, A. Weishaupt, T. Budde, and H. Wiendl. 2008. The two-pore domain potassium channel TASK3 functionally impacts glioma cell death. *Journal of neuro-oncology*. 87:263-270.

Mindell, J.A. 2008. The chloride channel's appendix. *Nature structural & molecular biology*. 15:781-783.

Mitchell, R., and M. Singer. 1965. Respiration and cerebrospinal fluid pH in metabolic acidosis and alkalosis. *Journal of applied physiology*. 20:905-911.

Olsen, M., S. Schade, S. Lyons, M. Amaral, and H. Sontheimer. 2003. Expression of voltage-gated chloride channels in human glioma cells. *The Journal of neuroscience*. 23:5572-5582.

Papandreou, I., R.A. Cairns, L. Fontana, A.L. Lim, and N.C. Denko. 2006. HIF-1 mediates adaptation to hypoxia by actively downregulating mitochondrial oxygen consumption. *Cell metabolism*. 3:187-197.

Pappas, C.A., and B.R. Ransom. 1994. Depolarization-induced alkalinization (DIA) in rat hippocampal astrocytes. *Journal of neurophysiology*. 72:2816-2826.

Park, H., J. Lyons, T. Ohtsubo, and C. Song. 1999. Acidic environment causes apoptosis by increasing caspase activity. *British journal of cancer*. 80:1892.

Ransom, C.B., J.T. O'Neal, and H. Sontheimer. 2001. Volume-activated chloride currents contribute to the resting conductance and invasive migration of human glioma cells. *The Journal of Neuroscience*. 21:7674-7683.

Rooj, A.K., C.M. McNicholas, R. Bartoszewski, Z. Bebok, D.J. Benos, and C.M. Fuller. 2012. Glioma-specific cation conductance regulates migration and cell cycle progression. *Journal of Biological Chemistry*. 287:4053-4065.

Semenza, G.L., D. Artemov, A. Bedi, Z. Bhujwalla, K. Chiles, D. Feldser, E. Laughner, R. Ravi, J. Simons, and P. Taghavi. 2001. 'The metabolism of tumours': 70 years later. *In* The Tumour Microenvironment: Causes and Consequences of Hypoxia and Acidity: Novartis Foundation Symposium 240. Wiley Online Library. 251-264.

Sontheimer, H. 2011. Glutamate and tumor-associated epilepsy. *Oncotarget*. 2:823.

Stauber, T., S. Weinert, and T.J. Jentsch. 2012. Cell biology and physiology of CLC chloride channels and transporters. *Comprehensive Physiology*.

Stupp, R., W.P. Mason, M.J. Van Den Bent, M. Weller, B. Fisher, M.J. Taphoorn, K. Belanger, A.A. Brandes, C. Marosi, and U. Bogdahn. 2005. Radiotherapy plus concomitant and adjuvant temozolomide for glioblastoma. *New England Journal of Medicine*. 352:987-996.

Traynelis, S.F., and S.G. Cull-Candy. 1990. Proton inhibition of N-methyl-D-aspartate receptors in cerebellar neurons. *Nature*. 345:347-350.

Van Slyke, A.C., Y.M. Cheng, P. Mafi, C.R. Allard, C.M. Hull, Y.P. Shi, and T.W. Claydon. 2012. Proton block of the pore underlies the inhibition of hERG cardiac K+ channels during acidosis. *American Journal of Physiology-Cell Physiology*. 302:C1797-C1806.

Vinci, M., S. Gowan, F. Boxall, L. Patterson, M. Zimmermann, C. Lomas, M. Mendiola, D. Hardisson, and S.A. Eccles. 2012. Advances in establishment and analysis of three-dimensional tumor spheroid-based functional assays for target validation and drug evaluation. *BMC biology*. 10:29.

Waldmann, R., G. Champigny, F. Bassilana, C. Heurteaux, and M. Lazdunski. 1997. A proton-gated cation channel involved in acid-sensing.

Warburg, O. 1956. On the origin of cancer cells. *Science*. 123:309-314.

Warburg, O., F. Wind, and E. Negelein. 1927. The metabolism of tumors in the body. *The Journal of general physiology*. 8:519-530.

Watkins, S., and H. Sontheimer. 2011. Hydrodynamic cellular volume changes enable glioma cell invasion. *The Journal of Neuroscience*. 31:17250-17259.

Wykoff, C.C., N.J. Beasley, P.H. Watson, K.J. Turner, J. Pastorek, A. Sibtain, G.D. Wilson, H. Turley, K.L. Talks, and P.H. Maxwell. 2000. Hypoxia-inducible expression of tumor-associated carbonic anhydrases. *Cancer Research*. 60:7075-7083.

Xu, L., D. Fukumura, and R.K. Jain. 2002. Acidic Extracellular pH Induces Vascular Endothelial Growth Factor (VEGF) in Human Glioblastoma Cells via ERK1/2 MAPK Signaling Pathway MECHANISM OF LOW pH-INDUCED VEGF. *Journal of Biological Chemistry*. 277:11368-11374.

Zhao, Z., X. Li, J. Hao, J.H. Winston, and S.A. Weinman. 2007. The ClC-3 chloride transport protein traffics through the plasma membrane via interaction of an N-terminal dileucine cluster with clathrin. *Journal of Biological Chemistry*. 282:29022-29031.

APPENDIX

IRB APPROVAL FORM

THE UNIVERSITY OF ALABAMA AT BIRMINGHAM

Institutional Review Board for Human Use

DATE: December 19, 2012

MEMORANDUM

TO: Avinash Honasoge
Principal Investigator

FROM: Cari Oliver
Assistant Director
Office of the Institutional Review Board (OIRB)

RE: Request for Determination—Human Subjects Research
IRB Protocol #N121219002– pH Regulates Glioma Cell Physiology via K+ Channel Modulation

A member of the Office of the IRB has reviewed your application for Designation of Not Human Subjects Research for above referenced proposal.

The reviewer has determined that this proposal is **not** subject to FDA regulations and is **not** Human Subjects Research. Note that any changes to the project should be resubmitted to the Office of the IRB for determination.

470 Administration Building
701 20th Street South
205.934.3789
Fax 205.934.1301
irb@uab.edu

The University of
Alabama at Birmingham
Mailing Address:
AB 470
1530 3RD AVE S
BIRMINGHAM AL 35294-0104